

INFORMATION TO USERS

This manuscript has been reproduced from the microfilm master. UMI films the text directly from the original or copy submitted. Thus, some thesis and dissertation copies are in typewriter face, while others may be from any type of computer printer.

The quality of this reproduction is dependent upon the quality of the copy submitted. Broken or indistinct print, colored or poor quality illustrations and photographs, print bleedthrough, substandard margins, and improper alignment can adversely affect reproduction.

In the unlikely event that the author did not send UMI a complete manuscript and there are missing pages, these will be noted. Also, if unauthorized copyright material had to be removed, a note will indicate the deletion.

Oversize materials (e.g., maps, drawings, charts) are reproduced by sectioning the original, beginning at the upper left-hand corner and continuing from left to right in equal sections with small overlaps. Each original is also photographed in one exposure and is included in reduced form at the back of the book.

Photographs included in the original manuscript have been reproduced xerographically in this copy. Higher quality 6" x 9" black and white photographic prints are available for any photographs or illustrations appearing in this copy for an additional charge. Contact UMI directly to order.

U·M·I

University Microfilms International
A Bell & Howell Information Company
300 North Zeeb Road, Ann Arbor, MI 48106-1346 USA
313/761-4700 800/521-0600

Order Number 9234805

**Transcranial Doppler sonography: A new noninvasive method
for measuring toxicant-induced alterations in cerebral blood flow**

Drues, Michael Edward, Ph.D.

Iowa State University, 1992

Copyright ©1992 by Drues, Michael Edward. All rights reserved.

U·M·I
300 N. Zeeb Rd.
Ann Arbor, MI 48106

**Transcranial Doppler sonography:
A new noninvasive method for measuring
toxicant-induced alterations in cerebral blood flow**

by

Michael Edward Drues

A Dissertation Submitted to the
Graduate Faculty in Partial Fulfillment of the
Requirements for the Degree of
DOCTOR OF PHILOSOPHY

Major: Biomedical Engineering

Approved: _____

Signature was redacted for privacy.

In Charge of Major Work

Signature was redacted for privacy.

For the Interdepartmental Program

Signature was redacted for privacy.

For the Graduate College

Members of the Committee: _____

Signature was redacted for privacy.

Iowa State University
Ames, Iowa
1992

Copyright © Michael Edward Drues, 1992. All rights reserved.

TABLE OF CONTENTS

1. INTRODUCTION	1
2. BACKGROUND	4
2.1 Regulation of Cerebral Blood Flow	4
2.1.1 Influences of selected drugs and external stimuli on CBF	5
2.2 Measurement of Cerebral Blood Flow	6
2.2.1 Differences between rCBF and CBF	7
2.2.2 Relationship between BFV and CBF	7
2.2.3 Invasive measurements of rCBF	8
2.2.4 Invasive measurements of CBF at a point	8
2.2.5 Noninvasive measurements of rCBF	9
2.2.6 Noninvasive measurements of CBF at a point	9
2.3 Toxicology	10
2.3.1 Measurement of toxicity	10
2.3.2 Pyrethroids	11
2.3.3 Deltamethrin	12
2.4 Cerebral Vascular Anatomy	14
2.4.1 Extracranial anatomy	14
2.4.2 Intracranial anatomy	15

3. TRANSCRANIAL DOPPLER SONOGRAPHY	22
3.1 Transmission of Ultrasound through Bone	22
3.2 Theory of Ultrasound Operation	23
3.2.1 Pulsed vs. continuous wave Doppler	25
3.3 Accuracy of TCD Measurements	26
3.4 Probe Location	27
3.5 Artery Identification	28
3.6 TCD in the Canine	29
3.7 Summary of TCD	30
4. MATERIALS AND METHODS	31
4.1 Experimental Design	32
4.1.1 Justification of animal use	32
4.2 Phase I - Evaluation of TCD Equipment	33
4.3 Phase II - Dose-Response Pilot Study	35
4.4 Phase III - Deltamethrin Exposure in the Unconscious Dog	37
4.4.1 Blood pressure measurement	37
4.4.2 Cannula preparation	38
4.4.3 Cannula implantation	39
4.4.4 Experimental procedure	39
4.5 Phase IV - Deltamethrin Exposure in the Conscious Dog	41
4.6 Statistical Methods	43
4.6.1 Statistical design	44
4.6.2 Statistical analysis	45

5. RESULTS	47
5.1 Conditioning BFV Data	47
5.2 Physiological and Calculated Parameters	50
5.3 Results of Dose-Response Pilot Study	51
5.4 Concentration of Deltamethrin in Blood	53
5.5 Typical Results	53
5.6 Results of Physiological Parameters	55
5.6.1 Mean arterial pressure	60
5.6.2 Mean heart rate	61
5.6.3 End tidal CO ₂	63
5.6.4 Mean blood flow velocity	65
5.7 Results of Calculated Parameters	67
5.7.1 Systolic-to-diastolic ratio	67
5.7.2 Pourcelout pulsatility index	69
5.7.3 Gosling pulsatility index	71
5.7.4 Systolic upstroke	73
6. DISCUSSION	76
7. BIBLIOGRAPHY	81
8. ACKNOWLEDGEMENTS	85
9. APPENDIX A: CANNULA CONSTRUCTION	88
10. APPENDIX B: CANNULA IMPLANTATION	91
11. APPENDIX C: TCD DATA ANALYSIS PROGRAM	94
12. APPENDIX D: SAS CODE FOR STATISTICAL ANALYSIS	109

LIST OF TABLES

Table 2.1:	Summary of qualitative effects of O ₂ and C'O ₂ on cerebral blood flow [20]	5
Table 2.2:	Summary of commonly used anatomical abbreviations	17
Table 4.1:	Amount of deltamethrin administered to each dog for each exposure (N/A denotes where an animal has been removed from the study)	36
Table 4.2:	Randomization schedule (one replication). b=baseline (no deltamethrin), l=low-level dosage, h=high-level dosage	45
Table 5.1:	Period-block means for low-level exposure ($n = 12, \alpha = 0.05, df = 88$); see text for further explanation	58
Table 5.2:	Period-block means for high-level exposure ($n = 10, \alpha = 0.05, df = 72$); see text for further explanation	59
Table 6.1:	Summary of qualitative results of both low- and high-level experiments (N/C denotes no change with respect to control)	78

LIST OF FIGURES

Figure 2.1:	Effects of $p\text{CO}_2$ (A) and arterial pressure (B) on cerebral blood flow [20]	6
Figure 2.2:	Structure of deltamethrin, 3-(2,2-dibromoethenyl) 2,2-dimethyl cyclopropanecarboxylic acid cyano(3-phenoxyphenyl)-methyl ester	12
Figure 2.3:	Extracranial vessels in the human showing the primary path of blood from the heart to the circle of Willis	16
Figure 2.4:	Human circle of Willis and surrounding vessels [12]	18
Figure 2.5:	Canine circle of Willis and surrounding vessels (dorsal view) [2]	19
Figure 2.6:	Photograph showing corrosion-cast model of greyhound cerebrovascular system. All soft tissue is removed in this model leaving only bone, arteries (red) and veins (blue) intact	21
Figure 2.7:	Photograph showing plasticization model of greyhound head showing layers of bone and soft tissue in cross-section to the circle of Willis	21
Figure 3.1:	Typical velocity waveform from the human middle cerebral artery obtained during pilot work with the Medasonics Transpect TCD system	24

Figure 3.2:	Typical velocity waveform from the <i>canine</i> middle cerebral artery (MCA) obtained during pilot work with the Medasonics Transpect TCD system	24
Figure 4.1:	Photograph showing experimental setup in Phase III	42
Figure 4.2:	Photograph showing experimental setup in Phase IV	42
Figure 5.1:	Typical TCD recording obtained from the MCA of a 32kg Greyhound dog; vertical scale is velocity (cm/sec), horizontal scale is time (sec); data above the zero line is flow toward the probe, below the zero line is flow away from the probe; depth of sample volume is displayed in upper right	48
Figure 5.2:	Top: Original BFV waveform (from maximum frequency follower of TCD); Bottom: Conditioned BFV waveform	48
Figure 5.3:	Calculated parameters from the BFV waveform	51
Figure 5.4:	Two exposures of deltamethrin (7.5% LD ₅₀ immediately followed by a 10% LD ₅₀) in a 30kg Greyhound; upper graph shows measured physiological parameters; lower graph shows calculated parameters from the BFV waveform	52
Figure 5.5:	Concentration of deltamethrin in blood at 0, 5, 10, 15 and 30 minutes <i>post exposure</i> ; circles indicate low-level (5% LD ₅₀ exposure ($n=4$); squares indicate high-level (10% LD ₅₀ exposure ($n=4$); range represents standard error	54

- Figure 5.6: Control, solvent (glycerol-formal) and low level deltamethrin exposure (5% LD₅₀) in a 32kg greyhound; upper graph shows measured physiological parameters; lower graph shows calculated parameters from the BFV waveform 56
- Figure 5.7: Control, solvent (glycerol-formal) and high level deltamethrin exposure (10% LD₅₀) in a 32kg greyhound; upper graph shows measured physiological parameters; lower graph shows calculated parameters from the BFV waveform 57
- Figure 5.8: Mean arterial pressure (averaged over each minute for all dogs) in control, glycerol-formal and deltamethrin periods; circles indicate low-level (5% LD₅₀ exposure ($n=12$); squares indicate high-level (10% LD₅₀ exposure ($n=10$); range represents standard error 62
- Figure 5.9: Mean heart rate (averaged over each minute for all dogs) in control, glycerol-formal and deltamethrin periods; circles indicate low-level (5% LD₅₀ exposure ($n=12$); squares indicate high-level (10% LD₅₀ exposure ($n=10$); range represents standard error 64
- Figure 5.10: End tidal C'O₂ (recorded once every 5 minutes and averaged over all dogs) in control, glycerol-formal and deltamethrin periods; circles indicate low-level (5% LD₅₀ exposure ($n=12$); squares indicate high-level (10% LD₅₀ exposure ($n=10$); range represents standard error 66

Figure 5.11: Mean blood flow velocity (averaged over each minute for all dogs) in control, glycerol-formal and deltamethrin periods; circles indicate low-level (5% LD₅₀ exposure ($n=12$); squares indicate high-level (10% LD₅₀ exposure ($n=10$); range represents standard error 68

Figure 5.12: Systolic-to-diastolic ratio (averaged over each minute for all dogs) in control, glycerol-formal and deltamethrin periods; circles indicate low-level (5% LD₅₀ exposure ($n=12$); squares indicate high-level (10% LD₅₀ exposure ($n=10$); range represents standard error 70

Figure 5.13: Pourcelout pulsatility index (averaged over each minute for all dogs) in control, glycerol-formal and deltamethrin periods; circles indicate low-level (5% LD₅₀ exposure ($n=12$); squares indicate high-level (10% LD₅₀ exposure ($n=10$); range represents standard error 72

Figure 5.14: Gosling pulsatility index (averaged over each minute for all dogs) in control, glycerol-formal and deltamethrin periods; circles indicate low-level (5% LD₅₀ exposure ($n=12$); squares indicate high-level (10% LD₅₀ exposure ($n=10$); range represents standard error 74

Figure 5.15: Systolic upstroke or acceleration (averaged over each minute for all dogs) in control, glycerol-formal and deltamethrin periods; circles indicate low-level (5% LD₅₀ exposure ($n=12$); squares indicate high-level (10% LD₅₀ exposure ($n=10$); range represents standard error 75

1. INTRODUCTION

The purpose of this experiment was to determine if transcranial Doppler sonography (TCD) could be used in the dog to noninvasively measure changes in cerebral blood flow (CBF) resulting from a low-level exposure to the commonly used insecticide deltamethrin. TCD provides a means of noninvasively measuring blood flow velocity in the brain. Since changes in CBF may occur before behavioral or clinical symptoms of chemically-induced toxicosis [5, 7, 8], a means of measuring these changes could potentially be used as a screening procedure for early detection of exposure to hazardous substances. If changes in CBF can be detected by TCD before the occurrence of behavioral or clinical signs, then interdictive measures could be initiated very early in the exposure at a time when the effects of the toxicosis may be either minimal or reversible.

For TCD to be a useful method for detecting exposure to hazardous chemicals, it should be sensitive to chemically induced changes in CBF at exposure levels at or near established threshold limit values (TLVs) and be reliable and easy to use. This study sought to demonstrate that TCD can be used to noninvasively measure changes in CBF in the greyhound dog caused by low-level exposure to the widely used pyrethroid insecticide deltamethrin.

Several commercial TCD instruments available today are small, portable de-

vices that can be used by a trained registered vascular technician (RVT). Although TCD is a relatively new technique, it is finding use in an growing number of clinical applications, for example,

- in the diagnosis of cerebral vascular disease (including stenoses).
- in the determination of arterial-venous malformations (AVMs).
- in intraoperative monitoring (as during open-heart surgery and carotid endarterectomy).
- in the detection of vasospasm due to subarachnoid hemorrhage, and
- in the study of the effects of microgravity and Space Adaptation Syndrome aboard NASA's space shuttles.

To conduct this experiment, a computer-based system capable of detecting chemically induced changes in CBF in the dog was constructed. The system used TCD to noninvasively measure changes in CBF. Deltamethrin was dissolved in glycerol-formal¹ solvent and administered intravenously via a cannula in the jugular vein at dosage levels of 5% and 10% of the LD₅₀ value (as determined by a dose-response pilot study) to 12 dogs. Since the changes resulting from low-level deltamethrin exposure are subtle and occur over several minutes (rather than beat-by-beat changes), the data was stored on a PC for off-line post processing. These data included mean blood flow velocity (MBFV) in the middle cerebral artery, mean arterial blood pressure (MAP) in the aorta, end tidal CO₂ (pCO₂), mean heart rate (MHR) and concentration of deltamethrin in the blood. Data were measured during control, glycerol-

¹75% 5-hydroxy-1,3-dioxane and 25% 4-hydroxymethyl-1,3-dioxolane.

formal and exposure (deltamethrin in glycerol-formal) periods according to a randomized block factorial design. In addition to the aforementioned parameters, four additional parameters were calculated using the blood flow velocity waveform. They were systolic-to-diastolic ratio (SDR), Pourcelout pulsatility index (PPI), Gosling pulsatility index (GPI) and systolic upstroke (SU). An analysis of variance was performed on each parameter to determine if there were significant differences among the three treatment groups.

2. BACKGROUND

Proper functioning of the central nervous system (CNS) depends upon adequate cerebral blood flow for the delivery of oxygen, glucose and other nutrient materials and the removal of carbon dioxide and other metabolic byproducts from the brain. Blood flow to the brain is highly regulated and, therefore, the brain is highly susceptible to disturbances of the blood supply [20].

2.1 Regulation of Cerebral Blood Flow

CBF is regulated by changes in arterial blood pressure and cerebral blood flow resistance. Arterial blood pressure is regulated by circulatory reflexes (*i.e.*, the baroreceptor reflex and the cerebral ischemic reflex). Cerebral blood flow resistance is subject to several types of regulation (*i.e.*, blood viscosity, neural regulation and autoregulation). CBF is approximately linearly proportional to $p\text{CO}_2$ while it is relatively independent of arterial pressure within normal physiological limits [17] (see Figure 2.1). For example, inhalation of 5% CO_2 increases CBF by 50% and breathing 7% CO_2 doubles CBF. Conversely, breathing 100% O_2 lowers CBF about 13%; 10% O_2 raises it 35% (see Table 2.1) [17]. In most situations, CBF is positively correlated with glucose metabolism, *i.e.*, an increase in metabolic rate (\dot{M}) gives rise to an increase in glucose utilization (\dot{M}_{Gluc}) and an increase in cerebral blood flow (CBF)

Table 2.1: Summary of qualitative effects of O₂ and CO₂ on cerebral blood flow [20]

	Direction of Change
5% CO ₂ (hyperatmospheric)	↑
7% CO ₂ (hyperatmospheric)	↑↑
10% O ₂ (subatmospheric)	↑↑
100% O ₂ (hyperatmospheric)	↓

[4] or

$$\uparrow \dot{M} \Rightarrow \uparrow \dot{M}_{Gluc} \Rightarrow \uparrow CBF.$$

2.1.1 Influences of selected drugs and external stimuli on CBF

CBF is sensitive to many drugs. For example, CBF tends to decrease under general anesthesia (slowing of metabolism) while large doses of epinephrine tend to increase CBF. Barbiturates (*i.e.*, pentobarbital) are potent vasoconstrictors and can cause a potentially large decrease in CBF [5]. On the other hand, the inhalation anesthetics (*i.e.*, halothane) as a group are unique in that they all appear to uncouple the normally tight relationship between CBF and \dot{M}_{Gluc} . Therefore, halothane (used in this experiment) would be expected to increase CBF causing a corresponding decrease in \dot{M}_{Gluc} [21].

$$\downarrow \dot{M}_{Gluc} \Rightarrow HALOTHANE \Rightarrow \uparrow CBF$$

In addition, CBF is sensitive to many external stimuli. For example, blood flow in the occipital lobe increases during visual stimulation and blood flow in motor areas increases during limb movements [17].

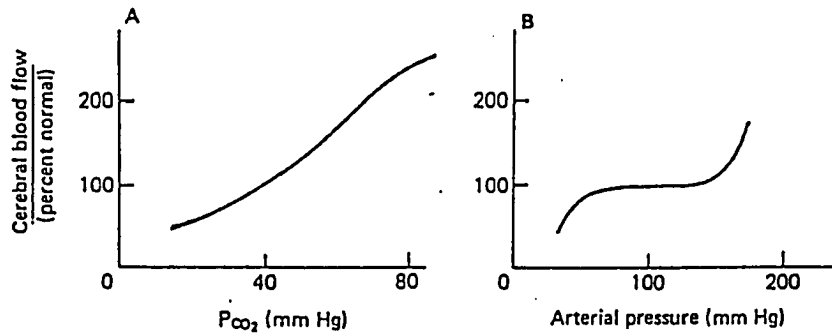


Figure 2.1: Effects of pCO₂ (A) and arterial pressure (B) on cerebral blood flow [20]

2.2 Measurement of Cerebral Blood Flow

Research in neurotoxicology seeks to determine the consequences of neurotoxicant exposure on central nervous system (CNS) function. Methods for examining CNS function may vary from the behavioral to the molecular level. The functional capacity of the CNS is dependent upon nutrient exchange, waste removal, fluid balance and temperature regulation which are in turn dependent upon cerebral blood flow. Although it is well known that several neurotoxicants alter CBF [19, 22, 28], the use of CBF measurement in neurotoxicology research has been very restricted because CBF has been difficult to measure. Indeed, many methods currently available require very sophisticated equipment and are extremely costly.

Methods for measuring blood flow in the brain can be divided into invasive and noninvasive techniques. They can be further subdivided into area measurements (*i.e.*, rCBF) or point measurements (*i.e.*, BFV).

2.2.1 Differences between rCBF and CBF

Typically, blood flow to and/or from a particular organ is reported in terms of the mass of tissue perfused by a given volume of blood per unit time. In the brain, this type of measurement is called the **regional cerebral blood flow (rCBF)** because it measures the blood flow supplying a particular region of the brain, for example, the cortex or the hypothalamus. It has dimensions of volumetric flow per unit mass, *i.e.*, ml/min/mg.

Flow through a particular vessel, regardless of the area that it serves, is called **cerebral blood flow (CBF)**. CBF is a volumetric flow and thus has typical dimensions of ml/min.

2.2.2 Relationship between BFV and CBF

Blood flow velocity (BFV) is the average instantaneous velocity of blood flowing through a given cross-sectional area of a vessel at a given time. BFV is *not* the same as CBF. They can be related through the continuity equation as:

$$CBF = BFV \times A$$

where A is the cross-sectional area of the lumen of the vessel of interest. It should be noted that A is rarely known in the cerebrovascular system. However, A seems to depend more on intracranial pressure (ICP) than CBF (which is *not* usually the case outside the cerebrovascular system), especially for the large cerebrovascular vessels, *i.e.*, the circle of Willis and its branches (see page 17) [1]. ICP is constant except after a cerebral vascular accident (CVA), for example, in head trauma resulting in subdural hematoma and increased fluid pressure on the brain. Therefore, if ICP does

not significantly change, then the cross-sectional area of a vessel will not change and, *in general*, an increase in BFV will result in a corresponding increase in CBF and *vice versa*, or

$$BFV \propto CBF.$$

2.2.3 Invasive measurements of rCBF

The most commonly used invasive technique to measure regional cerebral blood flow is the radioactive microsphere technique. This method involves sacrificing the subject to obtain a measurement thus it is strictly limited to use in research animals. Small latex spheres (or glucose molecules) are labeled with a radioactive tag (^{14}C -iodoantipyrine or 2-deoxyglucose) and injected into an extracranial vessel (usually the internal carotid artery). After a specified time, the animal is sacrificed and various parts of the brain are identified and removed. The amount of radiation detected in each sample can be related to the number of microspheres in the area which can in turn be correlated with rCBF for that area[9, 27]. As a consequence of having to sacrifice the animal, this method has the significant disadvantage that only one measurement can be obtained from each animal, thus, a large population is required. This technique is best suited for small animals (*i.e.*, rats and mice) which have relatively small brains and are inexpensive to obtain and house.

2.2.4 Invasive measurements of CBF at a point

To invasively measure CBF at a point involves surgically opening the skull, reflecting the brain tissue (if necessary) and using an electromagnetic flow meter, Doppler flow meter or similar device directly on the vessel of interest. This technique

is best suited for studying vessels on the surface of the brain, for example, the lateral middle cerebral arteries or the very small pial arteries.

An interesting use of TCD in dogs involves removing a piece of skull and placing a 8 MHz CW-Doppler probe directly on the dura to insonate the vessels of the circle of Willis, *etc.*, (see page 29). Although this approach may be effective, it can hardly be considered noninvasive and is certainly not transcranial.

2.2.5 Noninvasive measurements of rCBF

There are several noninvasive techniques for measuring regional cerebral blood flow. Such methods include: positron emission tomography (PET) scanning and magnetic resonance imaging (MRI). ^{133}Xe gas is typically introduced into the breathing stream (or dissolved and injected into the internal carotid artery) and, due to its high diffusion coefficient, it enters the brain where it may be detected by an array of sensors placed around the head. As in the microsphere technique described above, the amount of ^{133}Xe present can be correlated to the rCBF for that area [4, 14, 20]. These methods are expensive but have become routinely used in human medicine.

2.2.6 Noninvasive measurements of CBF at a point

Transcranial Doppler sonography is a new methodology which uses ultrasound to noninvasively measure blood flow velocity (BFV) at a point in a blood vessel within the brain. This method is described in detail in chapter 3.

Another interesting technique is called **quantitative angiography**. In this technique, a radio-opaque dye is injected into a vessel which makes the blood flow visible on a fluoroscope [4]. This information is fed into a computer and the volumetric

flow rate may be determined. This method is gaining in popularity in the human medical field.

2.3 Toxicology

To test the validity of TCD in this study, a chemical was chosen that had already been shown to alter CBF in lower mammals. Deltamethrin is a synthetic pyrethroid which had previously been shown to alter CBF in rats [7, 17]. It is widely used as an insecticide throughout the world and is commonly found in commercial and household products.

2.3.1 Measurement of toxicity

Deltamethrin is one of the most potent pyrethroids and is commonly used in agricultural and household insecticides. The relative toxicities of various substances are often compared by their LD₅₀ values¹. The LD₅₀ of deltamethrin in dogs is 3.440 mg/kg *i.v.*; in rats, it is 2-4 mg/kg; and in insects, it is 0.03 mg/kg (or 0.03 ng per insect) [7]. Threshold limit values² (TLVs), as well as permissible exposure limits³ (PELs), have not yet been established for deltamethrin.

¹LD₅₀ (lethal dosage 50%) is the dosage that if given to 100 animals, 50 of them will die [19].

²ACGIH annually publishes recommended Threshold Limit Values which are airborne concentrations of substances and conditions under which it is believed that nearly all workers may be repeatedly exposed day after day without adverse effect [26].

³OSHA is responsible for establishing legally enforceable Permissible Exposure Limits for industry in the United States.

2.3.2 Pyrethroids

The synthetic pyrethroids are a class of chemical insecticides that are highly toxic to a wide range of insects but are of relatively low toxicity to mammals. However, if absorbed in sufficient quantities, pyrethroids are also toxic to mammals [16]. In addition, pyrethroids degrade leaving no residues in the biosphere. Consequently, pyrethroids are commonly used to control a variety of agricultural and household pests. At present, the most commonly used pyrethroids are deltamethrin, fenvalerate and cypermethrin [13, 30]. These compounds are known to greatly affect CBF.

2.3.2.1 Clinical classification of pyrethroids Pyrethroids can be divided into two types based on the symptoms they produce [11]. *Type I* pyrethroids produce primarily tremor associated with increased sensitivity to external stimuli. *Type II* produce profuse salivation and choreoathetosis (withering convulsions). Some pyrethroids produce a mixture of the *Type I* and *Type II* syndromes [19]. At sublethal doses, the effects of pyrethroid intoxication are reversible, i.e., an animal can exhibit characteristic signs of pyrethroid poisoning and then fully recover [19].

2.3.2.2 Mechanism of action of pyrethroids All pyrethroids interact with sodium channels in excitable tissues [15, 31]. They do so by prolonging sodium current evoked by membrane depolarization [19, 25]. It has been suggested that the sodium channel is a likely site of action in mammals for pyrethroids that evoke both *Type I* and *Type II* behaviors [19]. One distinction between *Type I* and *Type II* pyrethroids is the duration of the prolonged sodium current. In insects and amphibians, *Type I* pyrethroids hold sodium channels open for relatively short periods

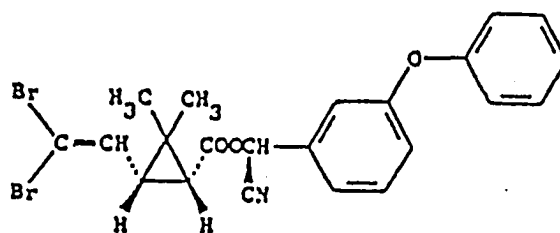


Figure 2.2: Structure of deltamethrin, 3-(2,2-dibromoethyl) 2,2-dimethyl cyclopropanecarboxylic acid cyano(3-phenoxyphenyl)-methyl ester

(msec), and *Type II* pyrethroids for longer periods (sec) [19]. Although this temporal difference between *Type I* and *Type II* compounds has been suggested to be the basis for the different behavioral effects observed in mammals, the magnitudes of these times are large compared to the times of normal synaptic events in the mammalian central nervous system. Deltamethrin is a *Type II* pyrethroid and thus holds sodium channels open for relatively long periods of time.

2.3.3 Deltamethrin

Since 1980, deltamethrin (see Figure 2.2) has been widely used throughout the world in the protection of crops, control of stored products and control of household insects [32]. It is, respectively, 100, 40 and 5–10 times as potent as DDT, parathion and other pyrethroids used in agriculture [6]. It is of interest to note that no clinical case of acute pyrethroid poisoning had been reported in the literature until outbreaks of acute deltamethrin and fenvalerate poisoning occurred in Chinese farm workers where application of pyrethroid insecticides was first started in 1982. Between 1982 and 1988, there were 573 cases of acute pyrethroid poisoning (including 229 occupational and 344 accidental poisonings) reported in the Chinese medical literature

alone [32].

Although there have been several studies on the effects of pyrethroids on the mammalian central nervous system, there has been only one study on the effects of pyrethroids on the cardiovascular system [10] and one on the effects of pyrethroids on the cerebrovascular system [7].

The change in CBF in the presence of deltamethrin or any other pyrethroid is as yet undetermined in the dog or any other higher mammal. However, some information about changes in regional cerebral blood flow (rCBF) is currently available. When dissolved in glycerol-formal and given intravenously, the LD₅₀ of deltamethrin was as low as $3.44 \pm 0.67 \text{ mg/kg}$ in anaesthetized dogs ($2-4 \text{ mg/kg i.v.}$ in rats) [6]. When administered intravenously, the toxicity of deltamethrin does not vary from one animal species to another [19]. In the rat, when deltamethrin (2 mg/kg i.v.) is administered, rCBF (as measured by ¹⁴C technique) in 14 areas of the brain studied increased between 150–300% [9]. A typical sequence of behavioral changes is as follows:

1. the onset of chewing at 1 minute,
2. salivation at 2 minutes,
... *significant increases in rCBF observed at this time.*
3. body twitches at 4 minutes.
4. head and forepaw movements at 6 minutes.

Other than in the cerebellum, a significant increase in rCBF was of early onset, occurring in rats showing salivation and chewing as the only symptoms after being

given deltamethrin. Low-level exposure to pyrethroids produces reversible symptoms in higher mammals. At higher exposure levels, the pyrethroid may cause permanent damage or perhaps even death. Alterations in rCBF have been associated with behavioral changes in pyrethroid exposures in the rat. It is not known, however, whether these rCBF alterations precede behavioral changes. Given that blood flow to the brain is so closely regulated, any change in CBF may be seen as an early indication of possible deltamethrin exposure. The mechanism for this change is a subject which merits further investigation.

2.4 Cerebral Vascular Anatomy

The anatomy and blood flow in the cerebral vascular system is quite complex and therefore will be discussed briefly. The application of TCD to the dog is complicated by the slight anatomical differences between the human and canine cerebral vascular systems. However, since this study was limited to the MCA, these differences were not pertinent and thus will not be discussed here. Commonly used anatomical abbreviations are summarized in Table 2.2.

2.4.1 Extracranial anatomy

The blood supply to the head and neck originates from the great vessels of the aortic arch in the superior mediastinum. After asymmetric origins, the arterial supply to/within the brain is generally symmetric. The aortic arch gives rise to three major trunk vessels: the brachiocephalic trunk (innominate artery), the left subclavian artery and the left common carotid artery. The brachiocephalic trunk is the first branch from the distal ascending aorta and divides to form the right subclavian

artery and the right common carotid artery. After asymmetric origins, the common carotid arteries ascend the anterolateral aspect of the neck in parallel and divide to form the internal and external carotid arteries in the mid-cervical portion of the neck. The subclavian arteries (providing blood supply to the arms) arise asymmetrically. The first major branch forms the vertebral artery. The vertebral arteries ascend the neck in parallel and enter the skull through the foramen magnum (see Figure 2.3).

2.4.2 Intracranial anatomy

The internal carotid arteries (ICA) are two of the four major arteries supplying the brain. They provide most of the flow to the frontal, temporal and parietal lobes. The ICAs pierce the dura mater anterior to the clinoid process, and each divides into two terminal branches: the anterior cerebral artery (ACA) and the middle cerebral artery⁴ (MCA). The circle of Willis is a vascular ring at the base of the brain which connects the two ICA systems with each other as well as with the posterior vertebral-basilar system.

2.4.2.1 Circle of Willis The circle of Willis provides the *most* important source of collateral circulation to the brain. It can be divided into an anterior portion and a posterior portion (see Figures 2.4 and 2.5). The anterior portion is composed of two internal carotid arteries, horizontal segments of both anterior cerebral arteries and the anterior communicating artery. The posterior portion is composed of the proximal segments of both posterior cerebral arteries and the two posterior communicating arteries (which arise from the ICA). The anterior communicating artery

⁴The middle cerebral artery was the principal artery of interest in this study.

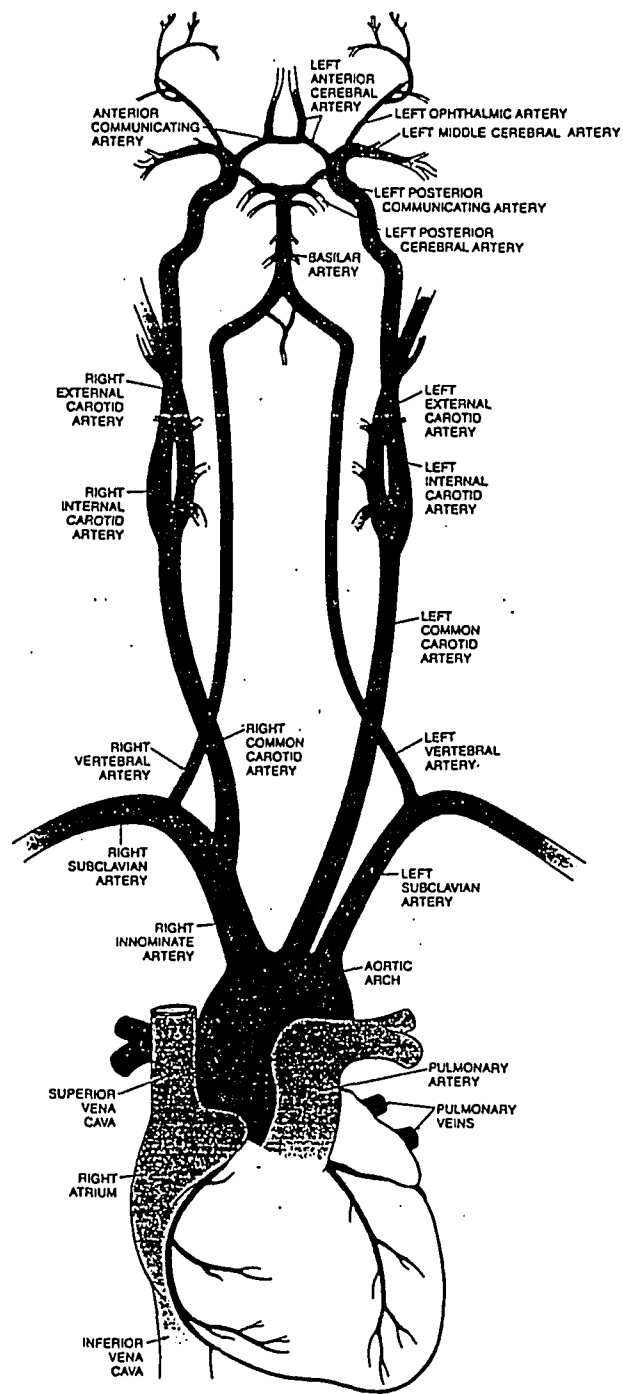


Figure 2.3: Extracranial vessels in the human showing the primary path of blood from the heart to the circle of Willis

Table 2.2: Summary of commonly used anatomical abbreviations

Abbreviation	Artery name
ACA	Anterior Cerebral Artery
ACoA	Anterior Communicating Artery
BA	Basilar Artery
ICA	Internal Cerebral Artery
MCA	Middle Cerebral Artery
PCA	Posterior Cerebral Artery
VA	Vertebral Artery

(ACoA) completes the anterior portion of the circle of Willis by joining the ACAs. It is interesting to note that only 18–20% of the general population have this balanced circle of Willis configuration.

2.4.2.2 Middle cerebral artery The middle cerebral artery (MCA) supplies a very extensive area, including most of the lateral surfaces of the cerebral hemispheres. The MCA is the larger of the two terminal branches of the ICA (recall the other is the ACA). The M-1 segment extends laterally and horizontally in the lateral cerebral fissure to the Sylvian fissure. The MCA turns upward around the island of Reil, branching and coursing posterosuperiorly within the depths of the Sylvian fissure. Although branching patterns are highly variable, anomalies are uncommon.

2.4.2.3 Additional arteries Although the MCA was the primary focus of this study, there are several other large arteries associated with the circle of Willis that, for the sake of completeness, will be briefly discussed.

The vertebral arteries (VA) are paired arteries that enter the skull through the

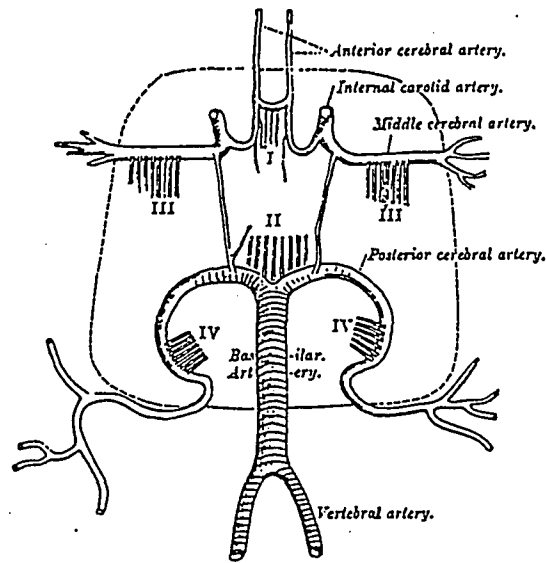


Figure 2.4: Human circle of Willis and surrounding vessels [12]

foramen magnum and proceed anteriorly to the upper medulla where they join to form the basilar artery (BA) at the junction of the medulla and the pons. The BA courses superiorly along the ventral surface of the pons and terminates at the interpeduncular cistern by dividing into the posterior cerebral arteries (PCA). The PCAs supply the temporal, parietal and occipital lobes as well as the thalamus, midbrain and other deep structures.

2.4.2.4 Models Due to the complicated nature of the geometry of the vessels involved in this project, two models were fabricated from greyhound dogs of comparable size to those used in this study to help visualize the anatomical relation-

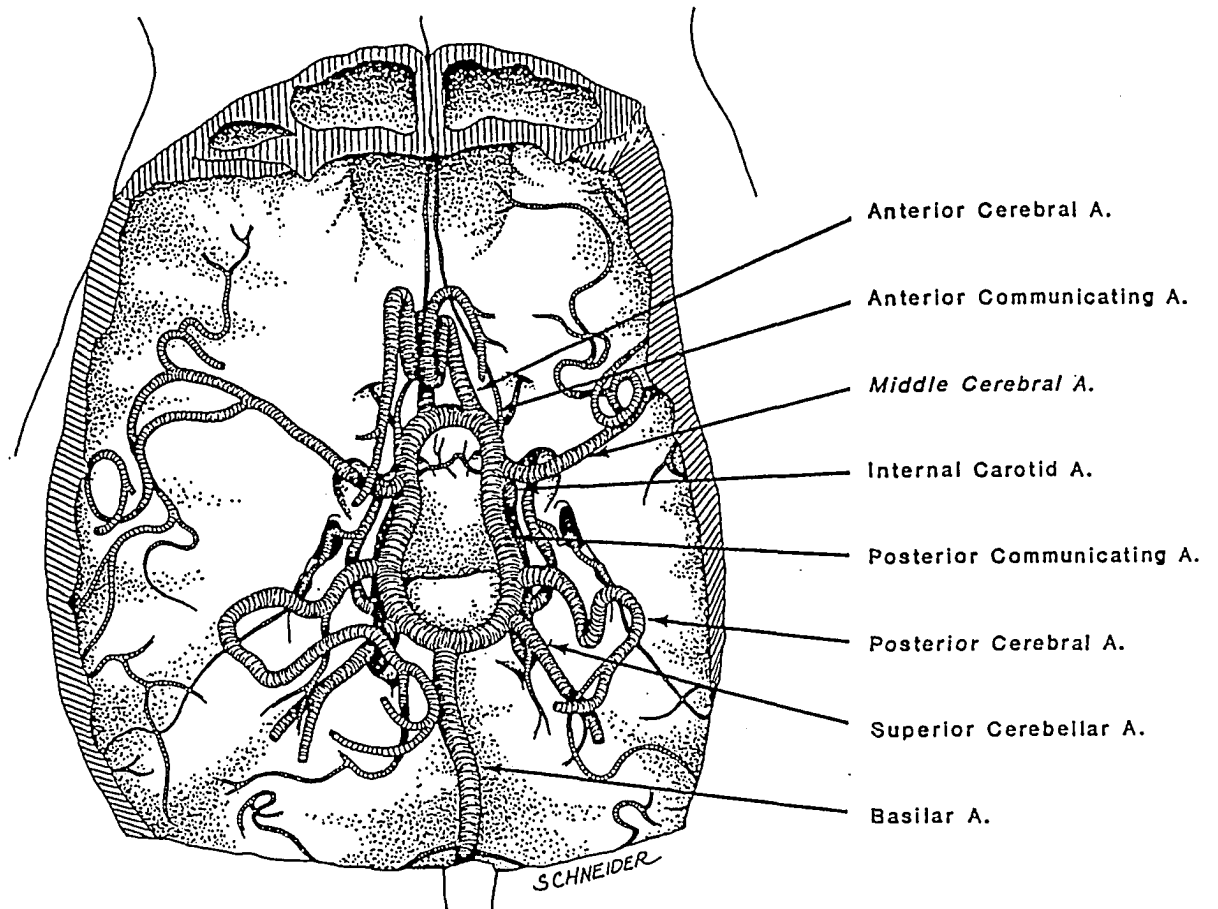


Figure 2.5: Canine circle of Willis and surrounding vessels (dorsal view) [2]

ships of vessels and to help find the optimum probe placement⁵. Although a small amount of shrinkage is expected while making these models, the shrinkage will be proportional in all dimensions to reflect the *in vivo* situation as closely as possible.

Plasticization model: This model is an entire head with the left side completely intact, but the right side has the skull and soft tissues removed revealing the cerebral vessels on the surface of the brain (see Figure 2.6).

Corrosion-cast model: This model shows only the skull and blood vessels. all other soft tissues are removed. The arterial system is shown in red and the venous system is shown in blue (see Figure 2.7).

⁵Model fabrication was done locally by an experienced veterinary anatomy technician.

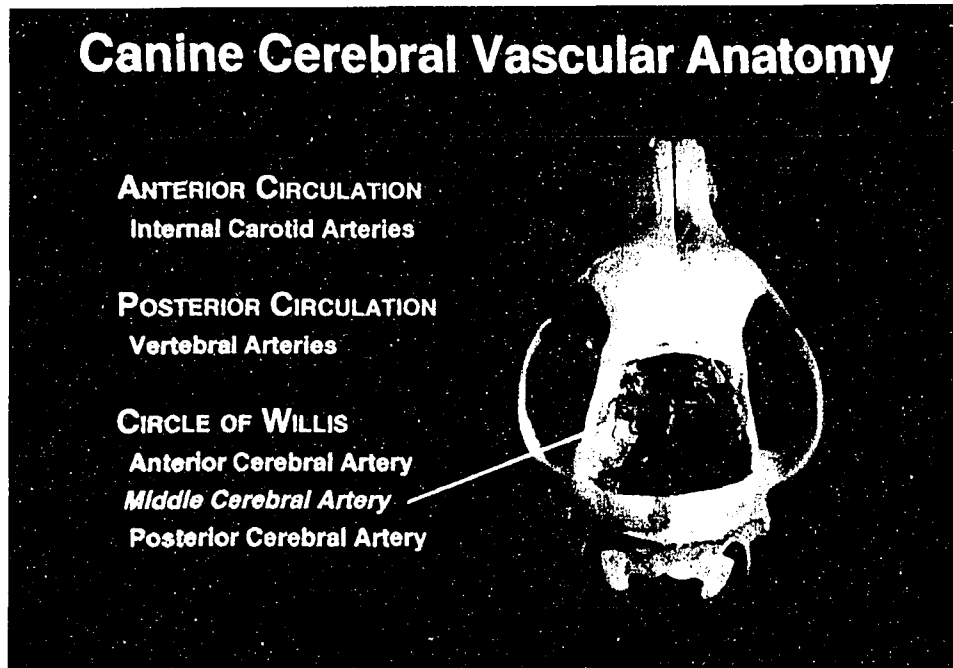


Figure 2.6: Photograph showing corrosion-cast model of greyhound cerebrovascular system. All soft tissue is removed in this model leaving only bone, arteries (red) and veins (blue) intact

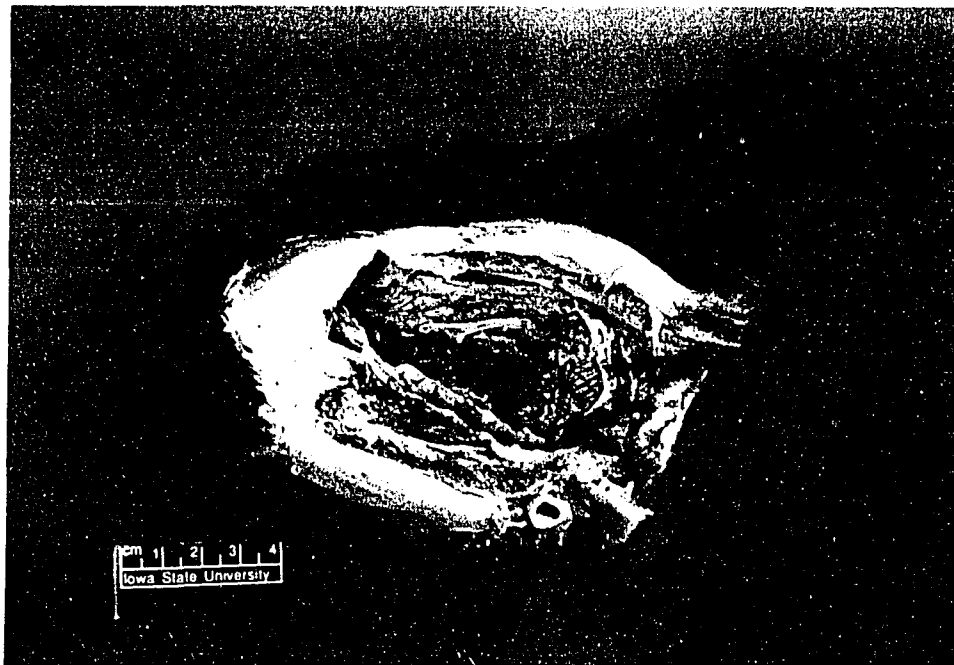


Figure 2.7: Photograph showing plasticization model of greyhound head showing layers of bone and soft tissue in cross-section to the circle of Willis

3. TRANSCRANIAL DOPPLER SONOGRAPHY

Transcranial Doppler sonography (TCD) provides a method by which ultrasound is used to obtain a real-time blood velocity waveform noninvasively from one of the larger vessels within the brain. Traditionally, ultrasound does an excellent job of penetrating the soft tissues (as evidenced by its use in obstetrics, gynecology, and cardiology); however, it does not penetrate hard tissue (*i.e.*, bone) nearly as easily. Since the brain, and therefore the blood supply to and from the brain, is nearly totally encompassed by the skull, ultrasound techniques could not, until recently, image brain tissue or measure blood flowing within the brain.

3.1 Transmission of Ultrasound through Bone

The problem of the acoustic properties of the skull were studied by White and co-workers in 1978 [36]. The skull consists of three layers of bone which influence ultrasound in different manners. The middle layer (diploe) has the most important effect on the attenuation and scattering of the ultrasound, especially when the bony spicules have a diameter comparable to the wave length of the ultrasound. However, these spicules are absent in the temporal region where the skull is the thinnest [1]. In addition, the skull has the effect of an acoustic lens, *i.e.*, bone tends to shorten the focal length of the ultrasound beam which may decrease sensitivity to blood flow

in deeper vessels (*i.e.*, 5–10 cm) [36].

3.2 Theory of Ultrasound Operation

In the simplest sense, a beam of ultrasound energy (the frequency of which can vary depending upon the probe selected) is emitted from a probe at the surface of the skin, penetrates the skull and tissues and is reflected by moving blood cells back to the probe. Typically, a 2 MHz pulsed-wave (PW) probe is used to insonate vessels within the cranium. The 4 and 8 MHz continuous-wave (CW) probes may be used to insonate deep and superficial peripheral vessels, respectively, *i.e.*, the common carotid (neck) and radial (forearm) arteries. The moving blood cells cause a shift in the frequency of the sound waves received by the detector in the probe. This shift in frequency is proportional to the velocity of the blood flowing through the vessel on which the beam is focussed [1]. This Doppler shift is given by the equation

$$\Delta f = \frac{2f_0 v \cos \theta}{c}$$

where Δf is the shifted frequency at the detector, f_0 is the emitted frequency at the source, v is the velocity of the moving blood cell, θ is the angle between the probe and the velocity vector and c is the velocity of sound in tissue (usually taken to be approximately 1540 *m/s*).

Figure 3.1 shows a typical velocity waveform from the middle cerebral artery in a *human* obtained during pilot work with the Medasonics Transpect TCD system. It is evident from the figure that the Doppler shift for blood flowing in arteries is not a pure frequency such as that from a single moving reflector. The signal received is a mixture of different frequency components coming from reflectors (*i.e.*, blood cells

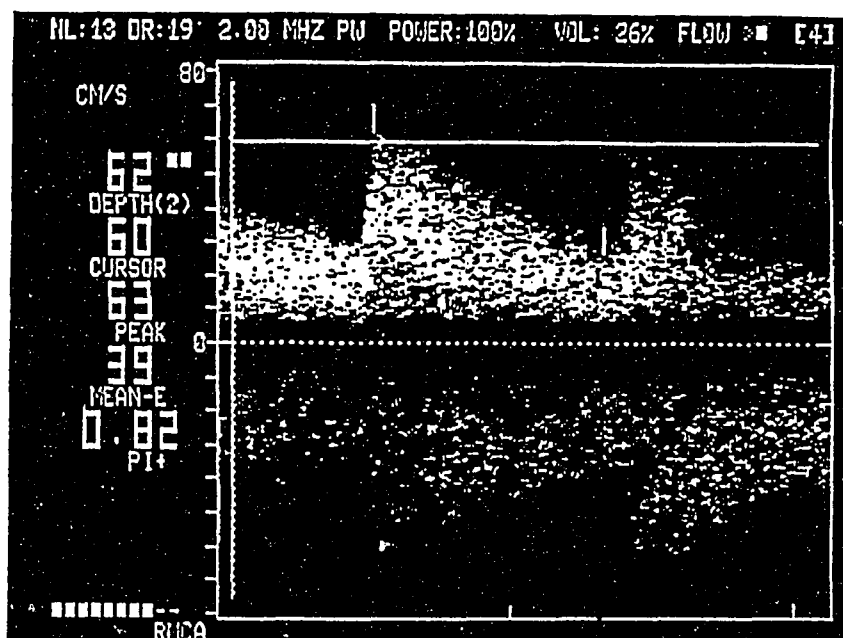


Figure 3.1: Typical velocity waveform from the human middle cerebral artery obtained during pilot work with the Medasonics Transpect TCD system

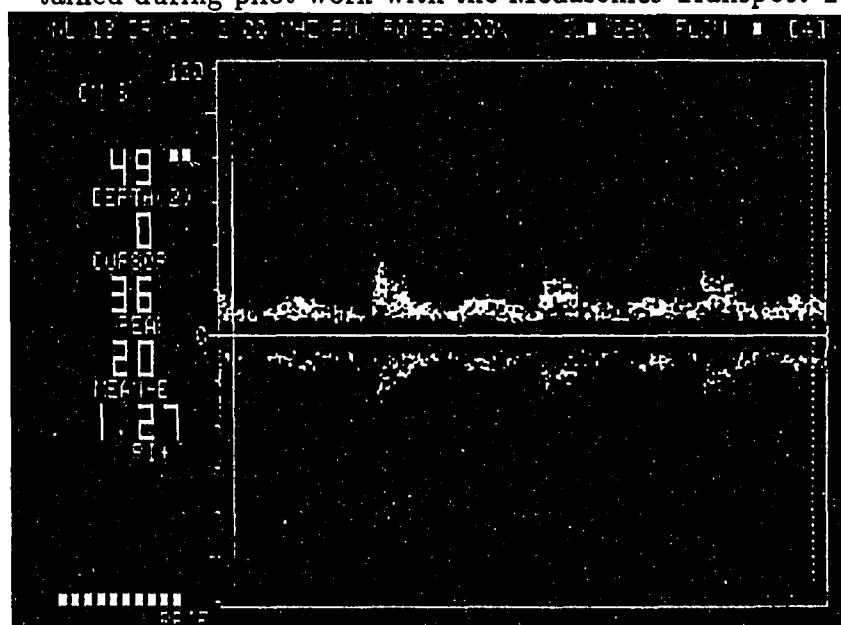


Figure 3.2: Typical velocity waveform from the *canine* middle cerebral artery (MCA) obtained during pilot work with the Medasonics Transpect TCD system

moving at different velocities. The spectral broadening effect is even more prominent in the transcranial approach than in cervical, peripheral or cardiac Doppler because the sample volume size is relatively larger compared to the dimensions of the arteries. Thus, not only is the entire cross-section of the lumen insonated, but branches, different segments of curves and nearby vessels all contribute to the Doppler signal received.

3.2.1 Pulsed vs. continuous wave Doppler

There are essentially two forms of Doppler ultrasound. They are known as *pulsed wave* (PW) Doppler and *continuous wave* (CW) Doppler.

3.2.1.1 Pulsed wave Doppler As mentioned above, TCD uses *pulsed wave* (PW) Doppler to measure blood flow velocity in the brain. In PW-Doppler, a single crystal is used as the source and the receiver. Bursts of ultrasonic energy are transmitted at regular intervals with a burst- or *pulse-repetition frequency* (PFR). These bursts travel (at velocity c) toward the reflector which is separated from the transmitter by a distance L . Some energy is reflected and travels back at the same propagation velocity. Thus, at a time $t = \frac{2L}{c}$ after the emission of the burst, the reflected echoes come back to the transducer. The echoes are transformed into electrical signals and amplified. The principle of range-gating is in practice realized by an electronic gate which opens and samples the signal for only a short period around the time t . Signals arriving from reflectors at different times and their effects are therefore eliminated from the sampled signal.

In PW-Doppler, PFR decreases as depth increases and vice versa ($PFR \propto$

$\frac{1}{\text{depth}}$). It has excellent range resolution by employing the idea of a *sample volume*. A sample volume is the volume in space from which the TCD signals are being obtained. As mentioned earlier, the sample volume is typically much larger than the diameter of the artery and thus encompasses not only the entire cross-section of the lumen insonated, but branches, different segments of curves and nearby vessels as well. The principal disadvantage of PW-Doppler is aliasing (Nyquist limit = $\frac{1}{2}PFR$ and PFR is limited by depth).

3.2.1.2 Continuous wave Doppler In contrast to PW-Doppler, *continuous wave* (CW) Doppler uses two crystals, one for the source and the other for the receiver. The source crystal emits a continuous sound wave which penetrates the tissues and is reflected back (same as the PW-Doppler case) to the receiver. In this fashion, information is obtained from the entire tissue *slice* in the line-of-sight of the transducer at all depths rather than from a particular depth as in PW-Doppler. The principal disadvantage of CW-Doppler is that it lacks range resolution but it does have an unlimited frequency response.

3.3 Accuracy of TCD Measurements

In recent studies, it has been shown that TCD does not provide an accurate measure of absolute BFV but can reliably detect relative changes in BFV [35]. The magnitude of these changes (as observed in humans) may be on the order of a few percent to several orders of magnitude. For example, in the middle cerebral artery (MCA), the BFV typically doubles during hyperventilation compared to at rest [34]. In the presence of a unilateral stenosis in an internal carotid artery, BFV in the MCA

may decrease 10% for a moderate stenosis (75–89% occlusion) to 25% or greater for a severe stenosis (90–99% occlusion) [24].

3.4 Probe Location

The first step in a transcranial Doppler examination is to localize a cranial window that the ultrasound can penetrate without being excessively damped. There are three commonly used approaches in human medicine. They are:

- **Transtemporal approach** to the basal cerebral arteries including the circle of Willis (see page 17).
- **Transorbital approach** through the orbit of the eye to the carotid siphon.
- **Transoccipital approach** through the foramen magnum near the base of the skull to the basilar artery and the intracranial segments of the vertebral arteries (see page 17).

Perhaps the most commonly used point of insonation is the transtemporal approach where the probe is positioned over the temporal bone. From this position, several vessels including the MCA, ICA and ACA can be well insonated (see Figures 2.4 and 2.5).

Using these three windows into the brain, any major cerebral vessel can be studied. Figure 3.2 shows a typical waveform from the middle cerebral artery via a *transtemporal* approach on a 72 lb. greyhound dog. Flow above the zero line indicates flow toward the probe while flow below the zero line indicates flow away from the probe. Note that the display indicates that the sample volume is at a depth of 6.2

cm. It is important to note that these are *TCD centimeters* and while this depth will likely be approximately equal to the actual depth, due to slight differences in c through the various tissue layers, it will not be exactly the same. The row of (white) back-lit boxes in the lower left corner of the display is the window-finder feature; the more boxes that are present, the more signal is getting through the bone.¹

3.5 Artery Identification

Once an adequate window is found and a blood flow velocity waveform is obtained, the location of the signal (*i.e.*, which vessel(s) is it coming from) must be determined. There are three main sources of information for artery identification. They are:

1. The spatial relation of the signal to other intracranial signals including both the depth of the sample volume and the angle of the probe.
2. The direction of flow (toward or away from the transducer) and the spectral distribution.
3. The response of the signal to (common carotid) compression or vibration maneuvers.

These three pieces of information must be used in conjunction with one another to accurately determine the location of the signal (see section 4.4.4). One cannot positively identify the location of a TCD signal from simply looking at the picture.

¹The window-finder feature was not available on the EME TC2-64 used in this study.

3.6 TCD in the Canine

After its development by Aaslid in Germany, TCD has been commercially available in U.S. since 1986. The vast majority of TCD research has been in the human clinical areas of neurology, neurosurgery and anesthesiology. Despite its obvious applications in a variety of research areas (both animal and human), TCD has had extremely limited use in animal research. TCD has been successfully used in pigs to measure the effectiveness of cardiopulmonary resuscitation (CPR) in maintaining adequate cerebral blood flow. Rabbits and cats have been used by a handful of TCD researchers with limited success. To date, the only study using TCD in dogs was reported by Werner in 1990 [35]. In this study, a portion of the skull was surgically removed and an 8 MHz ultrasound probe was placed directly on the dura mater to insonate various cerebral vessels. An extensive review of the literature revealed no published studies that employed TCD in toxicology or neurotoxicology.

Although the pilot work demonstrated that CBF measures can be obtained from the dog (see page 33), there were some problems which had to be resolved before this new technology could be routinely applied in animal research.

First, in human clinical applications, TCD is used to monitor CBF during procedures such as open-heart surgery and carotid endarterectomy where the probe placement is constant, or it may be used periodically over weeks or longer to follow the progress of a disease such as atherosclerosis. In these circumstances, only changes in the shape of the velocity waveform are of interest. In this study, repeated CBF measurements were made on different days, thus it was important to insure that measurements were consistently taken from the same area of a particular vessel. Therefore, probe placement was of primary importance. For human clinical applica-

tions, the probe is most often manipulated freely by hand to locate a target vessel, or the probe may be attached to a simple helmet to hold it in place. In the deltamethrin study, it was essential that probe placement be precise in 3-dimensional space.

Another concern is that of probe stability. The area where the beam is focused within the cranium (called the *sample volume*) is quite small with respect to the volume of the brain (on the order of several mm^3). Therefore, the anatomical location of the probe and the three-dimensional angle of incidence of the beam to the skull greatly affect the location of the sample volume. Thus, when using TCD, it is important to maintain a steady probe position to minimize noise and obtain accurate waveforms.

3.7 Summary of TCD

To use TCD effectively, the user must have a good understanding of cerebral vascular anatomy (human and dog) and the relative position of vessels with respect to one another to properly locate and identify TCD waveforms. However, for the purposes of this project, only the blood flow changes in the middle cerebral artery (MCA) were of interest. The MCA was chosen because it is a relatively large artery which supplies much of the lateral surface of the cerebrum [2]. In addition, it is usually easy to locate and obtain adequate signal quality using the TCD.

4. MATERIALS AND METHODS

This project was completed in four phases. The description of each phase below essentially outlines the chronological sequence of events of the project.

- **Phase I:** The goal of phase I was to answer the following initial questions:
 1. Could TCD be used to obtain blood flow velocity signals from various cerebral vessels within the brains of dogs?
 2. Was the signal-to-noise ratio of the blood flow velocity waveform large enough to provide adequate signal strength and integrity?
 3. Was TCD sensitive enough (in the dog) to detect changes in cerebral blood flow caused by breathing an increased concentration of CO_2 ?
 4. Which commercially available TCD instrument was best suited for use in this study?
- **Phase II:** The goal of phase II was to carry out a dose-response pilot study to determine the appropriate deltamethrin dosages (low and high) to be used.
- **Phase III:** The goal of phase III was to determine whether the system could detect changes in CBF in an *unconscious* (anaesthetized) dog.

- **Phase IV:** The goal of phase IV was to determine whether the system could detect changes in cerebral blood flow in a *conscious* (unanesthetized) dog. If so, any potential interaction between deltamethrin and the anaesthetic used in phase III could be eliminated.

Each phase had its own problems to be overcome and questions to be resolved before the project could progress to the next phase.

4.1 Experimental Design

It has been well established that pyrethroids have a pronounced effect on rCBF in rats and other lower mammals (see section 2.3.3). As discussed earlier, deltamethrin increased rCBF in 14 areas of the brain studied in rats by the microsphere technique (see section 2.3.3). Based on these findings, the null hypothesis of this study was: *Deltamethrin at 5 and 10% of the LD₅₀ administered intravenously will not alter the blood flow velocity in the middle cerebral artery of the dog.*

4.1.1 Justification of animal use

As is the case with most experiments in toxicology, it is not appropriate to purposely expose human subjects to potentially harmful toxic substances; therefore, an animal model was used to study the effects of toxicants on CBF. The greyhound dog was chosen as the animal model for this study for the following reasons:

- While there are some differences, the anatomy of the canine cerebral circulation is similar to that of humans,

- Dogs possess a large enough circle of Willis (see page 17) (compared with rats, for example) to allow TCD to distinguish signals from the various vessels within the cranium,
- The amount of extracranial muscle and soft tissue (*i.e.*, the distance between the skull and skin surface) is relatively small compared to other breeds and is the most similar to the human for the transtemporal approach,
- The greyhound has a relatively thin skull (1.4 mm thick¹) compared to the human (1.2–2.5 mm thick [1]) and therefore it should produce less attenuation of the transmitted and reflected signals [36],
- The greyhound is a domesticated subject and easy to work with,
- The greyhound racing industry is economically important in this state and dogs are readily available.

Unfortunately, greyhounds were more difficult to obtain than had originally been anticipated; therefore, it was necessary to use three large mongrel dogs in addition to the nine greyhounds to complete Phase III of this study.

4.2 Phase I - Evaluation of TCD Equipment

During Phase I of the project, several TCD instruments were brought into the laboratory for on-site evaluation and testing. The most promising instruments were the Transpect TCD from Medasonics (Mountainview, CA) and the TC2-64B from

¹Skull thickness measured in our laboratory of the temporal bone on a skull of a greyhound dog of comparable weight to those used in this study, at a point close to that used in the transtemporal approach.

Eden Medical Electronics (Kent, WA). In addition, the GenesisII from Biosound (Indianapolis, IN) was tried on a dog but was unsatisfactory due to a lack of signal strength. Further, the 500V from Multigon (Mt. Vernon, NY) was considered and rejected because of excessive cost. Since TCD is a relatively new technique and has not been used in dogs, both Medasonics and EME were willing to make their instruments available for a one month evaluation period. In both cases, 2 MHz probes were used to insonate the middle cerebral artery as well as several distinct bifurcations around the circle of Willis (transtemporal approach). CO_2 was introduced into the respired air and a distinct increase in CBF was detected. Both systems provide similar features with the following exception: the Transpect TCD has a window finder that indicates how much of the ultrasound signal is actually getting through the bone. Since no database of TCD usage in dogs existed at the time of the study, this feature was initially believed to be particularly useful in locating target arteries. Although exploratory work with transcranial Doppler sonography in dogs had just begun, this researcher was confident that CBF changes could be measured from several locations in the cerebral circulatory system and that responses to manipulations of CBF could be detected using TCD.

With substantial practice, it was determined that TCD could be adequately used in dogs and that changes in CBF caused by manipulation of CO_2 could be observed (data to support this observation was not recorded because there was no computer interface nor video printer available during Phase I). It was decided that because the EME TC2-64 supplied an (undocumented) analog voltage on a pin in the rear of the unit which corresponded to the mean envelope velocity of the BFV waveform (see page 47), the TC2-64 would be used rather than the Medasonics Transpect TCD

which did not provide this feature (or any other convenient way to store continuous BFV waveform data on a PC).

4.3 Phase II - Dose-Response Pilot Study

According to the National Institute for Occupational Safety and Health (NIOSH) Registry for Toxic Effects of Chemical Substances (RTECS) January, 1991 edition, the intravenous LD₅₀ for deltamethrin in dogs is $3.44 \pm 0.67 \text{ mg/kg}$. RTECS cites Chanh [6] as the source for this data. The protocol used by Chanh was as follows:

The dogs employed were mongrels of both sexes weighing 10-15 kg, anaesthetized with pentobarbital (Nembutal, 25 mg/kg *i.v.*). Deltamethrin was dissolved in glycerol formal (50 mg/ml) and less than 1 ml injected intravenously via the saphenous vein, or suspended in gum-arabic solution and administered by means of a duodenal cannula. In both cases, deltamethrin was given in a single dose and the treated animals were kept under observation for 5 hours after administration of the drug. The LD₅₀ values were calculated by the probit method. (page 127).

Using this as a starting point, various levels of exposure (each less than 10% of the LD₅₀) were tested.

As discussed earlier, based on previous experiments using rats, it was expected that deltamethrin would increase C'BF (see page 13). In general, barbiturates, (i.e., pentobarbital) are potent cerebral vasoconstrictors which elicit characteristic dose-related and potentially large decreases in C'BF (see page 5). However, it is very difficult to maintain a constant level of anaesthesia using an injectable anaesthetic such as pentobarbital. Therefore, halothane (a gas anaesthetic) was used to maintain a more constant level of anaesthesia. As discussed previously (see page 5), halothane

Table 4.1: Amount of deltamethrin administered to each dog for each exposure (N/A denotes where an animal has been removed from the study)

Dog Number	Mass of Dog (kg)	Mass of Deltamethrin (mg)	
		5% LD ₅₀	10% LD ₅₀
1	26.0	4.5	8.9
2	30.0	5.2	10.3
3	32.0	5.5	11.1
4	23.0	4.0	7.9
5	29.5	5.1	N/A
6	33.0	5.7	11.4
7	32.0	5.5	11.1
8	33.0	5.6	11.4
9	31.0	5.3	10.7
10	38.0	6.5	13.1
11	29.0	4.9	N/A
12	27.5	4.7	9.5

acts to increase cerebral blood flow (\uparrow CBF). Thus, both deltamethrin and halothane confound interpretations of data because both substances act to increase CBF.

Each animal was exposed to two levels of deltamethrin 48 hours apart. A low level (5% of the LD₅₀) and a high level (10% of the LD₅₀) of deltamethrin were used. Technical grade (\geq 98% purity) deltamethrin (Hoechst Chemical Co., Saskatchewan, Canada) was dissolved into glycerol-formal (Sigma Chemical Co., St. Louis, MO, #G1513) in concentrations of 5, 10, and 15 mg/ml. The volume of solution for each injection was held constant at 1 ml. Based on the weight of the animal, the amount of deltamethrin was calculated, withdrawn from the appropriate mixture into a 1-ml tuberculin syringe and diluted with pure glycerol-formal to make exactly 1 ml.

4.4 Phase III - Deltamethrin Exposure in the Unconscious Dog

These experiments were performed after approval of the Institutional Animal Use Committee. Deltamethrin was administered to 12 dogs weighing $30.3 \pm 3.8kg$ (9 greyhounds and 3 mongrels) of both sexes. It was given at two relatively low dosage levels, approximately 48 hours apart (see Table 4.3). Five physiological parameters were recorded during the control, glycerol-formal (no deltamethrin) and exposure (deltamethrin in glycerol-formal) periods. These parameters were mean blood flow velocity (MBFV) in the middle cerebral artery, mean arterial blood pressure (MAP) in the aorta, end tidal CO_2 , mean heart rate (MHR) and concentration of deltamethrin in the blood.

4.4.1 Blood pressure measurement

Approximately two to three days prior the first deltamethrin exposure, each dog had arterial and venous cannulas surgically implanted to facilitate direct arterial blood pressure measurements and to provide a consistent method for administering the deltamethrin and obtaining blood samples [29]. A cannula was inserted into the carotid artery contralateral to the side where TCD measurements were to be recorded. This minimized flow disturbances introduced by the presence of the cannula.² The arterial cannula tip was located in the aorta (or sometimes in the carotid) to record arterial pressure, and the venous cannula tip was located in the jugular vein (verification of tip placement was done *post mortem*).

²The cannula in the contralateral carotid artery should not alter CBF to any significant degree ipsilateral to the TCD probe due to the tremendous collateral circulation in the dog.

The construction and implantation of the cannulas are briefly described in the following two sections and described in greater detail in Appendices A and B.

4.4.2 Cannula preparation

Arterial and venous cannulas were obtained from Braintree Scientific, Inc., (Braintree, MA, model numbers RPC-080-18 and MRP- 080-18, respectively). Prior to implantation, the distal end of each cannula had a 2-way stopcock cemented to the hub end and a Dacron patch was sutured around the cannulas and secured in place using Silastic cement. This patch was to allow for secure attachment to the skin. A short piece of silastic tubing (0.889mm I.D., 0.254mm wall thickness) was soaked in xylene for approximately one minute to expand the silastic and then placed over the proximal tip of the venous catheter. The xylene evaporates in a few minutes and leaves a tight (shrink) fit of the silastic on the cannula. This flexible tip on the venous cannula decreased the possibility of a blood clot forming in the lumen of the cannula and of the cannula tip causing damage to the intimal tissues. The silastic tip was not placed over the arterial cannula because it would impede high fidelity blood pressure recordings. After sufficient curing (several days), each cannula was washed in a dilute Ivory soap flake solution to remove oils and other debris from the cannula, rinsed several times in sterile water and dried. Finally, the luminal surface of each catheter was coated with a highly concentrated heparin solution (Braintree Scientific, TDMAC-Heparin) to form a non-thrombogenic plastic surface. The cannulas were individually packaged and gas-sterilized using ethylene oxide (see Appendix A).

4.4.3 Cannula implantation

Under general anaesthesia (halothane) and sterile conditions, a five to seven centimeter midline incision was made on the ventral aspect of the neck. Another incision, approximately three to five centimeters in length, was made on the dorsal aspect of the neck just cranial to the level of the scapula. A stainless steel tube was inserted into the dorsal incision and run subcutaneously, exiting through the ventral incision. The distal ends of the cannulas were passed through the lumen of the tube from the dorsal to the ventral incision. The tube was removed leaving the cannulas in place. The skin of the dorsal incision was sutured to the Dacron patches and the incision was closed leaving the stopcocks exposed. The arterial cannula was inserted into the right carotid artery with the tip positioned at approximately the level of the aorta (verification of tip placement was done *post mortem*). The venous cannula was inserted into the right jugular vein. Both cannulas were secured to the vessel wall using a purse-string suture in such a fashion as to leave the vessel patent. Finally, the cannulas were secured to the surrounding muscle and connective tissue and the incision was closed. The cannulas were flushed daily with heparinized saline (see Appendix B).

4.4.4 Experimental procedure

The experimental procedure is outlined as follows: Each dog was anaesthetized using a mixture of Ketamine and Diazepam (equal volumes at 1 ml per 20 pounds), intubated, given halothane (approximately 1.5% as needed) and placed on a heated table in left lateral recumbency. A CO₂ analyzer (Datex Instrumentation Corp., Finland) was calibrated and attached to the endotracheal tube to monitor end-tidal CO₂.

A Statham P23Db pressure transducer was filled with saline (ensuring no air bubbles were present) and attached to the arterial cannula stopcock. The pressure transducer was attached to a Grass Model 7 Polygraph (Grass Instruments, Inc., Quincy, MA) that was in turn attached to a data acquisition system (Dataq Instruments, Inc., Model DI-420) connected to a Zenith 286 personal computer.

A 2MHz pulsed-wave transcranial Doppler (TCD) probe (Eden Medical Electronics, Santa Clara, CA, Model TC2-64) was used in a transtemporal approach to insonate a portion of the left middle cerebral artery (see Figure 4.1). Verification of the MCA signal was accomplished by using signals from other cerebral vessels as relative landmarks in addition to observing the direction and magnitude of blood flow, depth of the sample volume and overall shape of the blood flow velocity waveform. The TCD was used to locate and identify signals from a point on the middle cerebral artery (MCA) via transtemporal approach just downstream of the bifurcation with the circle of Willis. The MCA supplies most of the lateral surface of the cerebrum. This point was chosen because of its ease of location with the TCD and its close proximity to the MCA/ICA bifurcation which has a characteristic *butterfly* waveform. The BFV waveform spectrum from the TCD was stored on video tape while the maximum frequency follower (envelope velocity) signal was stored in the PC.

An Amiga 1000 personal computer and A1300 genlock (Commodore Business Machines, Westchester, PA) were used to superimpose text information on the video tape to identify different experimental conditions for post-experimental viewing. Finally, a video printer (Sony, Model UP-850) was attached to the TCD to allow periodic hardcopy recordings of the TCD signal.

After all the equipment was in place and functioning properly, thirty minutes of control recording were obtained. Next, 1 ml of pure glycerol-formal was injected into the venous cannula and another 30 minutes of data was recorded. Finally, either the low- or high-level dosage of deltamethrin (according to the randomization schedule in Table 4.2), dissolved in glycerol-formal, was injected into the venous cannula and an additional 30 minutes of data was collected. Arterial blood pressure and MCA blood flow velocity were recorded continuously for the entire 90 minute period (sampling frequency of 50 Hz per channel). End tidal CO_2 was recorded once every one to five minutes. Following the end of the 90 minute period, the dog was taken off anaesthesia and allowed to recover. This procedure was repeated two to three days later using the second dosage of deltamethrin.

Venous blood samples (approximately 3–5 mls) were obtained from 4 dogs via the venous catheter during both the low- and high-level exposure periods at 0, 5, 10, 15 and 30 minutes *post exposure*. These samples were analyzed by gas-liquid chromatography to determine the concentration of deltamethrin circulating in the blood [33].

4.5 Phase IV - Deltamethrin Exposure in the Conscious Dog

The final phase of this project involved administering deltamethrin and collecting data in a conscious (unanesthetized) dog. This would have a distinct advantage over Phase III because it would eliminate the possibility of an interaction between the deltamethrin and the anaesthetic. In addition, as previously mentioned, halothane and deltamethrin both tend to increase CBF. It would certainly be possible for the effects of anaesthesia to mask the effects of the deltamethrin. Eliminating the anaesthesia

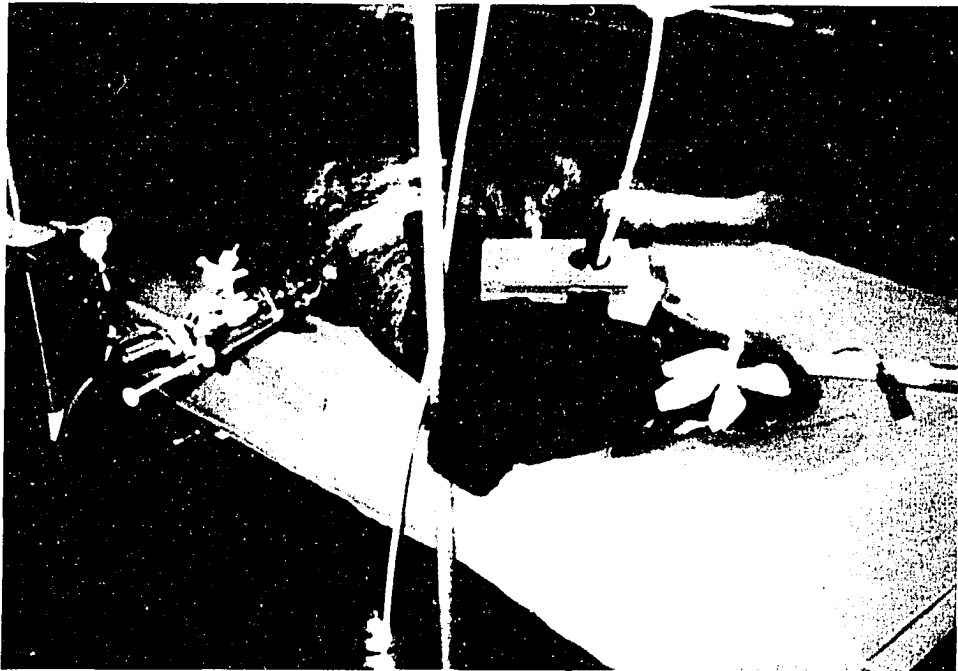


Figure 4.1: Photograph showing experimental setup in Phase III

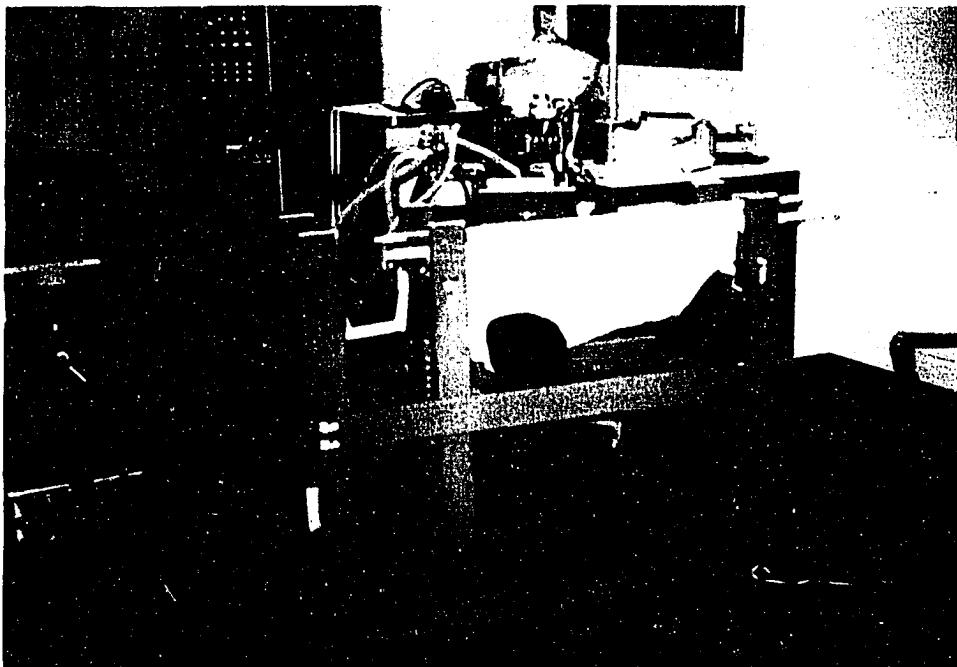


Figure 4.2: Photograph showing experimental setup in Phase IV

would eliminate the possibility of any masking of effects as well.

Since TCD is very sensitive to movement, the animal (while still conscious) must be restrained. This was accomplished by placing the dogs in a canvas sling device to suspend the body and head. A helmet apparatus was used to establish a fixed point of reference (see Figure 4.2). The TCD probe was securely attached to the helmet while still allowing 6 degrees-of-freedom to move the probe to obtain the desired signal. The 3-Space Isotrak system³ was used to determine exact probe placement so that repeated measurements could be reliably taken using a single probe. The 2 MHz TCD probe was attached to the Isotrak probe detector via a plexiglass tube to eliminate electromagnetic noise generated by the TCD. Unfortunately, no data was collected for any animals during Phase IV because, while the animals were conditioned to the sling, it was impossible to keep the head still enough to *verify* the location of a signal after it had been found. Consequently, all data presented in the remaining chapters was from Phases II and III.

4.6 Statistical Methods

For this experiment, each animal was subjected to three procedures. On day 1, the chronic arterial and venous cannulas were surgically implanted. On day 3, the first exposure to deltamethrin was carried out. Finally, on day 5, the second exposure to deltamethrin was completed. Following the second exposure, the animal was either used for another terminal experiment or euthanized and used in the Veterinary Anatomy teaching laboratory.

³Polhemus, Inc., Colchester, VT, (802) 655-3159.

4.6.1 Statistical design

All experiments consisted of three consecutive periods of 30 minutes each. Heart rate, arterial blood pressure and blood flow velocity were recorded continuously during each 30 minute period. End tidal CO_2 was recorded once every 5 minutes during each period. The first period was the control. Following the control period, 1 ml of glycerol-formal solution (no deltamethrin) was administered and data was recorded for 30 minutes. Finally, deltamethrin (in glycerol-formal) was administered (exposure period) and data was collected for an additional 30 minutes. Thus, for each dog, there were 3 periods per experiment and 2 experiments per dog (low and high) for a total of 180 minutes of continuous data collected.

A randomization table was used to determine the deltamethrin exposure schedule. In this design, two sources of variability were controlled. In this case, these nuisance variables were:

- **cumulative interactive effects** — one deltamethrin exposure that may interact with a future deltamethrin exposure in the same animal at a later time.
- **multiple animal subjects** — not all animals react exactly the same to the same level of exposure.

Three levels of exposure were used: a baseline level (b) which is solvent alone (no deltamethrin), a low-level (l) and a high-level (h) exposure. The low-level exposure was the level at which CBF changes were first observed and further CBF changes were anticipated at the high-level exposure.

Table 4.2 shows one replication of the exposure schedule which was used. Two replications ($n = 12$) were used to minimize standard error. Note that in Table 4.2.

Table 4.2: Randomization schedule (one replication). b=baseline (no deltamethrin), l=low-level dosage, h=high-level dosage

Exposure	Dog					
	1	2	3	4	5	6
1	b	b	b	b	b	b
	h	l	h	h	l	l
2	b	b	b	b	b	b
	l	h	l	l	h	h

the first exposure in each cell is always *b*, a baseline measurement, followed by either a low- or high-level exposure. This insured that there were no cumulative effects within any given cell (*i.e.*, *l* immediately followed by *h* within the same cell).

4.6.2 Statistical analysis

Each measured physiological parameter (*i.e.*, MAP, MHR, MBFV and pCO₂) and each calculated parameter (*i.e.*, SDR, GPI, PPI and upstroke) were calculated for each minute during each period. The control, glycerol-formal and deltamethrin periods were divided into three blocks (1–10 minutes, 11–20 minutes and 21–30 minutes). These *period-blocks* were denoted $C_1, C_2, C_3, G_1, G_2, G_3$, and D_1, D_2, D_3 , respectively. A randomized block factorial design and a Tukey studentized range test were used to test for significant differences between period-blocks.

In a randomized block factorial design (RBF-*pq*), the fixed-effects linear model is:

$$y_{ijm} = \mu + \alpha_i + \beta_j + \alpha\beta_{ij} + \pi_m + \varepsilon_{ijm}.$$

where μ is the grand mean of the treatment populations, α_i is the effect of treatment

i which is constant for all subjects within the treatment population i . β_j is the effect of treatment j , which is constant for all subjects within the treatment population j . $\alpha\beta_{ij}$ is the effect which represents the nonadditivity of effects α_i and β_j , π_m is a constant associated with block m , and ε_{ijm} is the experimental error [18].

For this experiment, there are three periods ($p = 3$) and three blocks ($q = 3$) within each period. Thus, an analysis of variance is performed using a RBF-33 design. Finally, Tukey's test declares two means significantly different if the absolute value of their sample differences exceeds a minimum significant difference (MSD) used for *all* comparisons[23]. In other words, if

$$|\bar{x}_1 - \bar{x}_2| \geq MSD$$

where \bar{x}_1 and \bar{x}_2 are period-block means (for example, C_1 and D_1), and MSD is the minimum significant difference, then there is sufficient evidence to reject the null hypothesis and conclude that C_1 and D_1 are significantly different. ⁴

⁴Unless otherwise indicated, all period-block mean comparisons were made using the Tukey test.

5. RESULTS

Figure 5.1 shows a typical TCD recording from a canine middle cerebral artery. This example shows that the blood flow velocity measured by the TCD is not a simple waveform but a spectrum of points representing a range of blood flow velocities for a given point in time. The TCD provides a voltage proportional to the maximum frequency follower (or envelope) velocity which is the maximum frequency (or velocity) at a given point in time. This velocity waveform was digitized and stored in the PC. However, due to the nature of the maximum frequency follower, the signal tends to be very noisy as evidenced by the example raw blood flow velocity waveform shown in Figure 5.2. Thus, some form of signal conditioning or filtering must be applied to be able to extract any useful data.

5.1 Conditioning BFV Data

Changes in CBF resulting from exposure to deltamethrin or other pyrethroids are very subtle and occur over several minutes. At low exposure levels, no beat-to-beat changes were expected. Therefore, the following algorithm (see Appendix D, page 94) was implemented to condition and condense the BFV data: First, the data was separated into one minute intervals. Due to the noisiness of the BFV signal, it was difficult to define each individual heart beat using the BFV waveform alone.

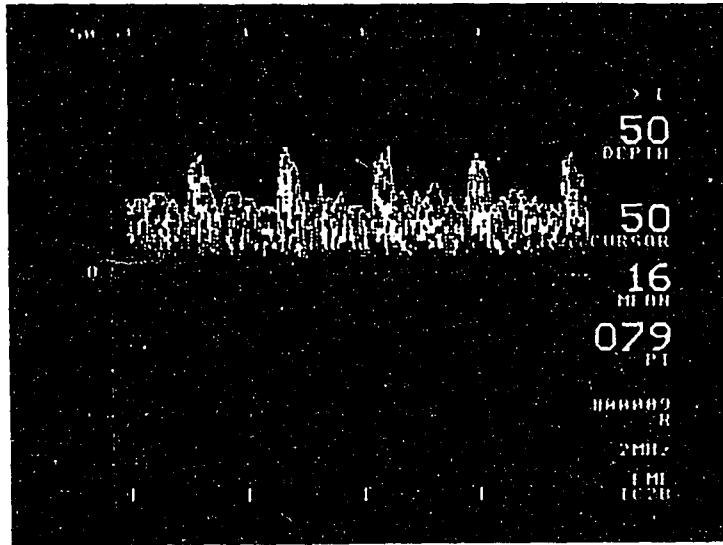


Figure 5.1: Typical TCD recording obtained from the MCA of a 32kg Greyhound dog; vertical scale is velocity (cm/sec), horizontal scale is time (sec); data above the zero line is flow toward the probe, below the zero line is flow away from the probe; depth of sample volume is displayed in upper right

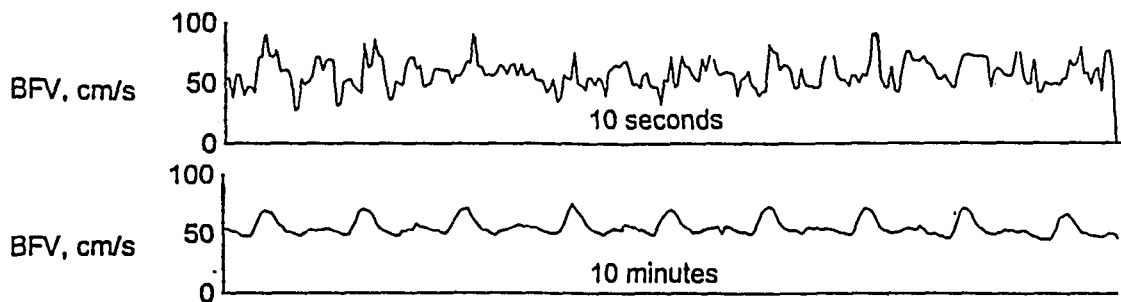


Figure 5.2: Top: Original BFV waveform (from maximum frequency follower of TCD); Bottom: Conditioned BFV waveform

Therefore, the minimum points on the blood pressure waveform (diastolic pressures) were used to define each heart cycle. These points were determined using the peak and valley detection algorithm in the Codas software package¹. Each minute of BFV data was then divided into individual heart cycles using the definition just described. The number of samples within each heart cycle is summed and the mean and standard deviation is calculated. Then, any heart cycle containing a total number of observations outside the range of the mean plus or minus one standard deviation ($\bar{x} \pm 1\sigma$) is discarded. Finally, the first observations for each heart cycle are averaged, followed by the second observations, and so on over the minute of data. The averaged points are put back together to form an average or composite BFV waveform representative of that particular minute of data. By eliminating those waveforms containing a total number of samples outside the $\bar{x} \pm 1\sigma$ range, the possibility of phase shifts occurring in the averaging and reconstruction is greatly reduced. This scheme had the secondary benefit of automatically discarding any section of data in which a cannula was flushed because the number of samples was significantly different from the normal heart cycles and thus was rejected.

The justification for using this type of signal conditioning is twofold: First, subtle changes occurring over several minutes and not beat-to-beat changes were expected. And second, the heart rate remained relatively constant over the one minute interval. If either of these conditions were false, then the method described above would not be appropriate for this analysis. In using this method, a much cleaner velocity signal was obtained (Figure 5.2), but at the expense of a significant amount of data. For a given

¹Dataq Instruments, Inc., 150 Springside Drive, Suite B220, Akron, OH 44333, 216-668-1444.

minute of data, initially perhaps 100 heart cycles (depending on heart rate) were present, and after conditioning, one heart cycle representative of the entire minute was obtained.

5.2 Physiological and Calculated Parameters

After obtaining a clean signal, mean arterial pressure (MAP), mean heart rate (MHR), mean blood flow velocity (MBFV) and end tidal CO_2 (pCO_2) in the control, glycerol-formal (solvent) and deltamethrin periods were compared. Additionally, there were four parameters that were obtained from the BFV waveform that are typically of clinical interest. They are:

1. Systolic to Diastolic Ratio (SDR)

$$SDR = \frac{V_A}{V_B}$$

2. Pourcelout Pulsatility Index (PPI)

$$PPI = \frac{V_A - V_B}{V_A}$$

3. Gosling Pulsatility Index (GPI)

$$GPI = \frac{V_A - V_B}{\bar{V}}$$

4. Average Systolic Upstroke (SU)

$$SU = \left[\frac{dV}{dt} \right] V(B,t) - V(A,t)$$

where V is blood flow velocity at points A and B (maximum systolic and minimum diastolic locations, respectively) as show in Figure 5.3.

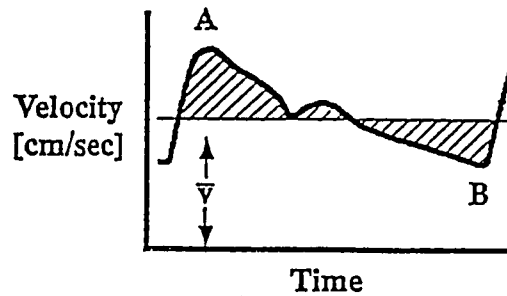


Figure 5.3: Calculated parameters from the BFV waveform

5.3 Results of Dose-Response Pilot Study

Two greyhound dogs were used in a pilot study to determine the low- and high-level deltamethrin exposure levels. It was hoped that the low-level exposure would correspond to a level where some changes *might* be detected and the high-level exposure would correspond to a level where some changes *would* be detected. No dogs were exposed to greater than 10% of the LD₅₀ because this would certainly be more than most individuals would be exposed to in the home or at the workplace.

Figure 5.4 (top) shows the results of a 7.5% LD₅₀ exposure immediately followed by a 10% LD₅₀ exposure on a 30kg female Greyhound. After each exposure, a slight increase in MAP, a distinct decrease in MHR and increase in pCO₂, and a definite increase in MBFV lasting approximately 10 to 15 minutes *post exposure* were observed. Figure 5.4 (bottom) shows the various BFV waveform parameters described previously. None of the four calculated parameters shown seems to indicate any observable changes that may be an indicator of exposure.

Based on the results of the pilot study, it was decided that the low- and high-level exposure levels would be set at 5% and 10% of the LD₅₀ value, respectively. These levels meet all of the exposure criteria mentioned previously.

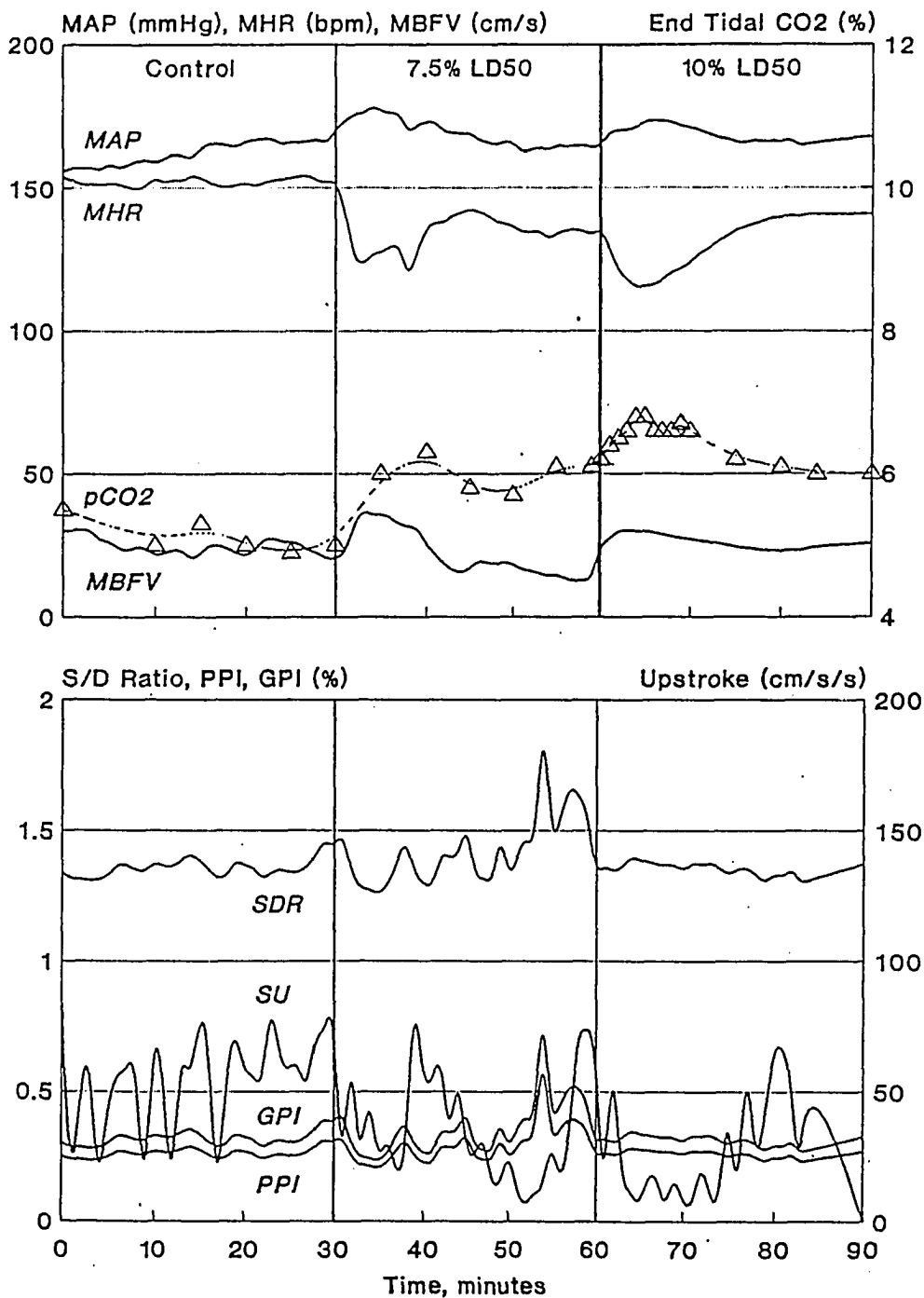


Figure 5.4: Two exposures of deltamethrin (7.5% LD₅₀ immediately followed by a 10% LD₅₀) in a 30kg Greyhound; upper graph shows measured physiological parameters; lower graph shows calculated parameters from the BFV waveform

5.4 Concentration of Deltamethrin in Blood

The concentration of deltamethrin in the blood as a function of time *post exposure* is shown in Figure 5.5. Notice that at $t = 0$ (just before injection of deltamethrin), there is no deltamethrin present in the blood. This indicates that waiting 24–48 hours between exposures was an adequate amount of time for the deltamethrin to be cleared from the circulation after a previous exposure. Of course, it is certainly possible that some deltamethrin was stored in adipose or other tissues and would not be present in the blood. Further, it is possible that some unnoticeable permanent alterations may be present that may bias the results from the second exposure. There was no indication that this occurred, and the randomization scheme described earlier should control for this possibility.

Although there is a limited amount of data available in Figure 5.5 on page 54 ($n = 4$ for each exposure), during both exposure levels, the concentration curves exhibit the characteristic rise and exponential decay ($y = ae^{-bt}$) expected after the injection of any substance that is slowly removed from the circulation. Deltamethrin is metabolized in the liver [3]. However, perhaps some is absorbed into the CNS and/or stored in adipose or other tissue. It is even possible that some may dissociate when exposed to blood.

5.5 Typical Results

Unfortunately, not all of the data obtained in these experiments exhibit the magnitude of responses shown in Figure 5.4 (top). Figures 5.6 and 5.7 show the results from low- and high-level deltamethrin exposures, respectively, done three days apart

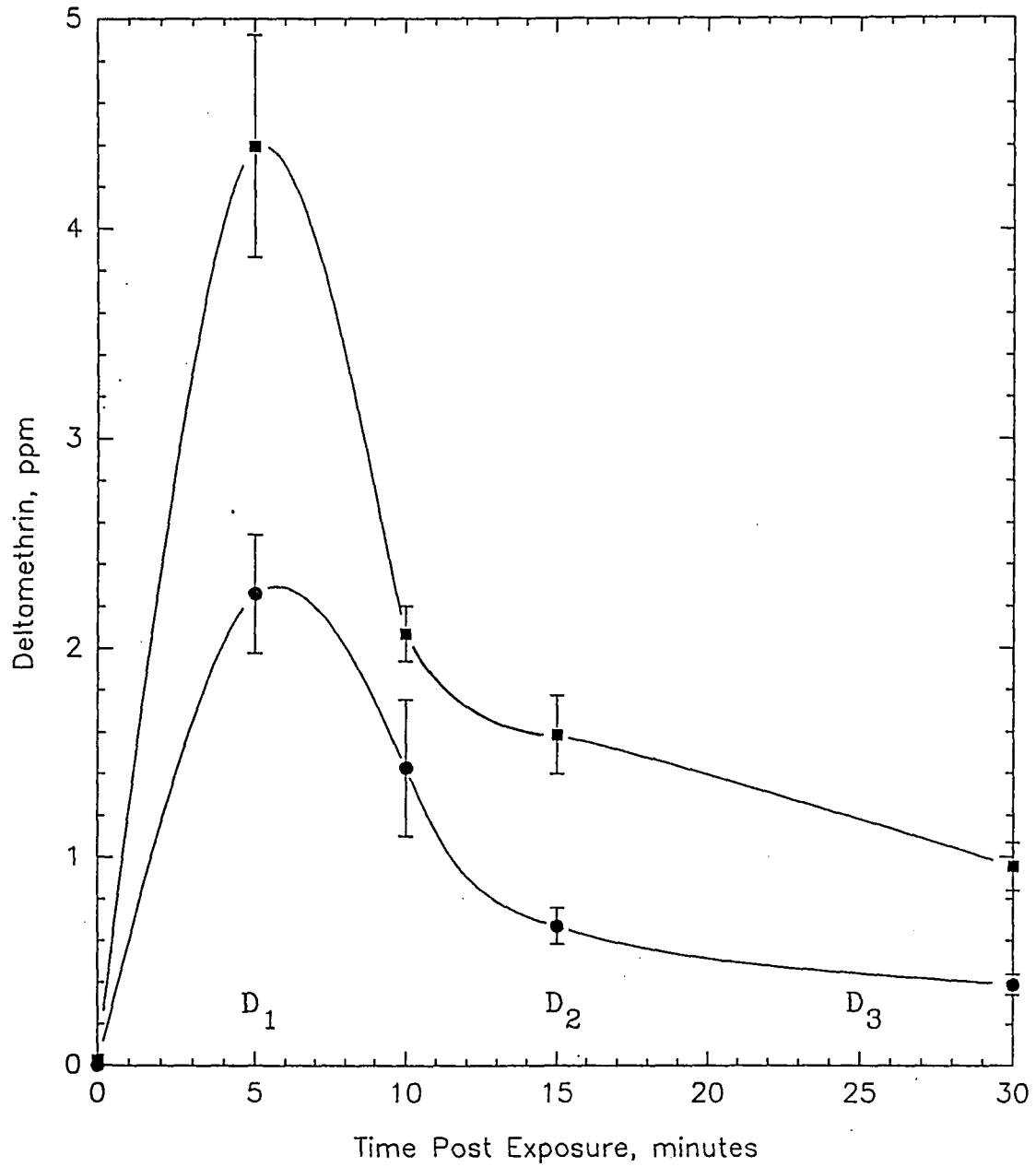


Figure 5.5: Concentration of deltamethrin in blood at 0, 5, 10, 15 and 30 minutes *post exposure*; circles indicate low-level (5% LD₅₀ exposure ($n=4$); squares indicate high-level (10% LD₅₀ exposure ($n=4$); range represents standard error

in a 32kg male Greyhound. Similar changes were observed in MAP, MHR, CO_2 and MBFV but to a much lesser degree compared to Figure 5.4. Again, Figures 5.6 and 5.7 show no consistent changes in calculated waveform parameters with the possible exception of some minor increases in pulsatility immediately following exposure.

5.6 Results of Physiological Parameters

In Phase III of this study (exposure to unconscious dogs), a total of 12 dogs weighing $30.3 \pm 3.8\text{kg}$ (9 greyhounds and 3 mongrels) were subjected to the low-level deltamethrin exposure. Two of the dogs that were subjected to the low-level exposure first developed complications which were unrelated to this study. Both dogs were removed leaving 10 dogs for the high-level exposure. An analysis of variance was carried out for each of the physiological and calculated parameters comparing the 9 period-blocks (treatment \times time) according to the procedure outlined in Section 4.6.2 (page 45).

Tables 5.1 and 5.2 summarize the period-block means for the measured and calculated parameters. In these tables, C_x is control period at time block x , G_x is glycerol-formal period at time block x , D_x is deltamethrin period at time block x , MSE is mean square error, CV is critical value of studentized range and MSD is minimum significant difference. In addition, the letters below each mean denote which means were *not* significantly different, *i.e.*, means with an *A* in a given column do not significantly differ, but one mean with an *A* and another mean with a *B* do significantly differ. These letters should be considered individually, in other words, the grouping *ABC* has no significance. For certain parameters (MHR, SDR and SU), the Tukey test does not detect significant differences between period-blocks when by

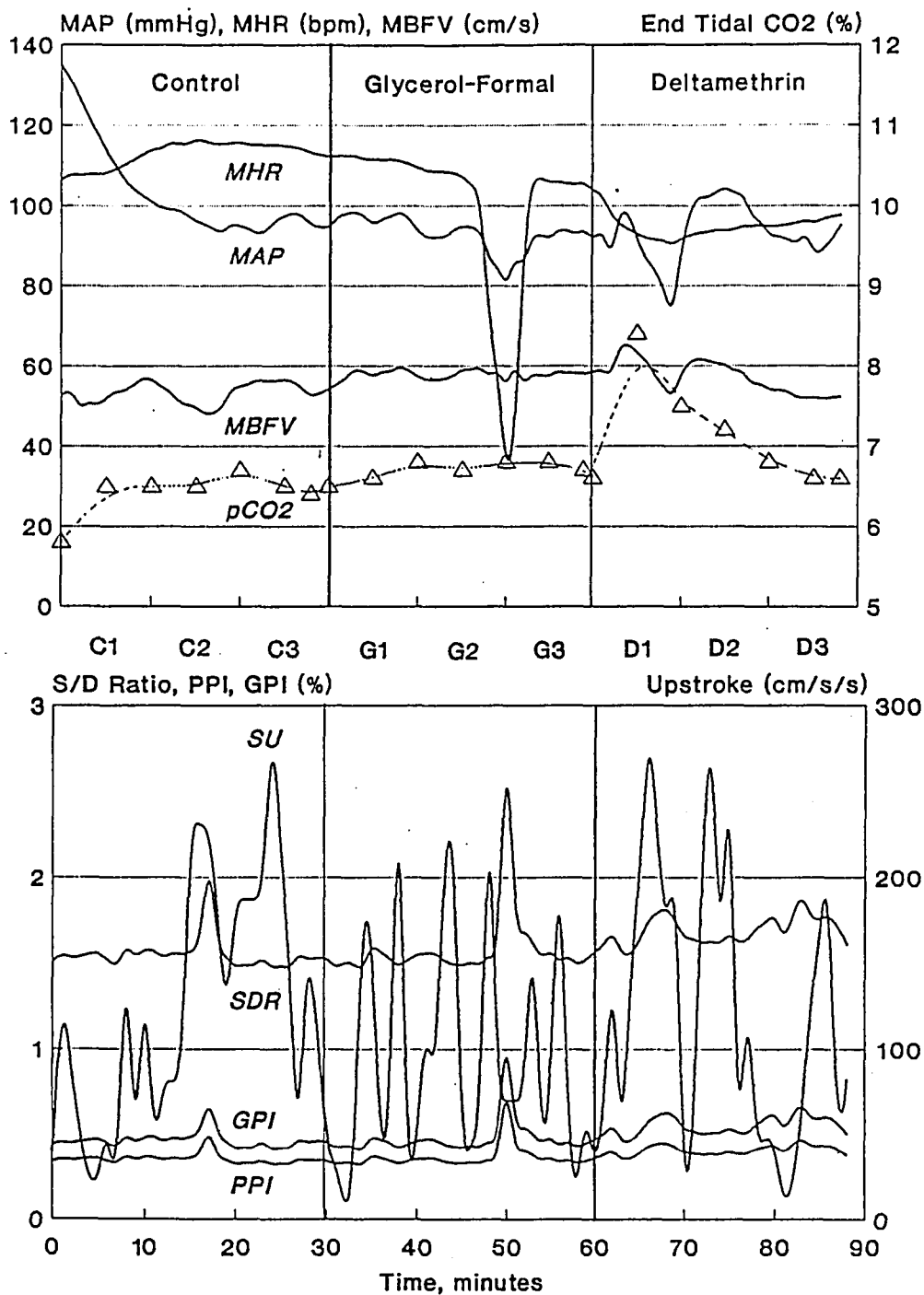


Figure 5.6: Control, solvent (glycerol-formal) and low level deltamethrin exposure (5% LD₅₀) in a 32kg greyhound; upper graph shows measured physiological parameters; lower graph shows calculated parameters from the BFV waveform

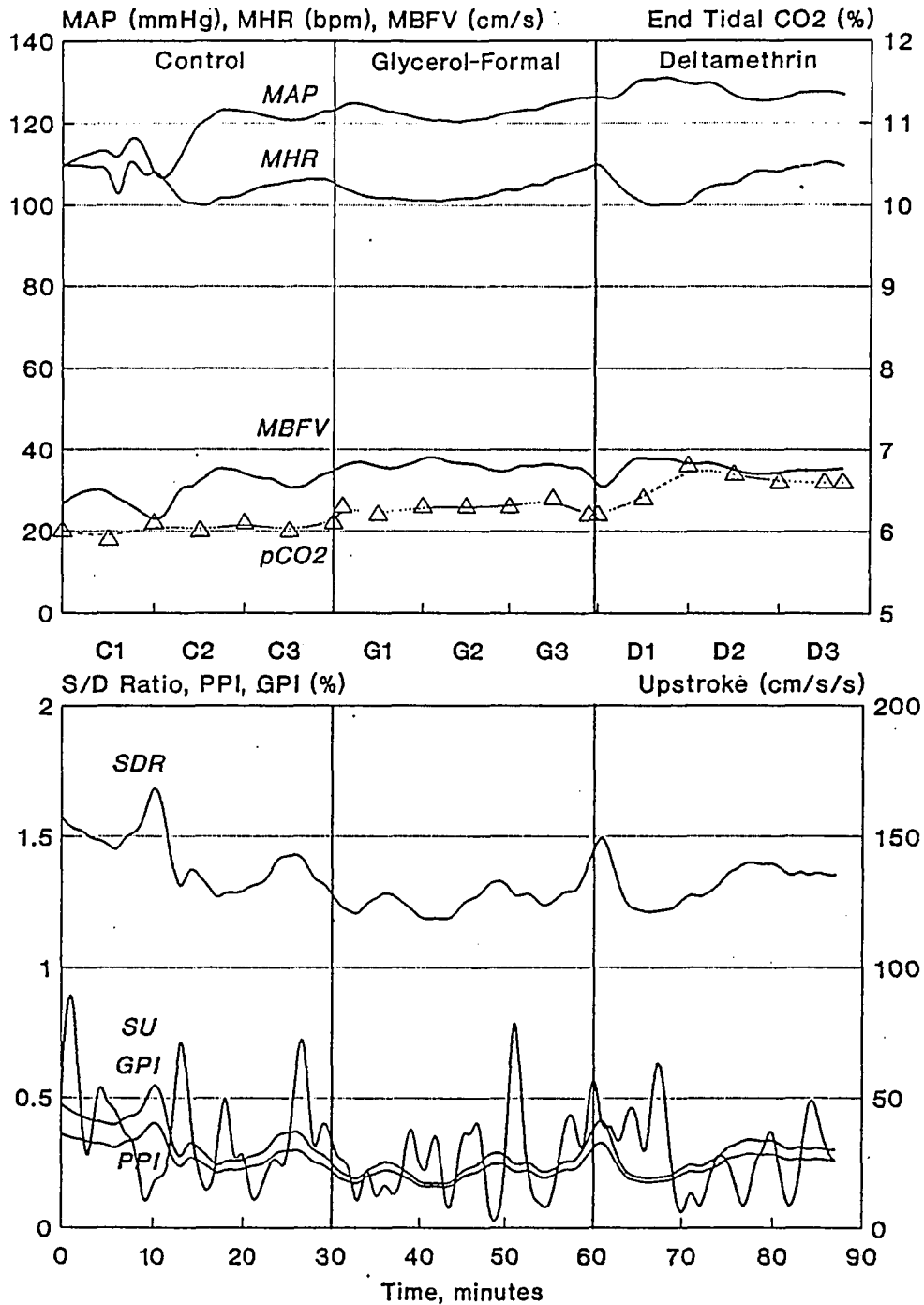


Figure 5.7: Control, solvent (glycerol-formal) and high level deltamethrin exposure (10% LD₅₀ in a 32kg greyhound; upper graph shows measured physiological parameters; lower graph shows calculated parameters from the BFV waveform

Table 5.1: Period-block means for low-level exposure ($n = 12, \alpha = 0.05, df = 88$), see text for further explanation

Period Block	Mean Arterial Pressure (<i>mmHg</i>)	Mean Heart Rate (<i>bpm</i>)	End Tidal CO_2 (%)	Mean Blood Flow Velocity (<i>cm/s</i>)	Systolic to Diastolic Ratio	Pourcelout Pulsatility Index (%)	Golsing Pulsatility Index (%)	Systolic Upstroke (<i>cm/s²</i>)
C_1	91.9 (A)	116.7 (ab- -)	6.8 (- -C)	33.2 (- -C)	2.61 (a-)	0.40 (A- -)	0.59 (A-)	29.07 (-b)
C_2	92.5 (A)	122.3 (a- - -)	6.9 (-BC)	34.6 (-BC)	1.93 (ab)	0.37 (ABC)	0.54 (AB)	50.85 (ab)
C_3	92.5 (A)	120.8 (ab- -)	7.1 (-BC)	35.8 (ABC)	1.66 (ab)	0.35 (ABC)	0.48 (AB)	50.82 (ab)
G_1	94.3 (A)	118.7 (ab- -)	7.1 (-BC)	37.4 (AB-)	1.54 (-b)	0.33 (-BC)	0.44 (-B)	32.22 (-b)
G_2	95.0 (A)	116.4 (ab- -)	7.3 (-B-)	37.9 (A- -)	1.51 (-b)	0.32 (- -C)	0.41 (-B)	41.97 (ab)
G_3	95.1 (A)	113.5 (-bc-)	7.2 (-BC)	36.8 (AB-)	1.61 (ab)	0.33 (-BC)	0.43 (-B)	39.86 (ab)
D_1	92.5 (A)	102.3 (- - - d)	7.9 (A- -)	37.7 (A- -)	1.68 (ab)	0.36 (ABC)	0.51 (AB)	47.95 (ab)
D_2	92.3 (A)	102.8 (- - - d)	7.9 (A- -)	36.1 (ABC)	1.66 (ab)	0.37 (AB-)	0.51 (AB)	61.37 (a-)
D_3	90.3 (A)	106.5 (- - cd)	7.9 (A- -)	35.4 (ABC)	1.66 (ab)	0.37 (ABC)	0.51 (AB)	47.22 (ab)
<i>MSE</i>	72.6	80.7	0.1	4.9	1.19	0.01	0.01	567.32
<i>CV</i>	4.4	(4.4)	4.4	4.4	(4.49)	4.49	4.49	(4.49)
<i>MSD</i>	11.0	(11.6)	0.44	2.89	(1.41)	0.05	0.14	(30.92)

Table 5.2: Period-block means for high-level exposure ($n = 10, \alpha = 0.05, df = 72$), see text for further explanation

Period Block	Mean Arterial Pressure (mmHg)	Mean Heart Rate (bpm)	End Tidal CO_2 (%)	Mean Blood Flow Velocity (cm/s)	Systolic to Diastolic Ratio	Pourcelout Pulsatility Index (%)	Golsing Pulsatility Index (%)	Systolic Upstroke (cm/s ²)
C_1	84.4 (- -C)	118.4 (a)	7.5 (-B)	25.7 (- -C)	1.68 (a -)	0.38 (A - - -)	0.53 (A - -)	26.26 (-bc)
C_2	88.7 (-BC)	117.8 (a)	7.3 (-B)	27.2 (ABC)	1.62 (a -)	0.35 (AB- -)	0.49 (AB- -)	24.27 (-bc)
C_3	89.9 (-BC)	118.9 (a)	7.4 (-B)	28.3 (ABC)	1.55 (ab- -)	0.33 (-BC- -)	0.44 (ABC-)	26.0 (-bc)
G_1	92.9 (ABC)	117.1 (a)	7.5 (-B)	30.1 (ABC)	1.47 (-bc-)	0.30 (- -CDE)	0.39 (-BCD)	22.1 (- -c)
G_2	96.1 (AB-)	118.5 (a)	7.6 (-B)	30.6 (AB-)	1.41 (- -c-)	0.27 (- - -DE)	0.35 (- -CD)	26.55 (-bc)
G_3	97.0 (AB-)	120.3 (a)	7.7 (-B)	30.8 (AB-)	1.38 (- -c-)	0.27 (- - - -E)	0.33 (- - -D)	32.56 (abc)
D_1	100.5 (A -)	103.2 (-b)	8.5 (A-)	31.0 (A -)	1.64 (a - -)	0.32 (-BCD-)	0.43 (-BCD)	50.69 (a -)
D_2	96.0 (AB-)	104.4 (-b)	8.4 (A-)	27.2 (ABC)	1.61 (a - -)	0.35 (AB- -)	0.48 (AB- -)	50.46 (a -)
D_3	92.7 (ABC)	108.5 (ab)	8.4 (A-)	26.3 (-BC)	1.60 (a - -)	0.35 (ABC- -)	0.48 (AB- -)	44.58 (ab-)
<i>MSE</i>	42.2	114.4	0.2	9.9	0.01	0.00	0.00	459.48
<i>CV</i>	4.5	(4.5)	4.5	4.5	(4.52)	4.52	4.52	(4.52)
<i>MSD</i>	9.2	(17.1)	0.6	4.5	(0.18)	0.05	0.10	(30.65)

observation, they would be expected. For example, in the high-level MHR experiment (Figure 5.9 bottom), the Tukey test showed no significant difference between C_1 and D_1 due to the large over-lapping standard errors between these two period-blocks. Thus, Duncan's multiple range test was used to compare these means. This is a slightly less conservative test than Tukey's test, but it is justified because it is very effective at detecting differences between means when real differences exist [23]. In order to make fair comparisons, however, the same test (either Tukey's or Duncan's) is used for both the low- and high-level experiments for any given parameter. For instance, Tukey's test is used for MAP in both experiments while Duncan's test is used for MHR in both experiments. In tables 5.1 and 5.2, means coded with capital letters (ABC) were compared using Tukey's studentized range test while those means coded with lowercase letters (abc) were compared using Duncan's multiple range test. For any given parameter, any two period-block means differ significantly if the absolute value of their difference exceeds the minimum significant difference (MSD) for that parameter. The results of this analysis are discussed below.

5.6.1 Mean arterial pressure

A plot of mean arterial pressure (MAP) versus time is shown in Figure 5.8 (see page 62). The upper graph (circles) represents the low-level exposure and the lower graph (squares) represents the high-level exposure. MAP remains fairly constant throughout the low-level exposure experiment, and there were no statistically significant differences between any periods or any time blocks.

For the high-level experiment, MAP tends to slightly increase through the control and glycerol-formal periods although these increases are *not* statistically significant.

There was a statistically significant difference between C_1 and D_1 ($\alpha = 0.05$, $MSD = 9.2$) indicating that the 10% LD_{50} exposure was causing a significant increase (19%) in MAP within the first 10 minutes *post exposure*. D_2 and D_3 do not significantly differ from C_2, C_3, G_1, G_2 or G_3 (B grouping for MAP column in Table 5.2) indicating that MAP returned to control levels after 10 minutes *post exposure*. Further, D_3 does *not* significantly differ from C_1, C_2, C_3 and G_1 indicating that MAP has returned to its starting level after 30 minutes *post exposure*.

5.6.2 Mean heart rate

A plot of mean heart rate (MHR) versus time is shown in Figure 5.9 (see page 64). The upper graph (circles) represents the low-level exposure and the lower graph (squares) represents the high-level exposure. MHR remained fairly constant during the control and glycerol-formal periods in the low-level experiment. There was an observable decrease in MHR immediately following exposure. There was a statistically significant difference ($\alpha = 0.05$, $MSD = 11.6$) between C_1, C_2, C_3, G_1, G_2 , and G_3 vs. D_1 and D_2 (a, b and c groupings for MHR column in Table 5.1). Further, there were no statistically significant differences between G_3 and D_3 (c grouping for MHR column in Table 5.1) indicating that there was a statistically significant decrease (12%) lasting 20 minutes *post exposure* and after 30 minutes, MHR had returned to pre-exposure (control and glycerol-formal) levels.

The results of the high-level experiment were similar to those of the low-level case (although there was greater variability in MHR during the high-level experiment). There was an observable decrease in MHR immediately following exposure. However, the Tukey test revealed *no* statistically significant differences between any period-

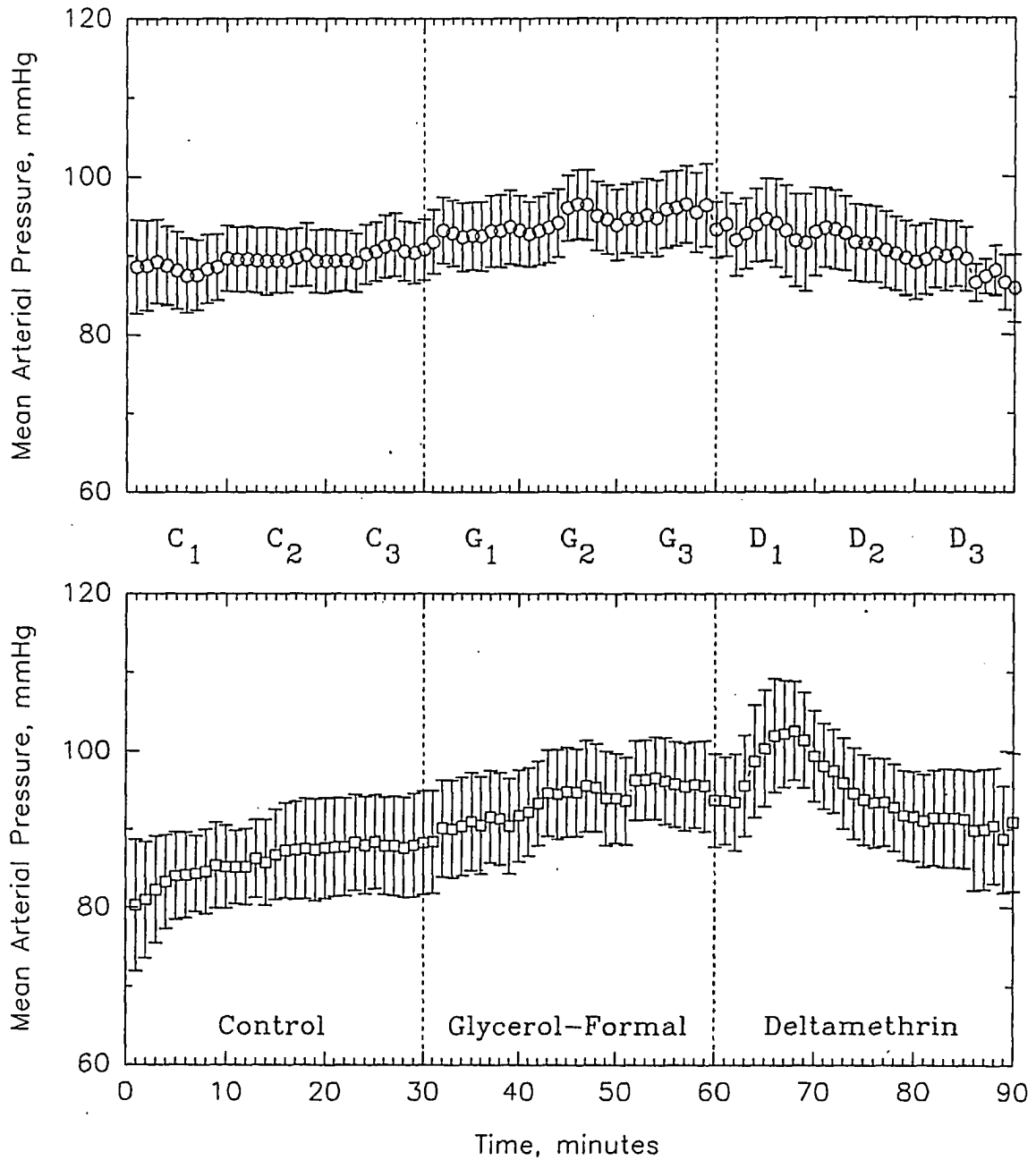


Figure 5.8: Mean arterial pressure (averaged over each minute for all dogs) in control, glycerol-formal and deltamethrin periods; circles indicate low-level (5% LD₅₀ exposure ($n=12$); squares indicate high-level (10% LD₅₀ exposure ($n=10$); range represents standard error

blocks. This was not a reasonable conclusion. Thus, a slightly less conservative Duncan multiple range test was used for MHR in the high-level exposure (indicated by lower case letters in the MHR column in Table 5.2). Applying this test, there was a statistically significant difference ($\alpha = 0.05$) between C_1, C_2, C_3, G_1, G_2 and G_3 vs. D_2 and D_3 (*a* and *b* groupings for MHR column in Table 5.2). This indicates that there were no significant differences between control and glycerol-formal heart rates but after the 10%LD₅₀ exposure, there was a significant decrease in MHR (13%) lasting approximately 20 minutes. Further, there were no statistically significant differences between C_1, C_2, C_3, G_1, G_2 and G_3 vs. D_3 indicating that heart rate had returned to control levels 30 minutes *post exposure*.

5.6.3 End tidal CO₂

A plot of end tidal CO₂ (pCO₂) versus time is shown in Figure 5.10 (see page 66). The upper graph (circles) represents the low-level exposure and the lower graph (squares) represents the high-level exposure. pCO₂ slowly increases (although not statistically significant) during the control and glycerol-formal periods in the low-level experiment. There was a statistically significant difference ($\alpha = 0.05, MSD = 0.4$) between C_1, C_2, C_3, G_1, G_2 and G_3 vs. D_1, D_2 and D_3 (*A* and *B* groupings for CO₂ column in Table 5.1). This indicated that there was a significant increase (17%) in pCO₂ immediately following the 5% LD₅₀ exposure and after 30 minutes, pCO₂ had not returned to control or glycerol-formal pre-exposure levels.

As was the case with MHR, the results for low- and high-level exposures for pCO₂ were similar. In the 10% LD₅₀ experiment, pCO₂ started out nearly a full 1% higher than in the low-level exposure experiment. There was a statistically significant

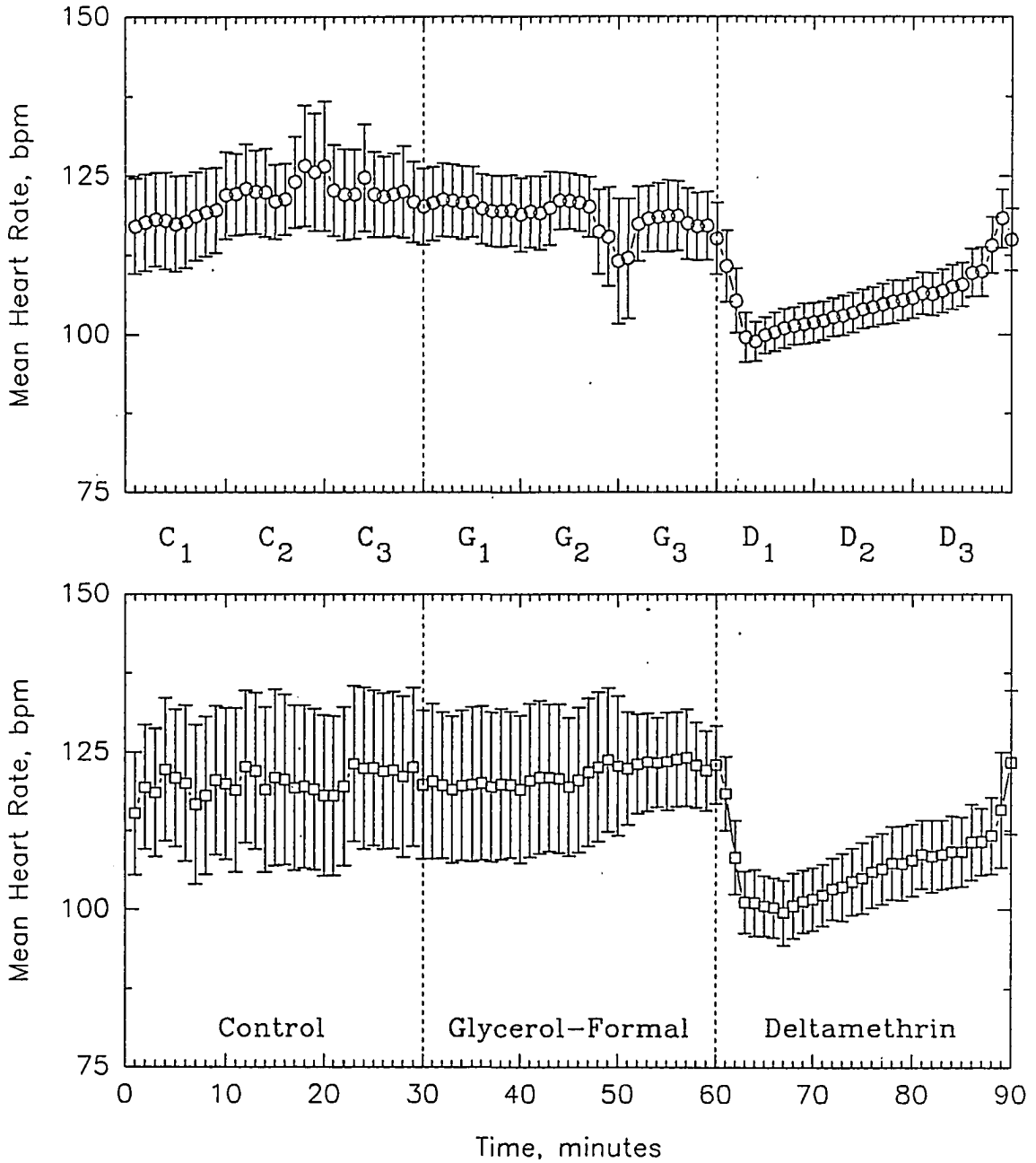


Figure 5.9: Mean heart rate (averaged over each minute for all dogs) in control, glycerol-formal and deltamethrin periods; circles indicate low-level (5% LD₅₀) exposure ($n=12$); squares indicate high-level (10% LD₅₀) exposure ($n=10$); range represents standard error

difference ($\alpha = 0.05$, $MSD = 0.6$) between C_1, C_2, C_3, G_1, G_2 and G_3 vs. D_1, D_2 and D_3 (*A* and *B* groupings for CO_2 column in Table 5.2). Again, this indicated that there was a significant increase in pCO_2 (14%) immediately following the 10% LD_{50} exposure and after 30 minutes, pCO_2 had not returned to control or glycerol-formal pre-exposure levels.

5.6.4 Mean blood flow velocity

A plot of mean blood flow velocity (MBFV) versus time is shown in Figure 5.11 (see page 68). The upper graph (circles) represents the low-level exposure and the lower graph (squares) represents the high-level exposure. In the low-level experiment, MBFV slowly increases during the control and glycerol-formal periods. However, the results of the Tukey test show no significant differences between C_1, C_2 and C_3 and further, there were no significant differences between C_2, C_3, G_1, G_3, D_2 and D_3 (*A* and *B* groupings for MBFV column in Table 5.1). There was a statistically significant difference between C_1 and D_1 ($\alpha = 0.05$, $MSD = 2.8$) although there was no difference between G_2 and D_1 . This indicated that MBFV did *not* significantly change during the control period; and, with the exception of an increase in the middle of the glycerol-formal period (G_2), MBFV remained constant until the 5% LD_{50} exposure. In addition, there was a significant increase in MBFV immediately following exposure, and after 10 minutes *post exposure*, it returned to original control and glycerol-formal levels.

As expected, there is a large degree of variability (large standard error) in each of the MBFV plots. In the high-level experiment, there were no significant differences between C_1, C_2, C_3, G_1, D_2 and D_3 (*C* grouping for MBFV column in Table 5.2).

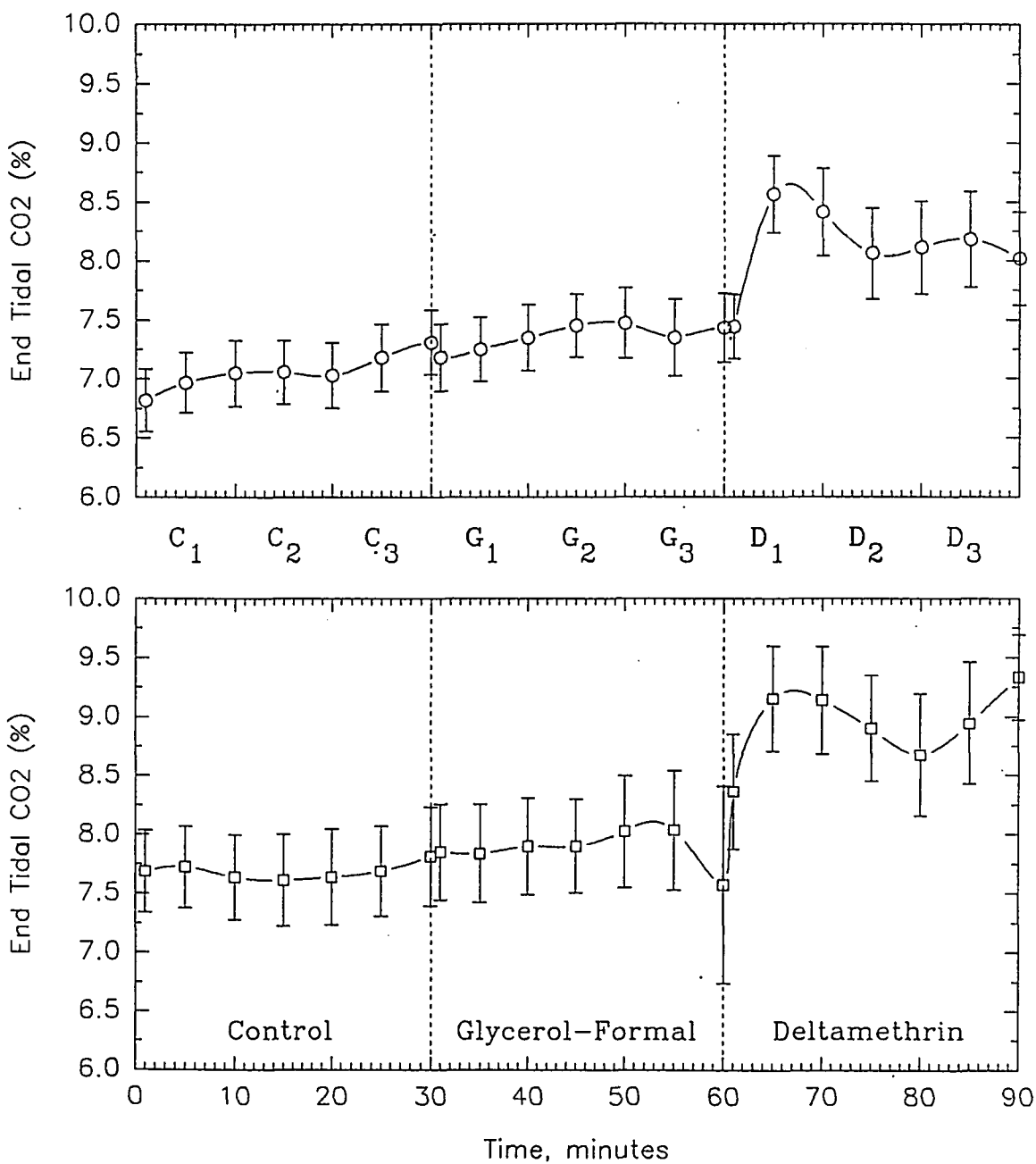


Figure 5.10: End tidal CO₂ (recorded once every 5 minutes and averaged over all dogs) in control, glycerol-formal and deltamethrin periods; circles indicate low-level (5% LD₅₀ exposure ($n=12$); squares indicate high-level (10% LD₅₀ exposure ($n=10$); range represents standard error

Further, there were no significant differences between $C_2, C_3, G_1, G_2, G_3, D_2$ and D_3 (B grouping for MBFV column in Table 5.2). There was a statistically significant difference ($\alpha = 0.05, MSD = 4.5$) between C_1 and D_1 . This indicated that MBFV did not significantly change during the control or glycerol-formal periods, but did significantly increase immediately following the 10% LD₅₀ exposure. It immediately returned to control and glycerol-formal levels after 10 minutes *post exposure*.

5.7 Results of Calculated Parameters

The next four sections describe the results of the parameters calculated from the blood flow velocity waveform. These parameters are systolic-to-diastolic ratio, Pourcelout pulsatility index, Gosling pulsatility index and systolic upstroke as defined on page 50.

5.7.1 Systolic-to-diastolic ratio

A plot of systolic-to-diastolic ratio (SDR) versus time is shown in Figure 5.12 (see page 70). The upper graph (circles) represents the low-level exposure and the lower graph (squares) represents the high-level exposure. During the control period of the low-level experiment, SDR is highly variable but seems to settle down during the glycerol-formal period. This phenomenon probably has little to do with the injection of the glycerol-formal because the variability tends to decrease through the control phase. The results of the Tukey test showed no significant differences between any period-block combinations. Applying Duncan's multiple range test revealed that only C_1 was significantly different from G_1 and G_2 ($\alpha = 0.05$). There was an observable increase in SDR (although not statistically significant) immediately following the

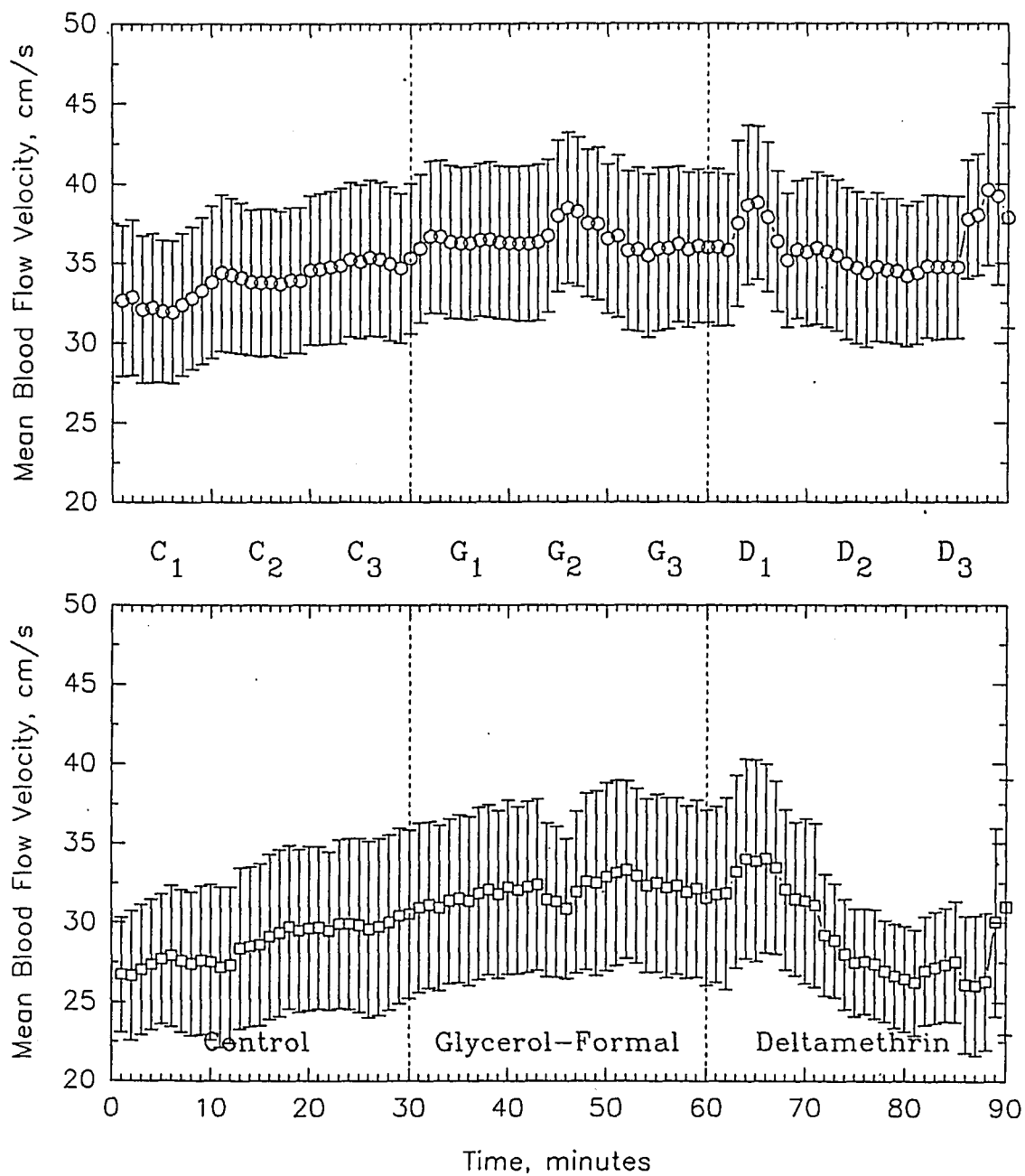


Figure 5.11: Mean blood flow velocity (averaged over each minute for all dogs) in control, glycerol-formal and deltamethrin periods; circles indicate low-level (5% LD₅₀ exposure ($n=12$); squares indicate high-level (10% LD₅₀ exposure ($n=10$); range represents standard error

injection of deltamethrin. It peaked approximately 5 minutes *post exposure* and lasted approximately 8 minutes.

In the high-level exposure experiment, SDR decreased slowly during the control and glycerol-formal periods and then gradually increased in the exposure period. There was a large degree of variability in SDR during C_1 and C_2 . The period-block groups C_1, C_2, C_3 , and C_3, G_1 , and G_1, G_2, G_3 , did not significantly differ; however, the differences between these groups were statistically significant ($\alpha = 0.05, MSD = 0.18$). In addition, there was a statistically significant difference between C_1 and G_3 . This indicates that SDR significantly decreased (12%) through the control and glycerol-formal periods and, after exposure to deltamethrin, returned to pre-exposure control levels.

5.7.2 Pourcelout pulsatility index

A plot of Pourcelout pulsatility index (PPI) versus time is shown in Figure 5.13 (see page 72). The upper graph (circles) represents the low-level exposure and the lower graph (squares) represents the high-level exposure. In the low-level experiment, PPI tended to decrease through the control and glycerol-formal periods and then to increase in the deltamethrin period. Tukey's test showed that there were no statistical differences between $C_2, C_3, G_1, G_2, G_3, D_1$ and D_3 (C grouping for PPI column in Table 5.1). There was, however, a statistically significant difference ($\alpha = 0.05, MSD = 0.05$) between C_1 and G_2 (A grouping for PPI column in Table 5.1). This indicated that the downward trend through the first two periods was significant (18%) and, following exposure, PPI increased and returned to the control level.

A similar trend for PPI was observed in the high-level experiment. There was a

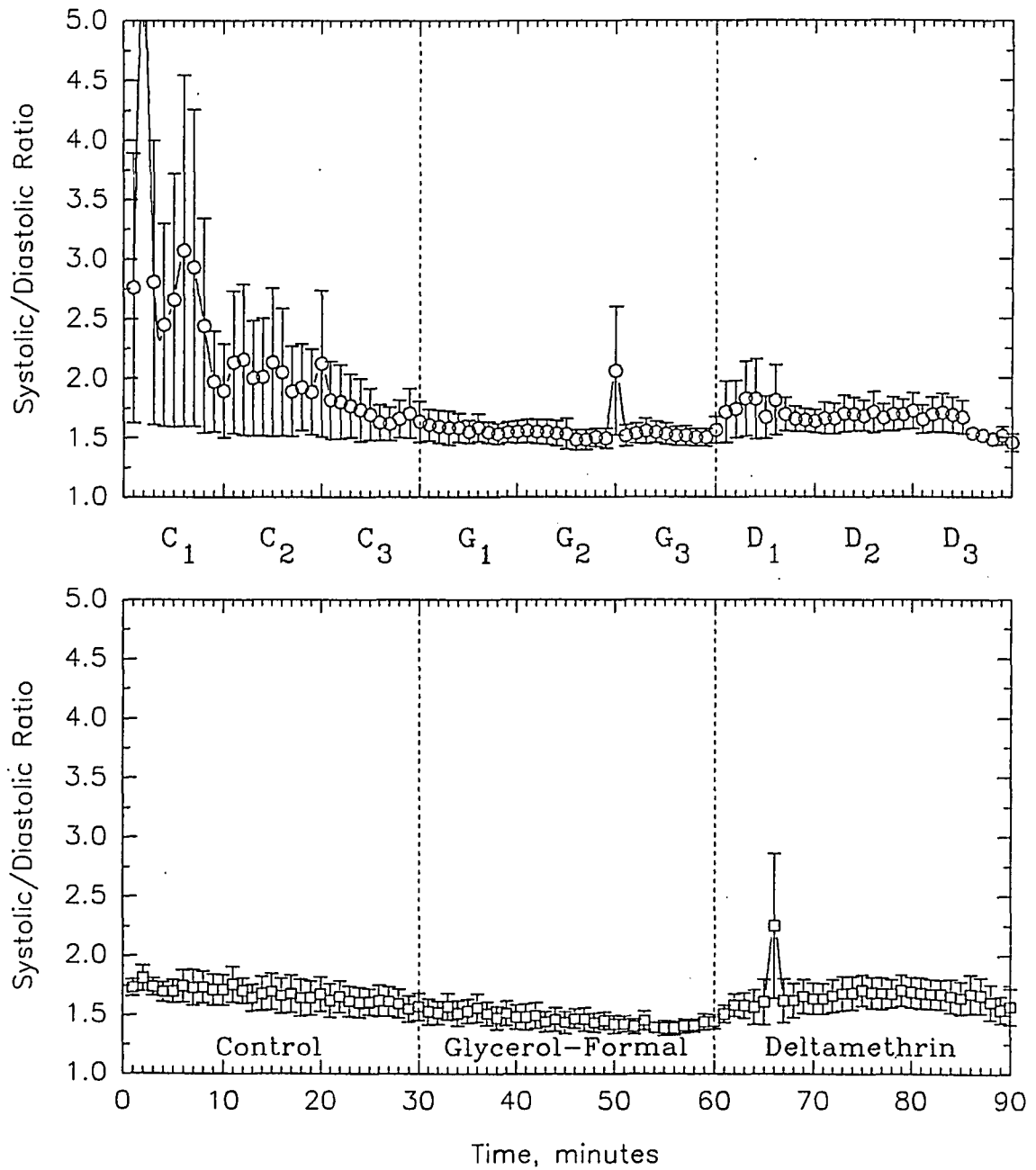


Figure 5.12: Systolic-to-diastolic ratio (averaged over each minute for all dogs) in control, glycerol-formal and deltamethrin periods; circles indicate low-level (5% LD₅₀ exposure ($n=12$); squares indicate high-level (10% LD₅₀ exposure ($n=10$); range represents standard error

statistically significant difference between C_1 and G_3 ($\alpha = 0.05$, $MSD = 0.05$). In addition, the period-block pairs C_1 and C_2 , C_2 and C_3 , C_3 and G_1 , and G_1 and G_2 do not significantly differ individually; however, the difference between these pairs was statistically significant ($\alpha = 0.05$, $MSD = 0.05$). Thus, as in the 5% LD_{50} case, the decrease in PPI, through the control and glycerol-formal periods, was significant (22%), and, after the 10% LD_{50} exposure, PPI increased and returned to the control level.

5.7.3 Gosling pulsatility index

A plot of Gosling pulsatility index (GPI) versus time is shown in Figure 5.14 (see page 74). The upper graph (circles) represents the low-level exposure and the lower graph (squares) represents the high-level exposure. The trend in the GPI data paralleled that of the PPI data; that is, in the control and glycerol-formal periods of both the low- and high-level exposure experiments, the GPI decreased and then increased during the deltamethrin period. In the low-level experiment, there was a statistically significant difference ($\alpha = 0.05$, $MSD = 0.14$) between C_1 vs. G_1, G_2 and G_3 (*A* and *B* groupings for GPI column in Table 5.1). There were no statistically significant differences between $C_2, C_3, G_1, G_2, G_3, D_1, D_2$ and D_3 . Thus, GPI significantly decreases (26%) through the control and glycerol-formal periods and then increases back to pre-exposure control levels during the deltamethrin period.

In the high-level experiment, the period-block groups C_1, C_2, C_3 , and C_2, C_3, G_1 , and C_3, G_1, G_2 , and G_1, G_2, G_3, D_1 did not significantly differ individually; however, the differences between these groups were statistically significant ($\alpha = 0.05$, $MSD =$

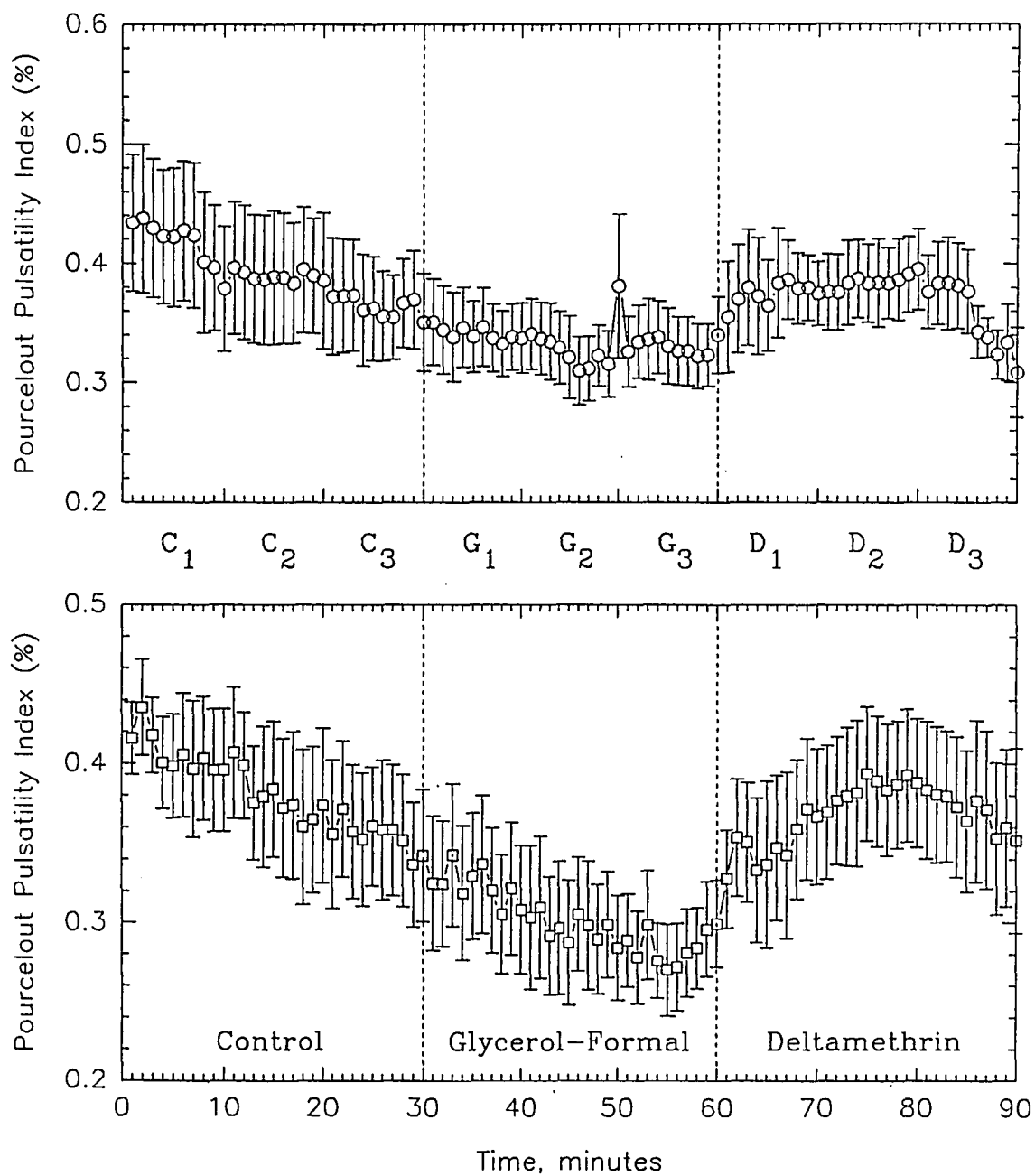


Figure 5.13: Pourcelout pulsatility index (averaged over each minute for all dogs) in control, glycerol-formal and deltamethrin periods; circles indicate low-level (5% LD₅₀ exposure ($n=12$); squares indicate high-level (10% LD₅₀ exposure ($n=10$); range represents standard error

0.10). In addition, there was a statistically significant difference between C_1 and G_3 . This indicated that GPI significantly decreased (27%) through the control and glycerol-formal periods, and after exposure to deltamethrin, returned to pre-exposure control levels.

5.7.4 Systolic upstroke

A plot of systolic upstroke (SU) versus time is shown in Figure 5.15 (see page 75). The upper graph (circles) represents the low-level exposure and the lower graph (squares) represents the high-level exposure. Systolic upstroke is really the mean acceleration of the blood from diastole to peak systole. SU is quite chaotic in all three periods in each experiment. There was an observable increase in SU immediately following exposure. The results of the Duncan test indicated that the only period-blocks that were significantly different ($\alpha = 0.05$, $MSD = 30.92$) were C_1 and D_2 . There were no other significant differences thus there was no consistent trend in SU through the low-level experiment.

In the high-level experiment, the Tukey test revealed no significant differences between *any* period-block combinations. Applying a Duncan's multiple range test on the high-level SU data indicated that there were statistically significant differences ($\alpha = 0.05$) between G_1 vs. D_1 and D_2 (*a* and *b* groupings for SU column in Table 5.2). Further, there were no statistically significant differences between C_1, C_2, C_3, G_1, G_2 and G_3 . This showed that there were no significant changes in systolic upstroke through the control and glycerol-formal periods and there was a significant increase (93%) in SU for 20 minutes *post exposure*. SU returned to the pre-exposure control level after 30 minutes *post exposure*.

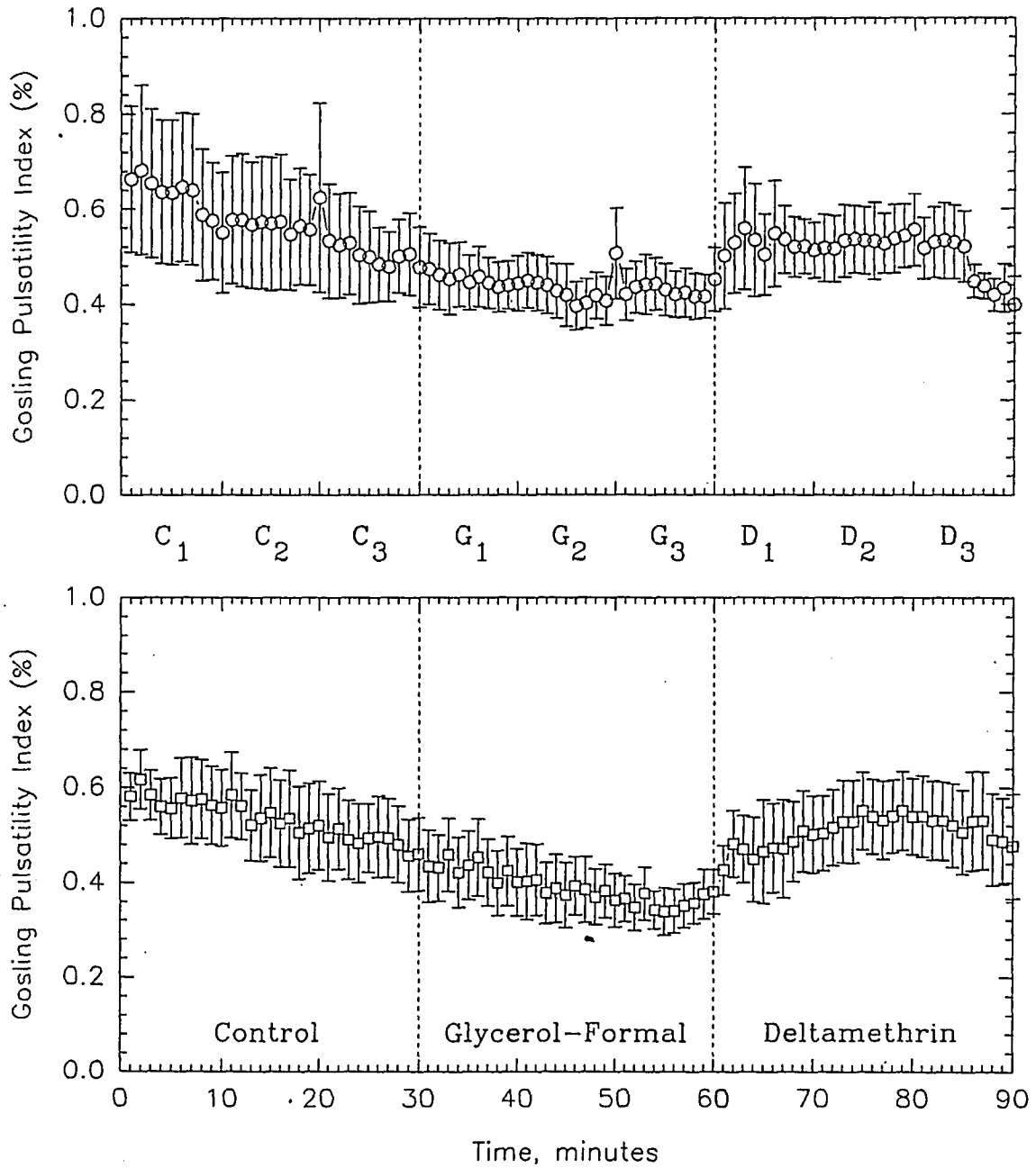


Figure 5.14: Gosling pulsatility index (averaged over each minute for all dogs) in control, glycerol-formal and deltamethrin periods; circles indicate low-level (5% LD₅₀ exposure ($n=12$); squares indicate high-level (10% LD₅₀ exposure ($n=10$); range represents standard error

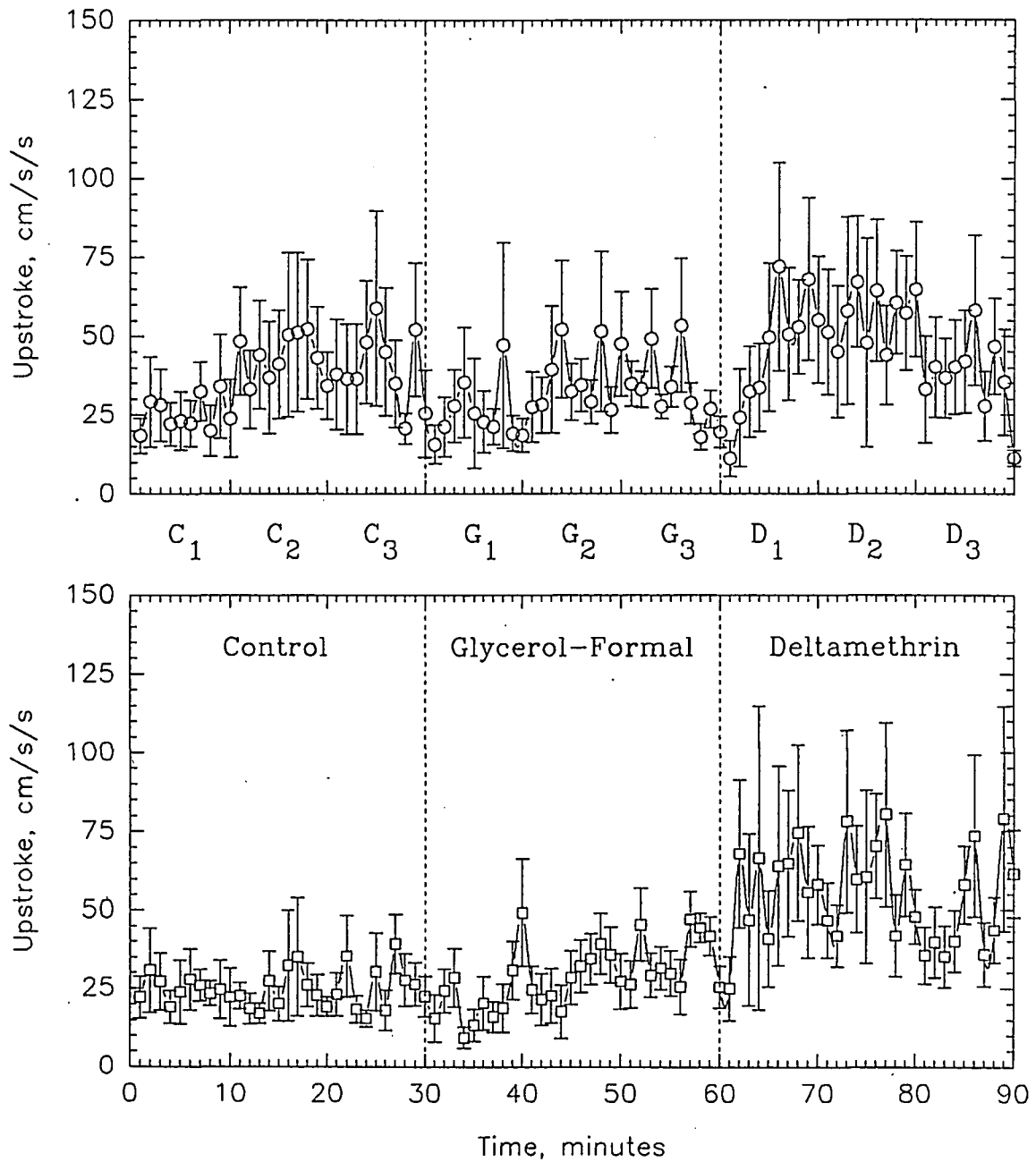


Figure 5.15: Systolic upstroke or acceleration (averaged over each minute for all dogs) in control, glycerol-formal and deltamethrin periods; circles indicate low-level (5% LD₅₀ exposure ($n=12$); squares indicate high-level (10% LD₅₀ exposure ($n=10$); range represents standard error

6. DISCUSSION

Each year, thousands of new chemicals are developed and many may eventually come into contact with people on the job or simply through every day activities. Although every effort is made to ensure that each chemical is safe for human exposure, any new testing procedure that may potentially detect subtle biological changes occurring before clinical symptoms are observed would certainly be worth further investigation. If these subtle changes can be detected early enough, perhaps the chance of permanent damage occurring could be reduced or even eliminated completely.

Transcranial Doppler sonography has been well established as a noninvasive and cost effective means of measuring cerebral blood flow in man. Although the use of TCD in animals has been limited, pilot work indicated that CBF can be measured by TCD in normal greyhound dogs. Further, it was shown that manipulations of CBF (using CO₂) can be detected using TCD. Deltamethrin had been previously shown to increase CBF in rats as determined by other techniques. The purpose of the proposed study was to determine whether:

- Deltamethrin increases cerebral blood flow in a higher mammal (*i.e.*, a greyhound dog), and whether
- Transcranial Doppler sonography can detect changes in CBF at very low exposure levels.

Although no data was obtained for the conscious dog experiments, the unconscious animal experiments did provide some useful information. These results are summarized in Table 6.1. With respect to control levels, glycerol-formal alone did not exhibit any significant effects on any of the physiological parameters measured. However, there was a significant decrease in SDR, PPI and GPI associated with the administration of glycerol-formal. This suggests that the shape of the blood flow velocity waveform changes in the presence of glycerol-formal without any corresponding changes in any directly measured physiological parameters. Specifically, a decrease in pulsatility and systolic-to-diastolic ratio suggest that the amplitude of the BFV waveform had diminished with *no* corresponding change in MBFV. This result would have not been known without the use of TCD to *continuously* measure the blood flow velocity waveform. It is possible that the glycerol-formal is acting directly on the cerebral vessels (specifically the MCA) by irritating the luminal surface and causing the vessels to become less compliant. Autoregulation would act to maintain mean flow even in the presence of these waveform alterations.

After exposure to deltamethrin, there is a significant increase in MBFV lasting 10 minutes *post exposure*, a significant increase in MAP and decrease in MHR each lasting 20 minutes *post exposure* and a significant increase in $p\text{CO}_2$ lasting at least 30 minutes *post exposure*. The increase in MBFV agrees with previously obtained data from rats for $r\text{CBF}$ [7]. In addition, significant decreases in heart rate and increases in $p\text{CO}_2$ and mean arterial pressure were observed during this same *post exposure* period indicating that the deltamethrin was having systemic effects on the cardiovascular and cerebrovascular systems. Further, this data is collaborated by circulating deltamethrin concentrations which peaked at approximately 5 minutes

Table 6.1: Summary of qualitative results of both low- and high-level experiments (N/C denotes no change with respect to control)

	Control	Gly-For	5% LD ₅₀	10% LD ₅₀	Duration
MBFV	—	N/C	↑ (13%)	↑ (21%)	10 min
MAP	—	N/C	N/C	↑ (19%)	20 min
MHR	—	N/C	↓ (12%)	↓ (13%)	20 min
pCO ₂	—	N/C	↑ (17%)	↑ (14%)	> 30 min
SDR	—	↓ (41%,12%)	N/C	N/C	—
PPI	—	↓ (18%,22%)	N/C	N/C	—
GPI	—	↓ (26%,27%)	N/C	N/C	—
SU	—	N/C	↑ (65%)	↑ (93%)	20 min

post exposure.

SDR, PPI and GPI returned to control levels following the administration of deltamethrin. Changes in these parameters suggest that there were actual changes in the *shape* of the blood flow velocity waveform occurring after deltamethrin exposure. The shape of the BFV waveform depends on a variety of factors including CBF resistance downstream (which is a function of glucose metabolic rate), vessel compliance and intracranial pressure. If CBF in the MCA increased while at the same time there was a decrease in heart rate, then not only would the mean BFV increase, but also the pulsatility would increase as evidenced by an increase in SDR, PPI and GPI.

There are several points in the methodology used in this experiment that may be improved upon in the future. First of all, the biggest question is anesthesia. Ideally, anesthesia should be eliminated completely from this experiment. Perhaps improvements could be made in the sling and helmet devices to enable restraint of a conscious dog for longer periods of time. In lieu of this, a gas anesthesia monitor may be used to more precisely control the level of anesthesia during experiments.

Also, while verification of TCD signals by traditional methods is certainly adequate in human clinical research, perhaps a more precise method should be developed to quantitate probe location. This is especially true in the dog where cerebral vessels are smaller and closer together, and the spectral broadening effect is even more prominent. Further, it would be useful to try lowering the exposure level of deltamethrin to 2.5% or perhaps even 1% of the LD₅₀ to determine if changes in MBFV could be detected by TCD at these very low levels.

Finally, this study showed that not only were there changes in the cerebrovascular system due to deltamethrin but systemic changes in the cardiovascular system as well. To separate these effects, it would be necessary to measure a systemic blood flow parameter, *i.e.*, cardiac output, or, ideally, blood flow in the carotid artery ipsilateral to the MCA being insonated by the TCD. Then, if there was a change in systemic blood flow caused by deltamethrin, this could be measured independently of blood flow velocity in the MCA. Perhaps additional parameters of the BFV waveform may be related to the cerebrovascular system. For example, systolic upstroke (or acceleration) is related to the force of contraction of the heart. The downslope of the BFV waveform is related to the downstream resistance or, in this case, the vascular resistance of the brain. It would be of interest to consider the effects of deltamethrin on the downstroke of the BFV waveform as a way to further understand how the brain reacts to a toxic substance.

TCD seems to have great potential as a screening methodology; however, prior to these experiments, it had not been used with animals nor had it been applied in the field of toxicology. In this research, it has been shown that TCD is sensitive enough to measure alterations in cerebral blood flow even when no other measurable

systemic changes occur. It is hoped that TCD may soon become a routinely used screening procedure for detecting the early effects of known (and perhaps even unknown) substances on people subjected to potentially hazardous materials at home or in the workplace.

7. BIBLIOGRAPHY

- [1] Aaslid, R. 1986. Transcranial Doppler sonography. Springer-Verlag, New York. 177 pp.
- [2] Adams, D.R. 1986. Canine anatomy. Iowa State University Press. Ames, Iowa. 513 pp.
- [3] Amdur, M.O., Doull, J., and Klassen, C.D. 1991. Casarret and Doull's toxicology: The basic science of poisons. 4th ed. Pergamon Press, New York. 1033 pp.
- [4] Angerson, W.J., Sheldon, C.D., Barbenel, J.C., Fisher, A.C. and Gaylor, J.D. 1989. Blood flow in the brain. Oxford Medical Engineering Series, Clarendon Press, Oxford, England. 138 pp.
- [5] Baugnman, V.L., and Hoffman, W.E. 1986. Effects of phenobarbital on cerebral blood flow and metabolism in young and aged rats. *Anesthesiology* 65(5):500-505.
- [6] Chanh, P.H., Navarro-Delmasure, C., and Clavel, P. 1984. Toxicological studies of deltamethrin. *International Journal of Tissue Reactions* 5(2):127-133.
- [7] Cremer, J.E., and Seville, M.P. 1985. Changes in regional cerebral blood flow and glucose metabolism associated with symptoms of pyrethroid toxicity. *Neurotoxicology* 6(3):1-12.
- [8] Cruickchank, J.M., and Neil, D.G. 1989. Acute effects of smoking on blood pressure and cerebral blood flow. *Journal of Human Hypertension* 3(6):443-449.
- [9] Cunningham, V.J., and Cremer, J.E. 1981. A method for the simultaneous estimation of regional rates of glucose influx and phosphorylation in rat brain using radiolabeled 2-deoxyglucose. *Brain Research* 221:319-330.

- [10] Forshaw, P.J., and Bradbury, J.E. 1983. Pharmacological Effects of Pyrethroids on the cardiovascular System of the Rat. *European Journal of Pharmacology* 91:207-213.
- [11] Gray, A.J. 1985. Pyrethroid structure-toxicity relationships in mammals. *Neurotoxicology* 6(2):127-138.
- [12] Gray, H. 1974 *Gray's anatomy. 40th ed.* Running Press, Philadelphia, Pennsylvania. 1257 pp.
- [13] He, F., Wang, S., Liu, L., Chen, S., Zhang, Z., and Sun, J. 1989. Clinical manifestations and diagnosis of acute pyrethroid poisoning. *Archives of Toxicology* 63:54-58.
- [14] Hartmann, A., and Hoyer, S. 1985. Cerebral blood flow and metabolism measurement. Springer-Verlag, New York. 618 pp.
- [15] Ishikawa, Y., Charalambous, P., and Matsumura, F. 1989. Modification by pyrethroids and DDT of phosphorylation activities of rat brain sodium channel. *Biochemical Pharmacology* 38(15):2449-2457.
- [16] Joy, R., Lister, T., Ray, D., and Seville, M. 1990. Characteristics of the prolonged inhibition produced by a range of pyrethroids in the rat hippocampus. *Toxicology and Applied Pharmacology* 103:528-538.
- [17] Kandel, E.R. 1985. Principles of neuroscience. *2nd ed.* Elsevier, New York.
- [18] Kirk, R.E. 1982. Experimental design: Procedures for the behavioral sciences. *2nd ed.* Brooks Cole Publishing, New York.
- [19] Klaassen, C.D., Amdur, M.O., and Doull, J. 1986. Toxicology: The basic science of poisons. Macmillan Publishing Company, New York.
- [20] Knezevic, S. 1988. Handbook of regional cerebral blood flow. Lawrence Erlbaum Associates, Hillsdale, NJ. 299 pp.
- [21] Michenfelder, John D. 1988. Anesthesia and the brain. Churchill Livingstone, New York. 215 pp.
- [22] Maximilian, V.A., and Riseberg, J. 1982. Regional cerebral blood flow and verbal memory after chronic exposure to organic solvents. *Journal of Regional Cerebral Blood Flow and Metabolism* 1(2):196-205.

- [23] Montgomery, D.C. 1991. Design and analysis of experiments. *3rd ed.* John Wiley and Sons, New York. 649 pp.
- [24] Lindegaard, K., and Bakke, S. 1985. Assessment of intracranial hemodynamics in carotid artery disease by TCD. *Journal of Neurosurgery* 63:890-898.
- [25] Narahashi, T. 1985. Nerve membrane ionic channels as the primary target of pyrethroids. *Neurotoxicology* 6(2):3-22.
- [26] O'Donoghue, J.L. 1985. CRC neurotoxicity of industrial and commercial chemicals. Vol. 1. CRC Press, Inc., Boca Raton, Florida.
- [27] Ohno, K., Pettigrew, K.D., and Rapoport, S.I. 1979. Local cerebral blood flow in the conscious rat as measured with ^{14}C -antipyrine, ^{14}C -iodoantipyrine and ^3H -nicotine. *Stroke* 10:62-67.
- [28] Orbaek, P., and Risberg, J. 1985. Effects of long-term exposure to solvents in the paint industry. *Scandinavian Journal of Work, Environment and Health* 11:1-28.
- [29] Palm, U., and Boemke, W. 1991. Prevention of catheter-related infections by a new, catheter-restricted antibiotic filling technique. *Laboratory Animals* 25:142-152.
- [30] Ray, D.E. and Cremer, J.E. 1979. The action of decamethrin (a synthetic pyrethroid) on the rat. *Pesticide Biochemistry and Physiology* 10:333-340.
- [31] Soderland, D.M. 1985. Pyrethroid-receptor interactions: Stereospecific binding and effects on sodium channels in mouse brain preparations. *Neurotoxicology* 6(2):35-46.
- [32] Shujie, W., Qinglang, Z., Lan, Y., Bohong, X., and Yurui, L. 1988. Health survey among farmers exposed to deltamethrin in cotton fields. *Ecotoxicology and Environmental Safety* 15:1-6.
- [33] Stahr, H.M. 1991. Analytical methods in toxicology. *1st ed.* John Wiley and Sons, New York.
- [34] Vriens, E., and Kraaier, V. 1989. TCD Measurements of blood velocity in the MCA: reference values at rest and during hyperventilation in healthy volunteers in relation to age and sex. *Ultrasound in Medicine and Biology* 15(1):1-8.
- [35] Werner, C., and Kochs, E. 1990. The effects of angiotensin-induced arterial hypertension on canine cerebral blood flow velocities in correlation to cerebral blood flow. *Anesthesia and Analgesia* 70:S450.

- [36] White, D.N., Curry, G.R., and Stevenson, R.J. 1978. The acoustic characteristics of the skull. *Ultrasound in Medicine and Biology* 4:225-252.

8. ACKNOWLEDGEMENTS

This project was supported by grant **1 R03 OH02932-01** from the National Institute for Occupational Safety and Health of the Centers for Disease Control. I would also like to thank Hoechst Canada, Inc. for their donation of deltamethrin used in this study and Eden Medical Electronics, Inc., and Polhemus, Inc., for donating a portion of their equipment costs for the TCD and Isotrak systems used in this study.

On a more personal note, I would like to thank the many people who have assisted on this project and who have helped me to get where I am today. First, I'd like to thank **Dr. Mary Helen Greer** and the many professors and graduate students in the Biomedical Engineering Program whom I have worked with over the years in my many academic and research pursuits. I would like to specifically thank **Dr. Donald Young** for acting as my major professor during my master's degree and for serving on my Ph.D. program of study committee. I would also like to thank **Dr. David Carlson** for serving as my co-major professor for my Ph.D., on my program of study committee for my master's and as a continuing source of technical advice on the many little unexpected glitches that pop up during any good research project.

I certainly owe **Dr. Douglas Lange** a huge amount of thanks for countless hours spent in surgery and animal experiments during both this project for my Ph.D.

and my corresponding blood pressure study as well. Doug, a practicing veterinarian, surgical resident and graduate student himself, found the time between surgeries and solving differential equations to help me perform the many surgeries and animal experiments necessary for this project, often working on weekends and at ungodly hours of the night stretching into the wee hours of the morning. I hope those many trips to "Little Tai Pay" showed, in some small way, how grateful I am to you for all your help and advice.

Now, to **Dr. David Hopper**, my major professor, mentor and friend, I am reminded of the following story:

In a forest, a fox bumps into a little rabbit and says "Hi junior. what are you up to?"

"I'm writing a dissertation on how rabbits eat foxes," said the rabbit.

"Come now, friend rabbit, you know that's impossible!"

"Well, follow me and I'll show you." They both go into the rabbit's dwelling and after a while the rabbit emerges with a satisfied expression on his face.

Comes along a wolf. "Hello friend rabbit, what are you up to these days?"

"I'm writing the second chapter of my thesis, on how rabbits devour wolves."

"Are you crazy? Where is your academic honesty?"

"Come with me and I'll show you." As before, the rabbit comes out with a satisfied look on his face and a diploma in his paw.

Finally, the camera pans into the rabbit's cave and, as everybody should have guessed by now, we see a mean-looking, huge lion sitting next to some bloody and furry remnants of the wolf and the fox.

The moral: *It's not the content of your thesis that is important — it's your Ph.D. advisor that really counts.*

Dr. Hopper, you have been more than just a major professor to me these past years. You have been a source of support and encouragement through some very trying times. Not only do I hope to have made some lasting impressions in my professional career, but around your *homestead* as well. Just think, how will I spend my Saturdays now?

Finally, I would like to dedicate this project to my family for putting up with me through the trials and tribulations of graduate school. To my grandmothers, **Betty Winokur** and **Valerie Druess**, for your continued support and endless confidence in me when sometimes I wasn't even sure of myself. To my now deceased grandfathers, **Max Winokur**, whom I barely remember, and **Dr. Lionel Druess**, whom I never met, I somehow feel that this work is a tribute to your sacrifice and your undying love of family and education. I hope that someday I can pass on these beliefs to my grandchildren as well.

Last, and certainly far from least, to my sister **Susan**, and my parents **Marshall** and **Paula**, I look back on what I have accomplished and realize that without your support, encouragement, caring and love, all of this would be meaningless. You have taught me to strive for excellence, to help others around me and to always try to leave every situation a little better than the way I found it. I hope I have done that. This work, as well as all my past accomplishments, is a reflection on you as much as it is on me.

To all of you and everyone else who has influenced me over the years, you have my utmost respect, admiration and thanks — without you, I would not be where I am today!

9. APPENDIX A: CANNULA CONSTRUCTION

Materials List

From Braintree Scientific, Inc., Braintree, MA:

1. RPC-080-18 Renapulse rigid catheter kit used for artery.
2. MRP-080-18 Micro-Renathane compliant infusion catheter kit for vein.
3. SCS-2 red stopcocks.
4. SCS-2 blue stopcocks.
5. Polysciences, Inc. 3813 TDMAC-Heparin 7% (25ml).

Other Materials Used:

1. Dacron felt.
2. Silastic glue.
3. 32 gauge stainless steel wire.
4. Silastic tubing (0.035 I.D., 0.010 wall thickness).
5. Zip Bond glue (Cole-Parmer) Cat. No. L-08776-00 1 oz. bottle.
6. 3-0 Mersiline.

Construction

1. Cut a rectangular piece of Dacron felt $1\frac{1}{2}$ inches long and wide enough to wrap around the cannula $1\frac{1}{2}$ times.

2. Cut a piece of stainless steel wire 12-18 inches long. Wrap the wire around the cannula (under the Dacron pad) and anchor the Dacron pad to the cannula. Place the Dacron pad about 1 inch from the bottom of the light blue (winged) plastic hub on the cannula.
3. Snugly wrap the stainless steel wire around the cannula tubing in the area where the Dacron pad will be placed. Make sure the pad will completely cover the wire. Tie the wire to itself, leaving two tails, each about 3 inches long.
4. Wrap the Dacron felt around the cannula $1\frac{1}{2}$ times. Tape the pad shut and remove it from the tubing so that it can be sutured closed away from tubing (to avoid puncturing cannula).
5. Suture the pad closed with 3-0 Mersilene. Attach a suture needle to the end of the stainless steel wire tails on the cannula and insert the needle inside the sutured Dacron pad. Push the needle and wires through the pad. Thread the end of the cannula through the Dacron pad and bring the pad up to just below the wrapped wire. Apply a layer of Silastic glue all around the tubing and wire in an area which will be completely covered by Dacron pad. Immediately slide the pad over the glue, wire and tubing. Wrap wire tails around outside of the pad and tie. Air dry Silastic glue for 24 hours.
6. To make a flexible tip on the distal end of the venous cannula, cut a $2\frac{1}{2}$ inch piece of Silastic tubing and immerse in Xylene for 2-3 min. After removing the Silastic tubing from the Xylene, immediately pull the Silastic over the end of the cannula tubing. Cover the distal $1\frac{1}{2}$ inches of the venous cannula leaving an additional 1 inch of Silastic tubing extending beyond the end of the cannula tip. Do not place a Silastic tip on the arterial cannula.
7. Next, coat the inside of both cannulas with TDMAC-Heparin. Using a syringe filled with TDMAC-Heparin and a blunt needle on the syringe, inject the TDMAC-Heparin into each cannula (use gloves and a fume hood). Leave the TDMAC-Heparin in cannula for 1 minute. Remove the heparin from cannula. Attach the cannula to the end of an air hose and run a stream of air through the cannula overnight.
8. After the cannula is air-dried, glue the 3-way stopcock (blue for venous, red for arterial) to the cannula with Zip-Bond glue. After the Zip-Bond is dry, gas sterilize the cannulas using ethylene oxide.
9. IMPORTANT - The plastic 3-way stopcocks must be glued on *after* the TDMAC-Heparin has been added and dried. If the TDMAC-Heparin is added after the

stopcocks have been glued, the solvent in the TDMAC-Heparin will dissolve the stopcocks.

10. APPENDIX B: CANNULA IMPLANTATION

1. Initially make sure the cannulas are filled with fluid (non-heparinized saline) and there are no air bubbles in the lumen. Be sure the stopcocks are securely in the off position. Place a sterile drape under the neck area of the animal before surgery starts. This area will be redraped later.
2. With the animal in right lateral recumbency, make an 8 cm skin incision on the ventral midline of the neck. With gentle blunt dissection, expose the muscles in the neck area so they can be seen but do not cut through or disrupt them. Using scissors, make a pocket under the skin on the proximal ("up") side about the size of a half dollar coin.
3. Without moving the animal, make a 4-5 cm incision on the dorsal midline of the neck. Form a pocket under the skin about the size of a quarter by each side of the anterior end of the incision. Pass an aluminum tube from the posterior end of the incision, under the skin, to the ventral neck area and exit through the first incision. Pass the venous cannula through the tubing as far as possible and then pull the tube out through the ventral skin incision while holding the cannula stationary. The cannula should be under the skin connecting the two surgical sites. Next, starting at the anterior end of the incision, repeat the process for the placement of the arterial cannula. Form a pocket for the Dacron sleeve on one side of the midline. Place a loop of tubing in the anterior pocket and form another pocket under the skin for the sleeve of the other cannula on the opposite side of the midline.
4. Using a stainless steel suture (4-0), pass the attached needle through the end of the sleeve next to the valve, then through a layer of the skin (without going completely through), and return to the sleeve to take another pass. Pull the suture snugly, but not too tight, and tie. The knot should be buried when the incision is closed. Repeat the procedure for the other cannula.

5. After anchoring the cannula, suture the skin with an interrupted suture pattern using the same suture material used for the skin closure. Draw the skin up over the cannula sleeves and close the skin on the back of the neck. Loosely place the sutures about 3-4 mm apart.
6. Roll the dog over so that it is now in dorsal recumbancy. Redrape as needed and use a new set of surgical instruments on the new surgical site. Find the line separating the muscles on the ventral surface of the neck. Bluntly dissect along this line down to the trachea; a 6-7 cm exposure is required.
7. The carotid arteries lie on either side of and slightly below the trachea. Gently dissect around a carotid artery to expose about 3-4 cm of vessel. Separate the nerve from the vessel sheath but don't damage the nerve in any way. After the artery is free, expose and isolate 4-5 cm of the jugular vein (located just under the skin).
8. After the vein is exposed, prepare to cannulate it first. Select the site for the cannulation. Estimate the distance from that site to the third intercostal space (approximately the length of cannula placed inside the vessel). Leave as much connective tissue on the vessel wall as possible while still having a workable area for cannulation. Now put in a simple purse string suture pattern (twice the cannula diameter) using 3-0 Mersilene in the surface of the vessel. Enter only connective tissue and vessel wall being careful not to enter the lumen. Make one throw of a surgeons knot but do not draw it tight (clamp the end in a hemostat). Enter the vein with a cannula introducer (or an 18 gauge needle with the tip bent at a 80 degree angle). Use this to make a hole in the vessel wall by carefully placing the point of the needle in the center of the area delineated by the purse string. Without removing the introducer, insert the venous cannula. Grasp the small silastic tip gently between two fingers (or with small tip thumb forceps) and work the cannula into the vessel. If the introducer should come out, use the plastic cannula introducer to reenter the original opening. Place the venous cannula in the vessel lumen to the estimated length. Draw the purse string up snugly around the cannula and tie securely (using many throws). Next, place 6-8 clove hitch knots around the cannula with the same suture. Finally, anchor the cannula to some connective tissue 2-3 cm away from the vessel.
9. To cannulate the artery, follow the same procedure outlined above with the following exceptions:
 - (a) Use a vascular clamp (or two bulldog clamps) to control the bleeding. Remember that the carotid artery is a high pressure vessel.

- (b) After inserting the cannula tip into the lumen, release the clamp just enough to pass the cannula into the vessel the remaining distance.
 - (c) All hemorrhage must be controlled by the purse string suture. Remove all clamps and gently move the cannula to test for leaks.
10. Close the skin completely over the cannulas after placing the excess tubing in the prepared pocket under the skin.
 11. After the surgical procedure has been completed, flush both cannulas with heparinized saline. Be sure to close the valve while the heparin injection is being made; this will prevent blood from entering the cannula tip and clotting. Apply furacin powder (or paste) to the cannula entrance site and wrap the area securely using gauze or an orthopedic stocking. Flush both cannulas daily with heparinized saline to prevent clotting.

11. APPENDIX C: TCD DATA ANALYSIS PROGRAM

The following program takes the blood pressure and blood flow velocity waveforms from the Cudas software and processes the data as described in Chapters 4 and 5.

```

,,,,,,,,,,,,,,,,,,,,,,,,,,,,,,,,,,,,,,,,,,,,,,,,,,,,,,,,,,,,,,,,,,,,,,,,,,,,,,,,
' TCD Data Analysis Package by Michael Drues
'   March, 1992, Iowa State University Dept. of Biomedical Engineering
'
' File Name Convension for OPEN/CLOSE:
'
'   #1 --> original data (i.e., CONTROL.TXT)
'   #2 --> one minute data files from #1 (i.e., CTRL000.TXT)
'   #3 --> one heart beat files from #2 (i.e., WAVE000.TXT)
'   #4 --> result data files (i.e., RESUL000.TXT)
'   #5 --> heart beat files BEFORE checking mean+/-s.d. (TEMPO00.TXT)
'   #6 --> Cudas data denoting diastolic points (i.e., CONTROL.L2)
'   #7 --> summary of diastolic, systolic, MAP and HR for each minute
'   #8 --> Stats on filtered wave data, STATS.TXT
'
' Colors:
'   13 - purple ; 14 - yellow ; 12 - red ; 10 - green
'
,,,,,,,,,,,,,,,,,,,,,,,,,,,,,,,,,,,,,,,,,,,,,,,,,,,,,,,,,,,,,,,,,,,,,,,,,,,,,,,,
      starttime = TIMER
      DIM observation(200), numobs(200), bfvpt(200), bppt(200),
          dia(200), sys(200), map(200), hr(200)
again:

```

```

GOSUB myscreen
COLOR 14
LOCATE 13, 35: PRINT "1 = Control"
LOCATE 14, 35: PRINT "2 = Glycerol-Formal"
LOCATE 15, 35: PRINT "3 = Deltamethrin"
LOCATE 10, 25: INPUT "Select one:"; datatype
IF datatype = 1 THEN datatype$ = "CONTROL"
IF datatype = 2 THEN datatype$ = "GLY"
IF datatype = 3 THEN datatype$ = "DELTA"
IF datatype<>1 AND datatype<>2 AND datatype<>3 THEN GOTO again

```

```

GOSUB myscreen
COLOR 14: LOCATE 10, 25
PRINT "For the "; datatype$; " period,"
LOCATE 12, 10
INPUT "Enter path to FIND data files [D:\DATA\TCD\DATA\] > ";
  datapath$
BEEP
IF datapath$ = "" THEN datapath$ = "D:\DATA\TCD\DATA\"
LOCATE 14, 10
INPUT "Enter path to SAVE results files [D:\DATA\TCD\RESULTS\]
  > "; respath$
BEEP
IF respath$ = "" THEN respath$ = "D:\DATA\TCD\RESULTS\"
LOCATE 16, 10
INPUT "Enter path to SAVE temporary files [E:\TEMP\] > ";
  tempopath$
BEEP
IF tempopath$ = "" THEN tempopath$ = "E:\TEMP\"

```

```

GOSUB myscreen
COLOR 14: LOCATE 10, 25
PRINT "Enter parameters (DEFAULT):"
COLOR 12
LOCATE 12, 25
INPUT "Enter sampling rate (50 Hz): "; samplerate
IF samplerate = 0 THEN samplerate = 50

data$ = datapath$ + datatype$ + ".TXT"
OPEN data$ FOR INPUT AS #1

```

```
FOR i=1 TO 3: LINE INPUT #1, junk$: NEXT i: junk$ = ""
```

```

,,,,,,,,,,,,,,,,,,,,,,,,,,,,,,,,,,,,,,,,,,,,,,,,,,,,,,,,,,,,,,,,,,,,,,,,,,,,,,,,
' Break up original data file into one minute files
'   i.e, CONTROL.TXT --> CTRL000.TXT, CTRL001.TXT, ...
,,,,,,,,,,,,,,,,,,,,,,,,,,,,,,,,,,,,,,,,,,,,,,,,,,,,,,,,,,,,,,,,,,,,,,,,,,,,,,,,

```

```

minute = 0
obs = 1
totalobs = 1
numfiles = 0

```

```
breakup:
```

```

IF minute >= 0 AND minute <= 9 THEN outfile$ = datapath$ +
  "CTRL00" + LTRIM$(STR$(minute)) + ".TXT"
IF minute >= 10 AND minute <= 99 THEN outfile$ = datapath$ +
  "CTRL0" + LTRIM$(STR$(minute)) + ".TXT"
IF minute >= 100 AND minute <= 999 THEN outfile$ = datapath$ +
  "CTRL" + LTRIM$(STR$(minute)) + ".TXT"
IF minute > 999 THEN GOSUB myscreen: LOCATE 20, 25: PRINT
  "ERROR DETECTED - To many files!": GOTO finish
OPEN outfile$ FOR OUTPUT AS #2
GOSUB myscreen
COLOR 12: LOCATE 11, 25: PRINT "Extracting "; outfile$
LOCATE 12, 30: PRINT " from "; data$
COLOR 10
LOCATE 15, 25: PRINT USING "Total time analyzed thus far:
  ##### minutes"; minute;
LOCATE 16, 25: PRINT USING "Total observations thus far:
  ##### observations"; totalobs
DO WHILE obs / samplerate <= 60
  INPUT #1, bfv, bp
  IF EOF(1) THEN GOTO continue:
  PRINT #2, totalobs, bfv, bp
  obs = obs + 1
  totalobs = totalobs + 1
LOOP
numfiles = numfiles + 1
IF numfiles = 31 THEN GOTO continue
minute = minute + 1

```

```

obs = 1
CLOSE #2
GOTO breakup

```

```

,,,,,,,,,,,,,,,,,,,,,,,,,,,,,,,,,,,,,,,,,,,,,,,,,,,,,,,,,,,,,,,,,,,,,,,,,,,,,,,,
' Use Codas *.L2 file to separate each 1 minute file into 1 heart
' cycle files i.e.,
' CONTROL.L2 + CTRL000.TXT, ... --> WAVE000.TXT, WAVE001.TXT, ...
,,,,,,,,,,,,,,,,,,,,,,,,,,,,,,,,,,,,,,,,,,,,,,,,,,,,,,,,,,,,,,,,,,,,,,,,,,,,,,,,

```

continue:

```

GOSUB myscreen
BEEP: BEEP: BEEP
CLOSE
COLOR 12
LOCATE 10, 25: PRINT USING "Total number of files =
    #####"; numfiles
LOCATE 11, 25: PRINT USING "Total number of observations =
    #####"; totalobs

summary$ = respath$ + "SUMMARY.TXT"
OPEN summary$ FOR OUTPUT AS #7

OPEN datapath$ + datatype$ + ".L2" FOR INPUT AS #6
FOR i = 1 TO 9: LINE INPUT #6, junk$: NEXT i: junk$ = ""

k = 0
obs = 1
minute = 0
FOR result = 0 TO numfiles

IF k = numfiles THEN GOTO finish

IF result >= 0 AND result <= 9 THEN results$ = respath$ +
    "RESUL00" + LTRIM$(STR$(result)) + ".TXT"
IF result >= 10 AND result <= 99 THEN results$ = respath$ +
    "RESULO" + LTRIM$(STR$(result)) + ".TXT"
IF result >= 100 AND result <= 999 THEN results$ = respath$ +
    "RESUL" + LTRIM$(STR$(result)) + ".TXT"
IF result > 999 THEN GOSUB myscreen: LOCATE 20, 25: PRINT

```

```

"ERROR DETECTED - To many files!": GOTO finish
OPEN results$ FOR OUTPUT AS #4
    IF k >= 0 AND k <= 9 THEN infile$ = datapath$
        + "CTRL00" + LTRIM$(STR$(k)) + ".TXT"
    IF k >= 10 AND k <= 99 THEN infile$ =
        datapath$ + "CTRLO" + LTRIM$(STR$(k)) + ".TXT"
    IF k >= 100 AND k <= 999 THEN infile$ =
        datapath$ + "CTRL" + LTRIM$(STR$(k)) + ".TXT"
    IF k > 999 THEN GOSUB myscreen: LOCATE 20, 25:
        PRINT "ERROR DETECTED - To many files!": GOTO
        finish
    OPEN infile$ FOR INPUT AS #2
    INPUT #6, diastolic, systolic, map, hr,
        diaobs, sysobs
    DO WHILE obs < diaobs 'move to begining of
        heartbeat
        INPUT #2, obs, bfv, bp
        IF EOF(2) GOTO continue5
    LOOP
continue5:
    cycle = 1
    z = 1
waves:
    INPUT #6, diastolic, systolic, map, hr, diaobs, sysobs

    IF EOF(6) THEN GOTO continue2
    dia(z) = diastolic
    sys(z) = systolic
    map(z) = map
    hr(z) = hr
    z = z + 1
    n = 1
    IF cycle >= 0 AND cycle <= 9 THEN outfile2$ =
        temppath$ + "TEMPO0" + LTRIM$(STR$(cycle)) + ".TXT"

    IF cycle >= 10 AND cycle <= 99 THEN outfile2$ =
        temppath$ + "TEMPO" + LTRIM$(STR$(cycle)) + ".TXT"
    IF cycle >= 100 AND cycle <= 999 THEN outfile2$ =
        temppath$ + "TEMP" + LTRIM$(STR$(cycle)) + ".TXT"
    IF cycle > 999 THEN GOSUB myscreen: LOCATE 20, 25:

```

```

        PRINT "ERROR DETECTED - To many files!": GOTO
        finish
OPEN outfile2$ FOR OUTPUT AS #3
DO WHILE obs < diaobs 'identify heartbeat cycle
    COLOR 10
    LOCATE 13, 25: PRINT "Taking data from ";
    infile$
    COLOR 14
    LOCATE 15, 25: PRINT USING "Current
    observation is #####"; obs
    LOCATE 16, 25: PRINT USING "Next heartbeat
    begins at #####"; diaobs
    COLOR 12
    LOCATE 18, 25: PRINT "Saving in file ";
    outfile2$
    INPUT #2, obs, bfv, bp
    IF EOF(2) THEN GOTO continue2
    PRINT #3, n, bfv, bp
    n = n + 1
LOOP
observation(cycle) = n - 1
COLOR 10
LOCATE 20, 25: PRINT "Number of heart cycles is ";
    cycle
LOCATE 21, 25: PRINT "Number observations in this
    heartbeat: "; n - 1
CLOSE #3
cycle = cycle + 1
GOTO waves
continue2:
    CLOSE #2
    CLOSE #3
    FOR m = 1 TO z - 1
        diatotal = dia(m) + diatotal
        systotal = sys(m) + systotal
        maptotal = map(m) + maptotal
        hrtotal = hr(m) + hrtotal
    NEXT m
    diamean = diatotal / (z - 1)
    sysmean = systotal / (z - 1)

```

```

mapmean = maptotal / (z - 1)
hrmean = hrtotal / (z - 1)
FOR m = 1 TO z - 1
    diatemp1 = (dia(m) - diamean) ^ 2
    diatemp2 = diatemp1 + diatemp2
    systemp1 = (sys(m) - sysmean) ^ 2
    systemp2 = systemp1 + systemp2
    maptemp1 = (map(m) - mapmean) ^ 2
    maptemp2 = maptemp1 + maptemp2
    hrtemp1 = (hr(m) - hrmean) ^ 2
    hrtemp2 = hrtemp1 + hrtemp2
NEXT m
diadev = SQR(diatemp2 / (z - 1))
sysdev = SQR(systemp2 / (z - 1))
mapdev = SQR(maptemp2 / (z - 1))
hrdev = SQR(hrtemp2 / (z - 1))
diatotal = 0: systotal = 0: maptotal = 0: hrtotal = 0
diatemp1 = 0: diatemp2 = 0
systemp1 = 0: systemp2 = 0
maptemp1 = 0: maptemp2 = 0
hrtemp1 = 0: hrtemp2 = 0
FOR m = 1 TO z
    dia(m) = 0: sys(m) = 0: map(m) = 0: hr(m) = 0
NEXT m
GOSUB myscreen
LOCATE 10, 20
PRINT "For minute "; minute
LOCATE 12, 25: PRINT USING "Mean diastolic pressure = ###.#
    +/- ##.## mmHg"; diamean; diadev
LOCATE 13, 25: PRINT USING "Mean systolic pressure = ###.# +/-
    ##.## mmHg"; sysmean; sysdev
LOCATE 14, 25: PRINT USING "Mean arterial pressure = ###.# +/-
    ##.## mmHg"; mapmean; mapdev
LOCATE 15, 25: PRINT USING "Mean heart rate = ###.# +/- ##.##
    bpm"; hrmean; hrdev
LOCATE 17, 25: PRINT "Saving means and deviations in ";
    summary$
PRINT #7, minute; ", "; rejects; ", "; diamean; ", "; diadev;
    ", "; sysmean; ", "; sysdev; ", "; mapmean; ", "; mapdev; ", ";
    hrmean; ", "; hrdev

```

```
minute = minute + 1
```

```

,,,,,,,,,,,,,,,,,,,,,,,,,,,,,,,,,,,,,,,,,,,,,,,,,,,,,,,,,,,,,,,,,,,,,,,,
' Calculate AVERAGE, STND. DEV., and RANGE for number of observations
'   in each heart cycle file over the one minute interval.
,,,,,,,,,,,,,,,,,,,,,,,,,,,,,,,,,,,,,,,,,,,,,,,,,,,,,,,,,,,,,,,,,,,,,,,,

```

```

minimum = observation(1)
maximum = observation(1)
FOR i = 1 TO cycle - 1
    total = observation(i) + total
    IF minimum > observation(i) THEN minimum =
        observation(i)
    IF maximum < observation(i) THEN maximum =
        observation(i)
NEXT i
average = total / i
FOR i = 1 TO cycle - 1
    temp1 = (observation(i) - average) ^ 2
    temp2 = temp2 + temp1
NEXT i
stnddev = SQR(temp2 / i)
lowlimit = average - stnddev
highlimit = average + stnddev

```

```

,,,,,,,,,,,,,,,,,,,,,,,,,,,,,,,,,,,,,,,,,,,,,,,,,,,,,,,,,,,,,,,,,,,,,,,,
' Delete heart beats which have no. of obs. outside MEAN +/- S.D.
'   (to minimize phase shifts and remove bad data (i.e., flushing)
'   and rename TEMP*.TXT --> WAVE*.TXT files
,,,,,,,,,,,,,,,,,,,,,,,,,,,,,,,,,,,,,,,,,,,,,,,,,,,,,,,,,,,,,,,,,,,,,,,,

```

```

rejects = 0
j = 1
FOR i = 1 TO cycle - 1
    IF i >= 0 AND i <= 9 THEN temp1$ = temppath$ +
        "TEMPO0" + LTRIM$(STR$(i)) + ".TXT"
    IF i >= 10 AND i <= 99 THEN temp1$ = temppath$ +
        "TEMPO" + LTRIM$(STR$(i)) + ".TXT"
    IF i >= 100 AND i <= 999 THEN temp1$ = temppath$ +
        "TEMP" + LTRIM$(STR$(i)) + ".TXT"
    IF i > 999 THEN GOSUB myscreen: LOCATE 20, 25: PRINT

```

```

"ERROR DETECTED - To many files!": GOTO finish
IF observation(i) < lowlimit OR observation(i) >
highlimit THEN GOTO reject: ELSE GOTO accept:

```

```
reject:
```

```

KILL temp1$
LOCATE 20, 20: PRINT "Deleting "; temp1$
rejects = rejects + 1
GOTO continue9

```

```
accept:
```

```

IF j >= 0 AND j <= 9 THEN wave1$ = temp1path$ +
"Wave00" + LTRIM$(STR$(j)) + ".TXT"
IF j >= 10 AND j <= 99 THEN wave1$ = temp1path$ +
"Wave0" + LTRIM$(STR$(j)) + ".TXT"
IF j >= 100 AND j <= 999 THEN wave1$ = temp1path$ +
"Wave" + LTRIM$(STR$(j)) + ".TXT"
OPEN temp1$ FOR INPUT AS #5
OPEN wave1$ FOR OUTPUT AS #3
DO WHILE NOT EOF(5)
    INPUT #5, n, bfv, bp
    PRINT #3, n, bfv, bp
LOOP
CLOSE #3
CLOSE #5
j = j + 1
KILL temp1$
LOCATE 22, 20: PRINT "Renaming "; temp1$; " as ";

```

```
wave1$
```

```
continue9:
```

```

NEXT i
rejects = rejects / (cycle - 1) * 100
cycle = j
maximum = highlimit
GOSUB myscreen

```

```

,,,,,,,,,,,,,,,,,,,,,,,,,,,,,,,,,,,,,,,,,,,,,,,,,,,,,,,,,,,,,,,,,,,,,,,,,,,,,
' Count no. of first, second, etc. points across valid heart beats
,,,,,,,,,,,,,,,,,,,,,,,,,,,,,,,,,,,,,,,,,,,,,,,,,,,,,,,,,,,,,,,,,,,,,,,,,,,,,

```

```

LOCATE 10, 10: PRINT "Counting first points, second points,
etc., in each heartbeat."

```

```

FOR i = 1 TO cycle - 1
  IF i >= 0 AND i <= 9 THEN file1$ = temppath$ +
    "WAVE00" + LTRIM$(STR$(i)) + ".TXT"
  IF i >= 10 AND i <= 99 THEN file1$ = temppath$ +
    "WAVE0" + LTRIM$(STR$(i)) + ".TXT"
  IF i >= 100 AND i <= 999 THEN file1$ = temppath$ +
    "WAVE" + LTRIM$(STR$(i)) + ".TXT"
  IF i > 999 THEN GOSUB myscreen: LOCATE 20, 25: PRINT
    "ERROR DETECTED - To many files!": GOTO finish
  OPEN file1$ FOR INPUT AS #3
  pts = 1
  DO WHILE NOT EOF(3)
    INPUT #3, obs, bfv, bp
    numobs(pts) = numobs(pts) + 1
    pts = pts + 1
  LOOP
  CLOSE #3
continue7:
  NEXT i

' .....,
' Calculate MEAN and S.D. of first, second, third, etc. obs. across
' all valid heart beat files and store to RESULT*.TXT file
' .....,

GOSUB myscreen
FOR pt = 1 TO maximum
  COLOR 14
  LOCATE 13, 25: PRINT USING "Analyzing point ### of
    ###"; pt; maximum
  FOR i = 1 TO cycle - 1
    IF i >= 0 AND i <= 9 THEN file1$ = temppath$ +
      "WAVE00" + LTRIM$(STR$(i)) + ".TXT"
    IF i >= 10 AND i <= 99 THEN file1$ = temppath$
      + "WAVE0" + LTRIM$(STR$(i)) + ".TXT"
    IF i >= 100 AND i <= 999 THEN file1$ =
      temppath$ + "WAVE" + LTRIM$(STR$(i)) + ".TXT"
    IF i > 999 THEN GOSUB myscreen: LOCATE 20, 25:
      PRINT "ERROR DETECTED - To many files!": GOTO
      finish
  OPEN file1$ FOR INPUT AS #3

```

```

        j = 1
        DO WHILE NOT EOF(3)
            INPUT #3, obs, bfv, bp
            IF j = pt THEN GOTO continue4
            j = j + 1
        LOOP
continue4:
        bfvpt(i) = bfv
        bppt(i) = bp
        CLOSE #3
continue6:
        NEXT i
        IF numobs(pt) = 0 THEN GOTO zero
        FOR i = 1 TO numobs(pt)
            bfvtot = bfvtot + bfvpt(i)
            bptot = bptot + bppt(i)
        NEXT i

        bfvavg = bfvtot / numobs(pt)
        bpavg = bptot / numobs(pt)

        FOR i = 1 TO numobs(pt)
            bfvtemp1 = (bfvpt(i) - bfvavg) ^ 2
            bfvtemp2 = bfvtemp2 + bfvtemp1
            bptemp1 = (bppt(i) - bpavg) ^ 2
            bptemp2 = bptemp2 + bptemp1
        NEXT i

        bfvdev = SQR(bfvtemp2 / numobs(pt))
        bpdev = SQR(bptemp2 / numobs(pt))

        PRINT #4, pt; ", "; numobs(pt); ", "; bfvavg; ", ";
            bfvdev; ", "; bpavg; ", "; bpdev

        COLOR 10
        LOCATE 10, 25: PRINT USING "Average
            observations/heartbeat = ##.# +/- ##.##"; average;
            stnddev
        LOCATE 11, 25: PRINT USING "Range of observations =
            ### - ###"; minimum; maximum

```

```

COLOR 12
LOCATE 15, 25: PRINT USING "For point ###,"; pt
LOCATE 16, 30: PRINT USING "Blood Flow Velocity is
    ###.## +/- ##.## cm/sec"; bfvavg; bfvdev
LOCATE 17, 30: PRINT USING "Blood Pressure is ###.##
    +/- ##.## mmHg"; bpavg; bpdev
LOCATE 18, 30: PRINT "Number of beats containing this
    cycle is "; numobs(pt)
COLOR 10.
LOCATE 20, 25: PRINT "Writing results to: "; results$

zero:

    bfvtot = 0: bptot = 0
    bfvavg = 0: bpavg = 0
    bfvtemp1 = 0: bptemp1 = 0
    bfvtemp2 = 0: bptemp2 = 0
    bfvdev = 0: bpdev = 0
    FOR i = 1 TO 200
        bfvpt(i) = 0
        bppt(i) = 0
        observation(i) = 0
    NEXT i

NEXT pt
cycle = 1
n = 1
CLOSE #4
CLOSE #2
k = k + 1
KILL tempopath$ + "*.TXT"
GOSUB myscreen
FOR i = 1 TO 200
    numobs(i) = 0
NEXT i
total = 0
maximum = 0: minimum = 0
temp1 = 0: temp2 = 0
average = 0: stnddev = 0
lowlimit = 0: highlimit = 0

NEXT result

```

```

finish:
OPEN temp_path$ + "TEMP.TXT" FOR OUTPUT AS #10
PRINT #10, numfiles
CLOSE
BEEP: BEEP: BEEP
END

```

```

myscreen:
    SCREEN 12: CLS
    LINE (0, 0)-(639, 399), 9, B: LINE (1, 1)-(638, 398), 9, B
    COLOR 13: LOCATE 6, 20
    PRINT "TCD Data Analysis Package by Michael Drues"
    LOCATE 24, 50: PRINT USING "Execution time = #####.## min.";
(TIMER - starttime) / 60
    COLOR 10
    BEEP
RETURN

```

```

mycontinue:
    COLOR 12
    LOCATE 24, 55: PRINT "Continue (Y/n): "; INKEY$
    IF INKEY$ <> "" OR INKEY$ <> "Y" OR INKEY$ <> "y" THEN GOTO
finish
    COLOR 10
RETURN

```

The next program takes the results of the last program and calculates the SDR, PPI, GPI and SU from the BFV waveform.

```

' Calculate wave parameters on filtered data (i.e., RESUL000.TXT, ...)
DIM bfv(300), bp(300), m(100)
CLS
OPEN "D:\DATA\TCD\DATA\TEMP.TXT" FOR INPUT AS #1

```

```

INPUT #1, numfiles
CLOSE
OPEN "D:\DATA\TCD\RESULTS\STATS.TXT" FOR OUTPUT AS #1
FOR result = 0 TO numfiles - 1
    PRINT "Minute = "; result
    IF result >= 0 AND result <= 9 THEN results$ =
        "D:\DATA\TCD\RESULTS\RESULOO" +
        LTRIM$(STR$(result)) + ".TXT"
    IF result >= 10 AND result <= 99 THEN results$ =
        "D:\DATA\TCD\RESULTS\RESULO" +
        LTRIM$(STR$(result)) + ".TXT"
    IF result >= 100 AND result <= 999 THEN results$ =
        "D:\DATA\TCD\RESULTS\RESUL" + LTRIM$(STR$(result))
        + ".TXT"
    OPEN results$ FOR INPUT AS #2
    j = 1
    DO WHILE NOT EOF(2)
        INPUT #2, obs, totobs, bfv, bfverr, bp, bperr
        bfv(j) = bfv
        bp(j) = bp
        j = j + 1
    LOOP
    CLOSE #2
    samples = j - 1
    minbfv = bfv(1)
    maxbfv = bfv(1)
    FOR i = 1 TO samples
        bfvtot = bfv(i) + bfvtot
        bptot = bp(i) + bptot
        IF minbfv >= bfv(i) THEN minbfv = bfv(i): imin = i

        IF maxbfv <= bfv(i) THEN maxbfv = bfv(i): imax = i
    NEXT i
    meanbfv = bfvtot / samples
    meanbp = bptot / samples
    sdratio = maxbfv / minbfv
    ppi = (maxbfv - minbfv) / maxbfv
    gpi = (maxbfv - minbfv) / meanbfv
    j = 1
    FOR i = imin TO imax

```

```
        m(j) = (bfv(i + 1) - bfv(i)) * 50 '
            (upstroke, cm/sec/sec)
        j = j + 1
    NEXT i
    maxslope = m(1)
    FOR i = 1 TO j
        IF maxslope <= m(i) THEN maxslope = m(i)
    NEXT i
    upslope = maxslope
    PRINT #1, result; ", "; meanbp; ", "; meanbfv; ", ";
        sdratio; ", "; ppi; ", "; gpi; ", "; maxslope
    FOR i = 1 TO samples: bfv(i) = 0: bp(i) = 0: NEXT i
    bptot = 0: bfvtot = 0: minbfv = 0: maxbfv = 0
NEXT result
CLOSE #1
```

12. APPENDIX D: SAS CODE FOR STATISTICAL ANALYSIS

The following is the SAS source code used for performing the analysis of variance on the MBFV, MAP, MHR, pCO₂, SDR, PPI, GPI and SUS data. Simply change the dose and parameter variables for each analysis.

```
data tcd;
    infile '/home/drues/=stat/=tcd/data.txt' pad missover;
    input measure $ dog $ dose $ period $ minute value;
    if minute > 30 then delete;
    if 1 <= minute <=10 then block = 1;
    if 11 <= minute <=20 then block = 2;
    if 21 <= minute <=30 then block = 3;
    if dose = "High" then delete;
    if measure ne "MBFV" then delete;
run;

title 'Mean Blood Flow Velocity for Low Level Experiment';

proc sort data = tcd;
    by period block dog ;
run;

proc means data = tcd maxdec=4 mean noprint ;
    by period block dog;
    var value;
    output out=datamean mean= mvalue;
run;
```

```
proc sort data = datamean;
    by period block ;
run;
```

```
proc means data=datamean maxdec=4 noprint;
    by period block;
    var mvalue;
    output out=tempmean mean= mmean sum= smean;
run;
```

```
proc print data=datamean;
proc print data=tempmean;
run;
```

```
proc glm data = datamean ;
    classes period block dog;
    model mvalue = period block dog period*block;
    means period block dog period*block / duncan scheffe lsd tukey ;
run ;
```

```
data datamean;
    set datamean;
    if period='Control' and block=1 then perblk=1;
    if period='Control' and block=2 then perblk=2;
    if period='Control' and block=3 then perblk=3;
    if period='Glyfor' and block=1 then perblk=4;
    if period='Glyfor' and block=2 then perblk=5;
    if period='Glyfor' and block=3 then perblk=6;
    if period='Delta' and block=1 then perblk=7;
    if period='Delta' and block=2 then perblk=8;
    if period='Delta' and block=3 then perblk=9;
```

```
proc glm data = datamean ;
    classes perblk dog;
    model mvalue = perblk dog;
    means perblk / duncan scheffe lsd tukey ;
run ;
```